ILIR '99:
SSC San Diego
In-House Laboratory
Independent Research
1999 Annual Report

SSC San Diego

TECHNICAL DOCUMENT 3095
May 2000

ILIR '99:
SSC San Diego
In-House Laboratory
Independent Research
1999 Annual Report

Approved for public release;
distribution is unlimited.

SPAWAR
Systems Center
San Diego

SSC San Diego
San Diego, CA 92152–5001

DTIC QUALITY INSPECTED 4

ADMINISTRATIVE INFORMATION

JA

CONTENTS

INTRODUCTION

INTRODUCTION

New and innovative ideas proposed by the scientists and engineers of the Space and Naval Warfare Systems Center, San Diego (SSC San Diego) are supported and encouraged through the In-house Laboratory Independent Research (ILIR) program, which is administered by the Office of Naval Research (ONR). The ILIR program is implemented at SSC San Diego under the authority of the Deputy Executive Director for Science, Technology, and Engineering and is managed by the Science and Technology Office. This program supports basic scientific research in several areas of interest to the Navy, including command and control, communications, surveillance, and navigation.

Dr. Larry Flesner, Science and Technology Office, administered the FY 99 SSC San Diego ILIR program under the direction of Dr. Eric Hendricks, Head, Office of Business Development and Science and Technology, with assistance from Dr. George Dillard of the Intelligence, Surveillance, and Reconnaissance Department. The selection process began with the 25 March 1998 call for proposals in four ILIR Thrust Areas. These areas are Command and Control (C^2); Communications (COMM); Intelligence, Surveillance and Reconnaissance (ISR); and Other Research. Scientists and engineers responded with 79 written proposals, which were screened for scientific merit and Navy relevance and then evaluated by panels of experts. The panels comprised Dr. Flesner; Dr. George Dillard, Dr. Charles Hicks, Navigation and Applied Sciences Department; and SSC San Diego technical experts. Based on evaluations by the panels and an administrative review, 29 projects were selected.

ONR allocated $2,544,688 to SSC San Diego for FY 99. In December 1998, ONR placed a hold on $1M pending possible reallocation of funds to projects relating to stochastic resonance. The funding hold was eventually reduced to $500K, and final resolution of FY 99 funding occurred in August 1999. The final allocations included $200K redirected to stochastic resonance projects, $300K carried over from FY 99 to the FY 00 ILIR program, and other FY 99 projects funded at approximately 84% of their original recommended amounts. Thus, the amount invested in ILIR projects during FY 99 was approximately $2,240K. Funding delays and reductions caused significant adverse impacts on almost all FY 99 projects.

This report describes accomplishments of the ILIR program for the period 1 October 1998 through 30 September 1999. Included are lists of publications and patents, honors and awards, and tables consisting of the SSC San Diego FY 99 and FY 00 ILIR databases. Four main sections are designated by focus area and include concise descriptions of the FY 99 ILIR projects, highlighting their objectives and accomplishments. Other sections comprise significant impacts and transitions from the FY 99 program.

Program Changes for FY 00 and FY 01

The ILIR program at SSC San Diego is being restructured to increase the impact of limited ILIR resources. This restructuring will be accomplished by increasing the size of selected projects to better focus ILIR on areas identified in our corporate technical vision as most critical to the SSC San Diego mission. Between two and six large team projects will be selected. Each will be funded at approximately $300K per year or more and will generally last for 2 to 3 years. The rest of the program will

comprise smaller projects, each funded in the range $100K to $150K per year. The intent is to fund the most mission-critical projects at high levels to enable exceptional impacts and to fund all projects at adequate levels to generate useful results. As a consequence of these changes, a smaller number of projects overall will be funded in FY 01 than in previous years. For example, if the FY 01 ILIR program receives approximately $2.7M, it may comprise four projects with an average funding of $300K, and 12 smaller projects with an average funding of $125K.

Two large team projects were initiated in FY 00, *Knowledge Mining for Command and Control Systems* and *Robust Waveform Design for Tactical Communication Channels*. These projects are expected to continue for 2 to 3 years, and additional team projects will be selected in FY 01 and subsequent years.

The following table summarizes recent metrics for the SSC San Diego ILIR program.

	FY 95	FY 96	FY 97	FY 98	FY 99
Funding ($K)	2,463	2,763	2,521	2,300	2,240
Number of projects	29	31	29	25	29
Professional work-years	15.3	15.6	14.5	13.3	12.8
Refereed papers (published or accepted)	26	19	19	15	22
Refereed papers (submitted)	9	9	10	5	10
Books/Chapters	—	—	—	3	9
In-house publications	3	4	2	2	—
Proceedings*	—	—	—	30	26
Presentations to professional meetings	60	38	50	42	52
Patents issued	5	6	7	5	9–IR 2–IED
Statutory Invention Registration	—	—	1	—	—
Claims allowed, pending issue	2	—	2	4	5
Patent applications filed	6	11	12	11	7
Invention disclosures authorized	5	6	4	3	3
Invention disclosures submitted	7	7	10	13	17

* Counted within Presentations in previous years

PROJECT SUMMARIES

COMMAND AND CONTROL

Robust Control of Information Flow for Network-Centric Warfare

Objective(s): Mathematically model global information flow dynamics on a massive command and control (C^2) network system and devise control and game theoretic methods to counter network attacks.

Accomplishment(s): Fluid flow on manifolds and graphs was proposed as a first qualitative description of information flow on a network-centric warfare system. Mathematical analysis and control theory applied to this model was a natural generalization of several well-established theoretical works of the principal investigator in the field of optimal flow control. In FY 99, stochastic Navier–Stokes as well as stochastic magnetohydrodynamic models were investigated both in continuum and discrete-continuum view points. The discrete models considered were a prelude to the network-centric models in the sense that space-time jump processes on a discrete lattice were studied, and it was proven rigorously that equations governing these models converge to fluid equations. Impulse and stopping-time problems were analyzed for the stochastic Navier–Stokes equations for the first time and published in the literature.

MODELING PHILOSOPHY

Stochastic processes for modeling command and control (C^2) systems can be chosen from the following classes depending on the characteristics of the specific problem. The particular features of Network-Centric Warfare (NCW) such as heterogeneity (different time scales for different components of the command and control system) can be represented in terms of parameter variations in the *generator* of these stochastic processes:

1. *Multidimensional point processes, space-time jump processes, and fractional Brownian motions.* Point processes arise in multiclass queuing systems and large communication systems. Here the term "multiclass" represents different arrival rates, priorities, different service rates, and state dependence of the servers. Space-time jump processes generalize the multidimensional point processes to allow for non-integer values. In *notices of the American Mathematical Society (AMS)*, Bell Lab experts argue the importance of fractional Brownian motions in Internet modeling [1]. Developing prediction and control techniques to such processes may be feasible in the future.

2. *Continuous time models, Hodgkin–Huxley-type neuron models, and fluid/diffusion limits to "reflecting" Navier–Stokes-like models.* For very large C^2 systems, many features concerning information-flow quantities and command action can be obtained by working with the infinite limit case (infinite nodes and heavy traffic), which would yield various deterministic and stochastic differential equations. Such a fluid/diffusion limit is currently an active research area in communication networks [2]. The resultant differential equations differ from the conventional fluid-flow equations in two ways. First, the state variable is positive-valued so one gets "reflecting" stochastic processes (generalizations of reflecting Brownian motions). Second, there may be stochastic forcing terms with a diffusion term depending on the state variable in interesting ways (such as square-root-like dependence). The prediction theory for such a system would be a generalization of the current joint work by G. Kallianpur and the principal investigator on

stochastic calculus and white-noise prediction theory for the conventional (deterministic and stochastic) Navier–Stokes equation. Rules for command action for the above reflecting system can be derived by generalizing the works of the principal investigator on control of a conventional Navier–Stokes system [3].

QUANTIFICATION OF INFORMATION-FLOW ON THE INFORMATION GRID

Mathematical formulations described above indicate the way we model data flow through the command control system in terms of the language of stochastic processes. The statistics of these processes can now be characterized in terms of suitable martingale formulations (generalizing the work of Stroock and S. R. S. Varadhan [4]). The statistics can then be used to define various notions of self and mutual information in terms of suitable Shannon and Fisher entropies. We call this information *a priori* information. Command and control systems involve fewer monitoring points of data-flow than the actual dimension of the (data) processes. At this point, it is possible to define the notions of *information-authentication, information-assurance, and information forecasting* by suitably *conditioning* the *a priori* information (or state of the stochastic process) by the *observed* information (or process) at the monitoring points. It is then possible to derive equations for the time evolution of these conditional information quantities based on the white-noise theory of G. Kallianpur and R. Karandikar [5].

We carried out this analysis for the discrete and continuous time models described previously. One of the main challenges in the continuous-time models (such as the "reflecting fluid" network models) is the task of dealing with the added complexity of reflecting processes. These equations of evolution will describe the (conditional) information flow across the C^2 network hierarchy in real time. Preliminary analysis shows very interesting equations arising in this context with subtle relations between the time evolutions of Shannon and Fisher entropies. Time asymptotic behavior of the above information quantifiers are being studied since they characterize and guarantee C^2 system stability and quality of service.

INFORMATION-FLOW MANAGEMENT/CONTROL: CHERNOFF THEORY OF STATISTICAL DECISIONS TO COMMAND ACTION

The previous step provides a way of monitoring the data flow and characterizing the time evolution of conditional information-flow quantities in the information grid. We now describe the task of obtaining strategic command actions to regulate and manage the information flow. Among the various control ideas available for finite- and infinite-dimensional processes, we choose the stopping-time control of H. Chernoff combined with the impulse control of A. Bensoussan and J. L. Lions. In this case, the information flow is managed by certain C^2 actions at certain discrete times called optimal stopping times (optimal "instants" of command action) of Chernoff. At these times, certain control action on the network such as switching of queues is performed as dictated by control theory. The most obvious advantages are that control is not performed all the time, and the required calculations (whose degree of difficulty would vary depending on the particular C^2 system) can often be performed off-line, thus facilitating real-time information-flow management. Research tasks include generalizing the current joint work of the principal investigator with J. L. Menaldi (on impulse and stopping-time control theory for a conventional fluid system) to C^2 network models in their infinite and diffusion/fluid limit with "reflecting processes"; this would be a nontrivial step.

PREDICTION OF C² FAILURES AND RARE EVENTS: LARGE DEVIATION ANALYSIS

Characterization of the time evolution of information flow in terms of concrete equations and methods of real-time information management will pave the way to designing robust C^2 systems. In particular, if a certain subnetwork fails or is jammed by adversaries, then we can design C^2 systems to dynamically reconfigure the information flow as long as we have a good statistical estimate of failure probabilities. This leads to the third part of the research, which is the estimation of rare events by large deviation theory [6] and the task of designing command actions, which are risk-sensitive. In this part, we used the close relationship between large deviation theory (estimating the probability of rare events in C^2 dynamics) and risk-sensitive control (which is currently a hot topic in stochastic games and control) to address this issue for the network-centric system. Risk-sensitive control is closely related to a game theoretic formulation for the C^2 system with disturbance/uncertainties appearing as the opposite player. This connection is, in fact, a consequence of some results of Varadhan [6]. The task in this part has focused on developing these ideas for the C^2 stochastic models.

REFERENCES

1. Willinger, W. and V. Paxon. 1998. "Where Mathematics Meets the Internet," *Notices of the American Mathematical Society (AMS),* vol. 45, no.8, (Sept), pp. 961ff.

2. *Stochastic Networks.* 1995. F. Kelley and R. J. Williams, eds. Springer-Verlag.

3. Sritharan, S. S. 1998. *Optimal Control of Viscous Flow*, Society for Industrial and Applied Mathematics (SIAM).

4. Stroock, D. W. and S. R. S. Varadhan. 1997. *Multidimensional Diffusion Processes,* Springer–Verlag.

5. Kallianpur, G. and R. Karandikar. 1988. *White Noise Theory of Prediction, Filtering and Smoothing*, Gordon and Breach.

6. Varadhan, S. R. S. 1984. *Large Deviation Theory,* Conference Board of the Mathematical Sciences (CBMS) Regional Conference Series, SIAM.

Principal Investigator:
Dr. Sri S. Sritharan   ZU68
D73H
(619) 553–1201
srith@spawar.navy.mil

Innovative Methods for Alertness Management and Crew Workload Allocation

Objective(s): Further explore an SSC San Diego study [1] that found that fluctuations in operator alertness affect task performance for longer periods of time than previously thought. This phenomenon has significant implications for the design of ship system automation. Objectives of this ILIR effort were to validate the original set of human alertness indicators and quantify their effects on human–computer task performance; develop a mathematical model of these effects relevant to the design of command and control systems, specifically adaptive automation, workload allocation, and decision support tools; and confirm these effects in an operational (i.e., shipboard) setting.

Accomplishment(s): The cardiac analyses of the original data set (figure 1) have been confirmed regarding both experimental methods and statistical approach, and a journal article is being prepared [2] to reflect this expanded investigation that augments the results reported in [3]. Electroencephalogram (EEG) and ocular (i.e., eye blink) analysis methods have been developed in-house to support examination of additional alertness-performance relationships (e.g., figure 2), and a new EEG technique—Independent Components Analysis—is being evaluated in collaboration with the University of California at San Diego (UCSD) Institute for Neural Computing. In addition, a collaborative effort has been initiated with the University of Wisconsin Industrial Engineering Department to generate a discrete-event dynamic system model of alertness-performance effects, based on the cardiac results. Finally, recording equipment has been evaluated to allow ambulatory data collection from shipboard watch personnel, and an experiment has been designed in consultation with the UCSD Neurosciences Department to support a field study of these effects. The alertness-performance model will be validated against both the experimental and field data sets prior to the completion of this ILIR project, and discussions have begun regarding transitions of this project to current command-and-control acquisition programs.
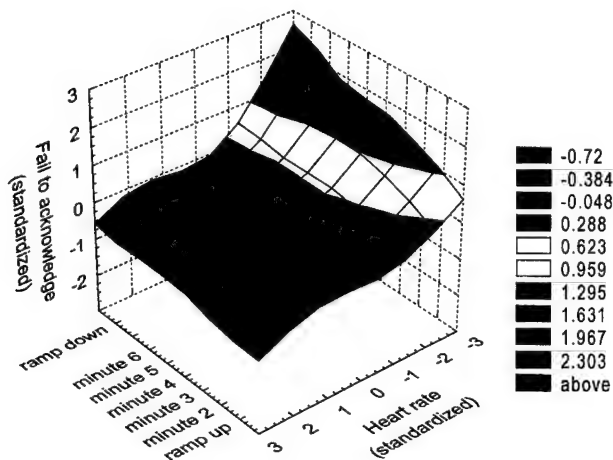
Figure 1. Alertness-performance effect for cardiac data. Reduced alertness is shown from left-to-right on the Heart-Rate scale, increasing error rates for a specific task are shown from bottom-to-top on the Fail-to-Acknowledge scale; and time duration of the task is shown from right-to-left on the Period scale.
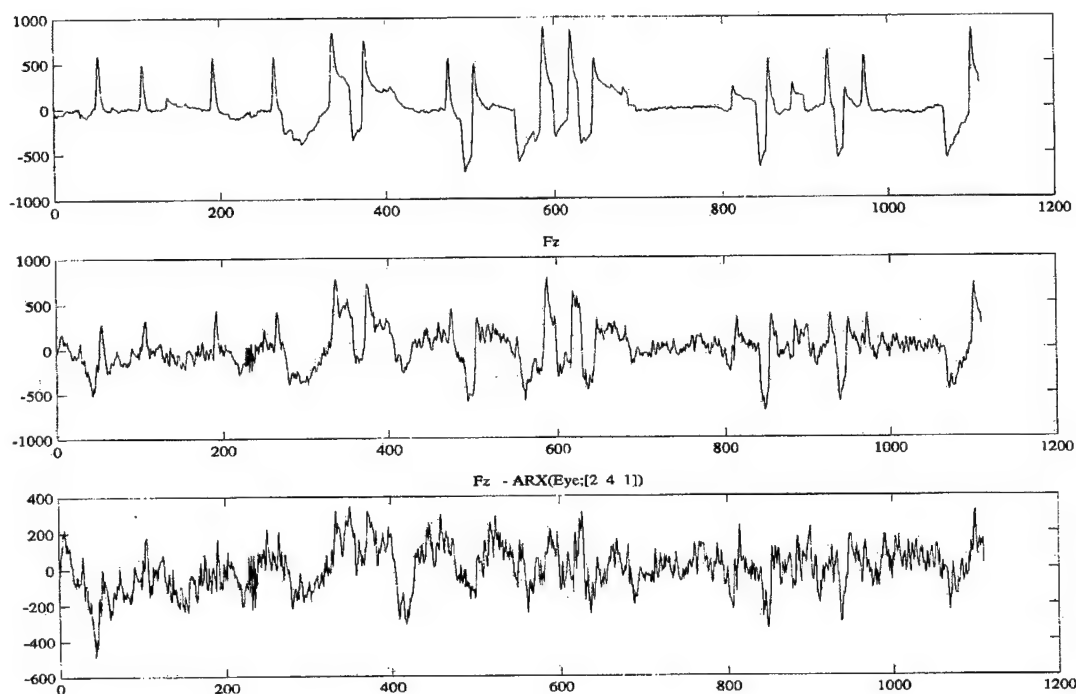
Figure 2. Example of muscle artifact signal (bottom), raw EEG signal contaminated by muscle artifact (middle), and signal with artifact removed (top) using in-house processing techniques.

BACKGROUND

The Navy desires smaller ship crew sizes as a means to reduce operating costs. Long periods of time spent with only sporadic stimulation, however, lead to lapses of alertness that can have critical consequences when competent task action is required [4, 5]. The success of a minimal-crewing policy, therefore, will depend on tools that extract maximum effectiveness from each crewmember in operations characterized by intermittent workload. Alertness levels must be measured and managed to ensure that no crewmember jeopardizes the viability of the ship at critical moments through fatigue, inattention, or confusion. Adaptive automation (i.e., dynamic allocation of workload between operator and machine) is an engineering method that can support operator effectiveness through comprehensive task management of crewmembers, sensors, and weapons [6]. Such automation schemes, however, necessarily rely on a real-time determination of operator readiness in order to function properly. Of critical importance is the operator's decision-making capacity in the initial moments after a problem arises (e.g., system emergencies, potential attacks); adaptive automation algorithms must have some assessment of operator state *before* workload-allocation decisions are implemented.

Of all the DoD research efforts in this area, shipboard applications may provide the best payoff opportunities. The stationary nature of many combat positions (e.g., Combat Information Center [CIC] workstations), where operators can be continuously monitored, and the readily available computer capability at these positions provide an ideal testing ground for new measurement concepts. Recent experimental results have shown several task-specific performance consequences from fluctuations in operator state, using real-time physiological measures [6]. The core of this ILIR effort is

13

to further examine and elaborate these results in order to provide an important enabling technology for the design of automated human–machine systems for the Navy.

A study of alertness classification based on heart, brain, and eye signals has already shown good predictive results of operator performance in a simulated air defense task. This work was distinctive because the experiment

1. was directly connected with real Navy workstation tasks,
2. involved realistic shift durations—a total of 8 hours per operator, and
3. gathered an exhaustive body of physiological and task performance data.

The essential contribution of this effort was to demonstrate that operator performance for even protracted tasks could be largely determined by brief physiology measures taken just before workload is introduced. This predictive model represents a unique approach in the human-performance literature.

APPROACH

This project more fully explored the existing data set in order to model the alertness (performance relationships) and seeks to extend these results to operational settings. Ongoing tasks include the following objectives:

1. With university collaboration, complete the signal processing and statistical analyses of the existing data. Apply additional analysis techniques (e.g., inferential statistics, improved artifact rejection methods) to the cardiac data, reduce the EEG data, and compare the use of these heart and brain measures to multiple indices of performance indices. The goal is thorough data mining, to guide future research and engineering efforts in this domain. To date, we have examined the correlation between task performance and spectral power in the alpha (8- to 12-Hz) EEG band and are currently replicating this analysis with both beta (13- to 20-Hz) and theta (4- to 7-Hz) bands. In addition, we are applying Independent Components Analysis (ICA) to the EEG data with the goal of developing a multidimensional predictor of task performance. Researchers at the UCSD Salk Institute (the development source for ICA methods) are assisting in this effort.

2. Develop a quantitative (i.e., discrete-event dynamic system) model of these effects that can improve the design of command and control systems. A rigorous model does not currently exist that addresses operator-alertness implications for adaptive automation, workload allocation, and decision support. Faculty and students at the University of Wisconsin–Madison have generated a preliminary discrete-event systems model, but the model has not yet been tested.

3. Test the model under operational conditions, using portable measurement equipment. This effort will commence later in FY 00, once results of (1) and (2) have been validated.

ACKNOWLEDGMENT

REFERENCES

1. Murray, S. A. 1997. "Effects of Operator Alertness on Human–Machine Interaction and Supervisory Control Performance," unpublished doctoral dissertation, University of Wisconsin–Madison, (contact author).

2. Murray, S. A. "Operator Alertness Fluctuations and Cognitive Function," to be submitted to *IEEE Transactions on Systems, Man, and Cybernetics.*

3. Murray, S. A. and B. S. Caldwell. 1998. "Operator Alertness and Human–Machine System Performance during Supervisory Control Tasks," (M. Scerbo and M. Mouloua eds.), *Automation Technology and Human Performance: Current Research and Trends* Lawrence Erlbaum, Mahwah, NJ.

4. Krulewitz, J. E., J. S. Warm, and T. H. Wohl. 1975. "Effects of Shifts in the Rate of Repetitive Stimulation on Sustained Attention," *Perception and Psychophysics*, vol. 18, pp. 245–249.

5. Ryan, T. G., S. G. Hill, T. K Overline, and B. L. Kaplan. 1994. "Work Underload and Workload Transition as Factors in Advanced Transportation Systems," *Workshop Proceedings* (EGG-HFSA-11483), Idaho National Engineering Laboratory, Idaho Falls, ID.

6. Pope, A. T. and E. H. Bogart. 1992. "Identification of Hazardous Awareness States in Monitoring Environments," *Society of Automotive Engineers (SAE) 1992 Transactions: Journal of Aerospace,* section 1, vol. 101, pp. 449–457, Warrandale, PA.

Principal Investigator:
Dr. Steven A. Murray   ZU67
D374
(619) 553–6350
murrays@spawar.navy.mil

Deduction in Data Fusion Based upon Algebraic Representation of Probabilistic Models

Objective(s): Develop a comprehensive and implementable algebraic-based theory of deduction and logical reasoning relative to multivalued phenomena that can arise in data fusion—such as involving conditional and/or set bounded information—and show that this applies to both classical deduction methods and statistical decision theory, as well as to linguistic-based information and decisions.

Accomplishment(s): During FY 99, the derivation of a novel Bayesian universal algebraic theory of conditional-probabilistic deduction, Second-Order Probability Logic (SOPL) was begun, significantly extending the preliminary results of FY 98. Furthermore, extensions of SOPL to a fuzzy-logic setting were also begun. The new theory is a conceptual improvement upon other previous *ad hoc* or limited approaches that are either at odds with commonsense reasoning or are compatible only in a general limiting sense—but not at specific fixed non-unity premise conditional-probability thresholds. Simple numerical experiments were conducted verifying this improvement. SOPL—and its extension to fuzzy logic—is based on the concept of the posterior-averaged deduction level (PADL). PADL has been derived by integrating, in a new way, three mathematical tools: second-order probability theory, Boolean conditional event algebra, and one-point random set coverage representations of fuzzy logic, the latter leading to deductive treatment of natural language descriptions and operators. The work was accomplished in conjunction with efforts by Prof. H. T. Nguyen (at SSC San Diego as a Summer American Society for Engineering Education [ASCEE] fellow) from New Mexico State University and interaction with Dr. R. P. Mahler (Lockheed-Martin, Eagen, MN).

SUMMARY

Deduction, or logical reasoning, apropos to a data-fusion setting, is the third general aspect (usually in temporal sequence) of the basic trilogy—(hypotheses testing; estimation and confidence setting; and deduction)—that we will call pre-action, comprising the basic analysis leading to decision-making actions. This analysis is often carried out with uncertainty present, relative to both newly arriving and prior multisource-, multisensor-based information. Such (arriving and prior) information typically contains both linguistic-based and probability-based aspects. In addition, the prior information often contains not only unconditional but conditional or relative information in the form of inference rules with differing antecedents. Thus, in light of the Navy's fundamental goal of improving its data-fusion capabilities, a comprehensive and applicable theory of pre-action operating upon such varying types of information is most desirable.

Unfortunately, prior to the onset of Artificial Intelligence and Fuzzy Logic, theories of pre-action were necessarily restricted to operating only on probabilistic-based information. Consider the case where a general theory of probability-based optimal hypotheses testing (such as in [1] or parts of classic texts such as [2]) and probability-based optimal estimation and confidence setting (such as [3] or Rao's famous treatise [4]) are available, with on-going research extending these results further (such as perusal through any recent issues of *Mathematical Reviews* will show): even there, the

theory of classical logic deduction as it stands is not at all integrated with probability. (See, e.g., any of a number of elementary textbooks on classical logic deduction, such as [5] or [6]—where, in the case of the latter, there is a section on probability, but no attempt to relate it directly with deduction!) Moreover, this disconnect at the unconditional level has exacerbated the problem of integrating, in a natural manner, classical logic deduction applied to conditional statements with possibly differing antecedents (usually via the so-called material conditional operator, the only one of the 16 classical or Boolean binary operators that reasonably models conditional statements) and conditional probability evaluations of uncertain information.

In fact, one of the three mathematical tools leading to PADL (and SOPL), conditional event algebra, was originally developed to address this issue, analogous to the role an ordinary Boolean algebra or, equivalently, classical logic of propositions, plays with respect to all unconditional probability evaluations over it. (See, e.g., [7] or [8].) Later, Goodman and Nguyen [9] extended this idea further by showing that such conditional event algebras could be established in a fully Boolean setting, compatible with the standard construction in probability theory of a product probability space formed out of a countable infinity of (unconditional) probability spaces. Consequently, these conditional event algebras could be used to (1) extend to conditional probabilities and conditional events in a natural way *all* of the standard unconditional relations involving probabilities and unconditional events, such as that of the probability of a disjunction of events expanded out as an alternating signed sum of the probability of the various subconjunctions of the events; laws of large numbers; central limit laws; and estimation and hypotheses testing, among others; and (2) establish novel uses applicable to Artificial Intelligence and related areas, such as determining similarities/dissimilarities and consistency/inconsistency of inference rules. (See, e.g., [10], part 3.) Still further use of Boolean conditional event algebra was brought about in FY 99 by applying it directly to establish a unified conditional probabilistic and Boolean conditional event algebra setting for *all* three components of pre-action, especially for deduction. (See [11], sections 3.1 and 4.)

Another mathematical tool contributing critically to the development of SOPL is that of the one-point random set coverage representation of fuzzy logic. (See, e.g., [12] and more recently [13].) In general, this tool shows that any model based on first-order fuzzy logic (which is essentially the level considered here) can be shown mathematically equivalent to a collection of corresponding probability evaluations involving the one-point coverage function of random sets (the weakest natural way to partially describe random sets, analogous to the way that expectation weakly describes a random variable). A basic consequence of this is that linguistic-based and probability-based information may be fully integrated as probability-only information, with appropriate introduction of multiple-choice random sets. (See, e.g., [14] on using random sets in fuzzy logic.) Additional use of one-point random set coverage representation of fuzzy logic was started in FY 99 by applying it to extend PADL in the previously mentioned Boolean conditional event algebra format to include linguistic-based information. (See [11], sections 3.2 and 4.)

Finally, unlike the two previously mentioned mathematical tools, developed completely at SSC San Diego under the ILIR program, the third key factor in deriving PADL, and hence SOPL, is that of second-order probability theory, which until recently was simply an obscure branch of probability theory, useful in certain restricted applications. (For a thorough treatise on second-order probability and its previous applications, see the text of Aitchison [15].) Second-order probability theory is concerned with probabilities or distributions of probabilities and the consequences of such. (See also

Goodman & Nguyen [16] for an application to information updating.) During FY 99, the following observations and assumptions were made leading to PADL (although hints of this process were recognized but not fully acted upon in FY 98):

The first step was to recognize that commonsense reasoning involving conditional expressions with uncertainty present—where each such expression separately can be reasonably measured by a conditional probability—generally extends a corresponding classical logic deductive expression with no uncertainties and with a fixed pattern of events making up the premise and potential conclusion. For example, consider the deduction class, *transitivity-syllogism* that in commonsense reasoning has the form of Premise: ["If c, then b," "If b, then a"] and Conclusion: ["If c, then a"], where, in general, there may be some uncertainty in the validity of each if–then statement, because of obvious exceptions to the rule or uncertainty in the relations stated. In conditional probability form, the premise becomes $[P(b|c) = s, P(a|b) = t]$, where one may well have in place of the equalities in the premise, inequalities (of the form $\geq$) relative to any reasonable choice of thresholds s, t in the unit interval. The potential (but not necessarily actual) conclusion can take the form $[P(a|c) = f(s,t)]$, where function f is to be determined in some best sense, so that the potential conclusion can be a real conclusion according to the laws of probability theory and basic reasoning at the metalevel. However, one can easily show (see, e.g., [11], section 5 as well as Pearl's comments on this key issue throughout [17]) that probabilities P exist for which $P(a|b)$, $P(b|c)$ are less than unity—although quite close to it—yet $P(a|c)$ is very low or actually zero! On the other hand, commonsense reasoning tells us that: "on the average, everything else being equal," $P(a|c)$ should be high, approximating the classical logic relation or the conditional-probability form closest to it, i.e., where, in effect, all conditional probabilities involved being unity allows for a valid deduction relation. The classical logic counterpart of transitivity-syllogism is originally attributed to at least Aristotle or earlier in its pure classical-logic-no-uncertainty form of premise ["If c, then b," "If b, then a"] and conclusion ["If c, then a"]. (See, e.g., [18] for a detailed history of this pattern of deduction.)

The second and most critical step was to interpret the fragment "on the average, everything else being equal" as applying to the fixed pattern of events involved in both premise and potential conclusion and varying the Ps uniformly over all possible choices, subject to the constraints generated by the premise thresholds (s, t in the transitivity-syllogism example).

The third and final step was to compute the average or expectation of the resulting possible conclusion probabilities as the Ps move randomly as above. Thus, in the example, one computes the expectation of $P(a|c)$ subject to constraints $P(a|b) = s$, $P(b|c) = t$, where P is considered in some sense a random variable (more properly, a random vector relative to the atoms derived from events, a, b, c). Mathematically, this means we need to consider the second-order probability distribution of the Ps—which is a uniform one—subject to the allowable constraints generated by the premise, and its effect on the computation of the mean of P of the given conclusion conditional in the form of its mean (at the second order). This is the essence of PADL, and in turn, SOPL.

All of the above, set in a completely rigorous framework, leads to computations for a wide variety of types of deduction schemes, agreeing with the common-sense reasoning counterpart (from both informal extensive polls of individuals queried and inspection of the forms). The expectations themselves, for even relatively simple-appearing deductions such as transitivity-syllogism (although creating a formidable open issue in the literature—again see [11]), can result in rather complicated,

but closed-form expressions of PADL. (In the case of transitivity-syllogism, this takes the form of the simple expression $st + (1 - t)/2$ minus a correction term, which is in the form of a more complicated rational polynomial in s and t. (See [11], sections 5 and 6 for more details.)

Comparing PADL and SOPL with previous approaches to conditional-probabilistic deduction only shows work concerned with the more restrictive case of premise conditional-probability thresholds actually approaching unity (such as the maximum entropy approach of [19] or attempts to deal with the fixed-threshold-value case by extremal approaches, rather than averaging techniques, most typified by Adams' *minimum conclusion function* [20, 21], in effect, replacing PADL by picking out that single probability measure satisfying premise constraints that *minimizes* the consequent (conditional or unconditional) probability in the simple case of one conclusion component. In turn, when in the limit, the premise-probability-thresholds-approaching-unity uniformly implies that the conclusion probability does also. Adams dubs this as *high probability deduction*. The essential drawback here, despite the widespread use of his approach and its generalizations (called ε-calculi—see [17] again) is that a number of commonsense deduction schemes are invalid relative to this criterion, including transitivity-syllogism.

Returning to the general problem of constructing a satisfactory universal theory of pre-actions in data fusion, it is readily seen that FY 97 work was directed to the first or hypotheses-testing aspect, using not only Boolean conditional event algebra, but also an extension of it, relational event algebra, which plays a role relative to general functions of individual unconditional probabilities of events analogous to Boolean conditional event algebra's role relative to arithmetic division of individual unconditional probabilities (with a suitable nesting restriction of relevant events). (A good summary of this direction of work, based on critical use of probability metrics and their computations via Boolean conditional event algebra is found in [10], section 3.) FY 98 work was directed toward the second or estimation and confidence-setting aspect, in which random set theory proper was used to produce a general way of algebraically combining information, once the hypotheses-testing aspect determines such a combination is appropriate. Documentation can be found in [22, 23]. Numerical experiments related to hypotheses testing for similarity of models and algebraic combining of information can be found in [24]. Thus, FY 99 was a fundamental continuation of previous work in attempting finally to deal with the third part of a general theory of pre-actions, namely, deduction.

Finally, in addition to the successful commencement of SOPL, mention should be made of the related but independent work of Bamber [25], who also considers second-order probability, but only in the more restrictive limiting-premise threshold case, for which he has derived rather deep results fully characterizing this case in algebraic terms and relating it to other limiting-premise threshold work, such as that of [26]. ILIR work in FY 00 is expected to combine both Bamber's and this investigator's efforts in a unified deduction approach applicable to both fixed-nontrivial-premise thresholds and the unity-limiting case.

REFERENCES

1. Lehmann, E. L. 1959. *Testing Statistical Hypotheses,* John Wiley, New York, NY.

2. Wilks, S. S. 1963. *Mathematicla Statistics,* John Wiley, New York, NY.

3. Gelb E. (ed.). 1974. *Applied Optimal Extimation,* MIT Press, Cambridge, MA.

4. Rao, C. R. 1973. *Linear Statistical Inference and Its Applications,* 2nd Edition, John Wiley, New York, NY.

5. Bergmann, M., J. Moor, and J. Nelson. 1980. *The Logic Book*, Random House Publishers, New York, NY.

6. Copi, I. M. 1986. *Introduction to Logic*, 7th Edition, MacMillan, New York, NY.

7. Calabrese, P. G. 1987. "An Algebraic Synthesis of the Foundations of Logic and Probability," *Information Sciences*, vol. 42, pp. 187–237.

8. Goodman, I. R., H. T. Nguyen, and E. A. Walker, 1991. *A Theory of Measure-Free Conditioning*, North-Holland, Amsterdam, Holland.

9. Goodman, I. R. and H. T. Nguyen. 1995. "Mathematical Foundations of Conditionals and Their Probabilistic Assignments," *International Journal of Uncertainty, Fuzziness, & Knowledge-Based Systems*, vol. 3, no. 3, (Sept), pp. 247–339.

10. Goodman, I. R., R. P. Mahler, and H. T. Nguyen. 1997. *Mathematics of Data Fusion*, Kluwer Academic, Dordrecht, Holland.

11. Goodman, I. R. 1999. "A Decision-Aid for Nodes in Command and Control Systems Based on Cognitive Probability Logic,*" Proceedings of the 1999 Command and Control Research and Technology Symposium*, vol. 2, pp. 898–941.

12. Goodman, I. R. and H. T. Nguyen. 1985. *Uncertainty Models for Knowledge-Based Systems*, North-Holland, Amsterdam.

13. Goodman, I. R. and G. F. Kramer. 1997. "Extension of Relational and Conditional Event Algebra to Random Sets with Applications to Data Fusion," *Random Sets: Theory & Applications* (J. Goutsias, R. P. Mahler, and H. T. Nguyen, eds.), Springer–Verlag, New York, NY, pp. 209–242.

14. Goodman, I. R. and H. T. Nguyen. 1999. "Application of Conditional and Relational Event Algebra to the Defining of Fuzzy Logic Concepts," *Proceedings of the SPIE Conference on Signal Processing, Sensor Fusion, and Target Recognition VIII,* vol. 3720, pp. 25–36.

15. Aitchison, J. 1986. *The Statistical Analysis of Compositional Data*, Chapman & Hall, London, U.K.

16. Goodman, I. R. and H. T. Nguyen. 1999. "Probability Updating Using Second Order Probabilities and Conditional Event Algebra," *Information Sciences*, vol. 21, pp. 295–347.

17. Pearl, J. 1988. *Probabilistic Reasoning in Intelligent Systems: Networks of Plausible Inference,* Morgan Kaufmann, San Mateo, CA.

18. Prior, N. et al. 1967. "History of Logic," *Encylopedia of Philosophy* (P. Edwards et al., eds.), Macmillan, New York, NY, vol. 4, pp. 513–571.

19. Goldszmidt, M., P. Morris, and J. Pearl. 1993. "A Maximum Entropy Approach to Non-monotonic Reasoning," *IEEE Transactions on Pattern Analysis & Machine Intelligence*, vol. 15, no. 3, (March), pp. 220–232.

20. Adams, E. W. 1975. *The Logic of Conditionals,* D. Reidel, Dordrecht, Holland.

21. Adams, E. W. 1996. "Four Probability Preserving Properties of Inferences," *Journal of Philosophical Logic*, vol. 25, pp. 1–24.

22. Goodman, I. R. 1998. "Application of Fréchet and Other Random Set Averaging Techniques to Fusion of Information," *Proceedings of the SPIE Conference on Signal Processing, Sensor Fusion, and Target Recognition VII,* vol. 3374, pp. 108–118.

23. Goodman, I. R. and H. T. Nguyen. 1998. "Adams' High Probability Deduction and Combination of Information in the Context of Product Space Conditional Event Algebra," *Proceedings of the International Conference on Multisource-Multisensor Information Fusion (Fusion '98),* Las Vegas, NV, pp. 1–8.

24. George, M. J. and I. R. Goodman. 1999. "Numerical and Implementational Studies of Conditional and Relational Event Algebra, Illustrating Use and Comparison with Other Approaches to Modeling of Information," *Proceedings of the Second International Conference on Information Fusion*, pp. 273–280.

25. Bamber, D. 2000. "Entailment with Near Surety of Scaled Assertions of High Conditional Probability," *Journal of Philosophical Logic,* vol.29, pp. 1–74.

26. Goldszmidt, M. and J. Pearl. 1991. "System Z+: A Formalism for Reasoning with Variable Strength Defaults," *Proceedings of the Ninth National Conference on Artificial Intelligence (AAAI'91)*, vol. 1, pp. 399–404.

Principal Investigator:
Dr. I. R. Goodman   ZU58
D44215
(619) 553-4014
goodman@spawar.navy.mil

Integration of Complex Information

Objective(s): Define a mechanism to allow the integration and use of complex non-specified information. The method explored uses open hypermedia architectures and lightweight inference to manage and use information.

Accomplishment(s): Representations of military plans and intelligence in hypermedia were investigated. Languages for representing semantic networks were researched, and Prolog was chosen as a language to represent the knowledge held in the open hypermedia base. Rules for translating hypermedia into Prolog were developed, and sample hypermedia translations were performed. The design of an interface module to an existing open hypermedia system was begun.

Command and control involves three fundamental processes that fit together in a tight cycle. Situation analysis provides the context on which to act. Decisions are made based on the analysis results. These decisions constitute planned movements, engagement orders, and many other possible actions. Decisions must be communicated to those who are to carry out the actions. The results of these actions are observed and folded into a new situation analysis.

As command, control, communications, computers, intelligence, surveillance, and reconnaissance (C4ISR) systems have evolved, system integration has been the general theme. Stand-alone systems, each with its own database, were first interfaced to allow some transfer of data. Data-management schemes were implemented to provide some consistency among databases and operational units. System federation gradually allowed multiple applications to run on users' workstations, thus preventing the need for specialized hardware and support software for large numbers of individual systems. The current state of system integration not only allows multiple applications to share hardware, operating system, and network platforms, but also uses a layered service architecture to eliminate redundancy of some capabilities.

The evolution of system integration has broadened the stovepipes that were so narrow in previous system generations. The resulting view is of a few very broad systems made up of many small applications, any of which may be accessible through the workstation in front of the user. Some applications can work on common data managed through centralized services. However, many categories of data still form separate stovepipes since they are maintained in separate data servers due to their differing technical natures and programmatic backgrounds. The users then must associate the tactical situation shown in one application with the results of a logistical query conducted through another.

INFORMATION COMPLEXITY

The focus on systems integration ignores the true goal in decision support. It is the information that is of ultimate value to the decision-makers. Integrating the information is the next step. However, military information is not a simple matter of collecting and crunching sales and inventory figures from various branch offices as found in data warehousing applications. The domain of the military environment is complex. The variety of concepts, events, and situations that can be described subjectively or measured and reported objectively is probably limitless. No ontological study can *a priori* determine all of the possible data types needed to describe the military environment. Therefore,

information integration is not going to be completely accomplished through bringing all data into a relational or object database.

A PATTERN OF ANALYSIS

In researching the requirements for an intelligence support system for the Defense Intelligence Agency (DIA), a pattern of analysis was uncovered that was common to what has been used in some other domains. The primary feature of this pattern is that an analyst's role is to create associations among existing data. An analyst rarely creates data but searches, filters, and reviews all available information. As analysts work, they form networks of related information.

Current practice has DIA intelligence analysts spending a portion of their time building up a private model of their area of expertise. The remainder of their time is spent responding to queries from DIA's various customers. The responses typically take the form of linear essays. Analysts also periodically produce background reports on particular matters of interest. These reports also take a strictly linear book-like form, even when delivered over a computer network.

The results of the current approach included the following problems:

- The products were static or updated on a paper publishing timeframe.
- Customers with local information could not share information with others.
- Only a particular question was answered, even if it was not the correct question.
- Analyst turnover causes a large loss of knowledge.

As a result of these insights, work was initiated to find a way to record the knowledge being built by the intelligence analyst and to communicate this knowledge to intelligence consumers. The goal was to move away from the linear essay and its strict segregation of reader and writer roles to a more collaborative method of communication that would allow for a continuous update of the knowledge jointly held between the intelligence agency and its customers.

RECORDING DECISIONS

Decisions also take the form of associations among data or information elements. A classic example may be the order for a surface combatant to engage a hostile aircraft. The decision-maker did not create the aircraft or the positional and attribute data held on that aircraft. Likewise, the surface combatant's information was not generated by the decision-maker. The value added by the decision-maker is that an engagement relationship (perhaps with other amplifying information) should exist between the two.

As the data on the two combatants change, the association must be reviewed but is not necessarily invalidated. Likewise, a reversal of the decision changes the relationship among the combatants but does not change any of their individual data. This fundamental distinction between the structural representation of the associations among concepts or real-world objects and the content that describes them is common between the knowledge created by analysts and decision-makers.

USING THE KNOWLEDGE

The intelligence analysis tool built for DIA allows for the storage and retrieval of information from the knowledge base. If this technique is to be used for command and control, the knowledge held in

the structure of the hypermedia must be able to be extracted and used. This knowledge can best be described in terms of properties. Some simple properties regarding connectedness and reachability have been defined for the hypermedia. More complex domain-specific properties regarding command and control will be defined using these primitive properties. Inference capabilities will then be added to allow new properties to be inferred and communicated to users.

Two methods of inference will be standard. The first will translate the hypermedia into a form available for processing with Prolog. This method has the benefit of being easily accomplished and will serve as a comparison for domain-specific lightweight inference techniques. The downside of using Prolog is that inference in the general case is undecidable without domain-specific heuristics. Prolog programs generated from hypermedia may never terminate. The second method to be studied involves the use of domain-specific lightweight interference.

Principal Investigator:
Douglas S. Lange
D4223
(619) 553–6534
dlange@spawar.navy.mil

ZU66

Speech Enhancement in High-Noise Environments

Objective(s): Investigate a recently reported advance in speech-enhancement technology and attempt to replicate and verify the results with respect to its ability to improve the intelligibility of speech signals degraded by severe random noise.

Accomplishment(s): This 1-year project independently implemented a new noise-suppression algorithm from a Greek effort [1, 2] that claimed the algorithm greatly increased the intelligibility of speech degraded by severe random noise. No one had claimed such large gains before. Our formal tests failed to show similar improvements to those reported. There was a small improvement in the more severe (–5-dB highway [HWY]) signal-to-noise (SNR) condition, but the algorithm actually degraded the intelligibility for signals with better (0-dB flat white noise [FWN]) SNR. There are difficult problems that limit the accuracy of the noise floor estimation. Any estimation errors result in an inappropriate spectral subtraction processing, which can actually add extra distortion to signals that are already only marginally intelligible. For signals more overwhelmed by noise, the current algorithms' processing did help more than it hindered, though only slightly.

BACKGROUND

The algorithmic approach is based on reducing the processing artifacts seen in the usual spectral subtraction by suppressing only the audible portion of the noise. The estimate of the specifics of just what is, in fact, the audible portion of the spectrum is based on a model of human perception.

The standard Diagnostic Rhyme Test (DRT) test corpus for speech intelligibility was corrupted by different noise conditions and then "cleaned" using this new algorithm. The intelligibility of the "cleaned" speech was compared to that for the corrupted speech. The most critical portion of this effort was in the correct performance of these formal tests.

During this investigation, it was found that a large part of the reported improvement was possibly due to the fact that the Greek researchers had worked with an unusually wide bandwidth for severe-noise corrupted speech. They worked with a bandwidth of 8 kHz, whereas 4 kHz or less is more typical in that domain. Even if their algorithm reduced BOTH the speech and noise above 4 kHz, they would still get considerable intelligibility improvements. Once this situation was discovered, the remainder of the investigation was focused on finding whether this "surgical" spectral subtraction approach could actually improve intelligibility in random noise in the more realistic domain of typical communications-channel bandwidth.

SUMMARY

Speech signals are often degraded by noise—many signals become unintelligible. Current algorithms are very effective against interfering tones and many types of impulse noise. Some algorithms also have been successful at reducing stationary noise, such as that generated by motors near a microphone. Since these noises are consistent and predictable, they are easier to correct than random noise.

Until recently, no one had claimed any significant improvement in intelligibility for speech covered by random, flat-spectrum communications-channel noise or even random shaped-spectrum noise.

The most effective noise-enhancement approach has always been the (somewhat heavy-handed) spectral subtraction pioneered by Dr. Steven Boll [3]. This approach arbitrarily subtracts some portion of the estimated noise from the corrupted signal. This is done in the same manner throughout the entire spectrum, changing every part, and it results in significant distortions and artifacts. The resultant "cleaned" speech sounds more acceptable to listeners, but the signal is no more "readable" (no more intelligible), probably due to these processing distortions. Essentially, the increased distortion artifacts offset any potential gain.

At EuroSpeech '97, Tsoukalas, Mourjopoulos and Kokkinakis, of the Wire Communications Laboratory at the University of Patras, Greece, presented work claiming significant improvement in speech intelligibility. They followed it with a journal publication in the *IEEE Transactions on Speech and Audio Processing* in November 1997 [2]. Their approach was based on an attempt to suppress more "surgically" only the audible portion of the noise by using a model of human perception as a guide.

Much of the noise in an audio environment is actually inaudible to humans due to some unique features and limits of human perception. Noise near prominent frequency peaks is inaudible due to adjacent-frequency masking. Some other portions of noise are inaudible due to the background masking effects of the (time, amplitude, and frequency varying) perceptual noise "floor." The idea of this perceptual approach is to only change those portions of the spectrum where the noise rises above these perceptual limits, and to subtract only enough to drop the noise below these limits. This results in far fewer and smaller processing changes to the data. The expectation is that there will be gains in acceptability similar to those of traditional methods, but that these more delicate and precise adjustments will result in significantly less processing distortion. The hope is that the improvement would suffer less offsetting distortion, thus giving a net gain over the older methods.

The Greek researchers reported large improvements as measured by the Diagnostic Rhyme Test, which is a standard measure of intelligibility in the speech community. They also played some demonstration audio at the EuroSpeech '97 conference that sounded convincing to many experienced listeners.

Dr. Bill Voiers [4, 5] created the DRT in an attempt to better measure intelligibility and "diagnose" specific areas of difficulty. He refined the rhyme tests of Fairbanks [6] to create word pairs whose only differences are the leading consonants. Examples might be "hit-fit" or "rat-cat," etc. Test subjects choose which of the pair they heard. The test score is the percentage correct. In addition, the test scoring attempts to classify (diagnose) any problems along the dimensions of voicing, nasality, sustension, sibilation, graveness, and compactness. Dr. Voiers formed a company, Dynastat, Inc., which is the premier testing group used by commercial activities, but far too costly for this effort. We used one of the several other research facilities with the ability to perform the test.

APPROACH

This ILIR project attempted to independently implement the Greek algorithm and verify the results. Verifying the results requires elaborate, formal testing, preferably by an independent group. These tests require considerable experience, appropriate equipment, sound isolation booths, and a pool of subjects. The testing was subcontracted to an experienced team headed by Dr. John Hansen, the

Associate Director of the Robust Speech Processing Laboratory at the University of Colorado at Boulder. Dr. Hansen also acted as an additional technical resource and advisor to the overall project.

Dr. Hansen's team used the standard DRT test corpus, corrupted with two kinds of random noises to form the "noisy" test sets. The team also used these same corrupted speech sets, after "cleaning" by the algorithm, as the "enhanced" test sets. Five listeners were recruited for the DRT test, and they listened to randomized selections from 116 word-pairs. The test took approximately 3 hours for each listener. Three of the listeners were native American speakers, and two were non-native speakers. (The original researchers tested native speakers in Greek and non-native speakers in English).

A pilot evaluation was done with two listeners to flat white noise (FWN) at 5-dB SNR and highway noise (HWY) at 0-dB SNR. Because of the different spectral balances of these two conditions, they actually suffer about the same amount of perceptual degradation. These levels produced too many correct responses (the speech was not corrupted enough to produce intelligibility errors). The test team decided to drop the SNR levels for both noise types by 5 dB before having all five listeners run through the complete test.

RESULTS

This investigation found that a large part of the Greeks' reported improvement was possibly due to the fact that they worked with an unusually wide bandwidth for severe noise-corrupted speech. They worked with a bandwidth of 8 kHz, whereas 4 kHz or less is more typical in that domain. This 4-kHz bandwidth restriction is normally used because the human perceptual system reacts to the total random noise power. Most of the critical speech information is in the lower 4 kHz (roughly the bandwidth of telephone communications). White noise is equally distributed throughout the frequency band, so cutting the bandpass down from 8 kHz to 4 kHz cuts the total noise in half, while losing little of the critical speech. This is a great intelligibility boost in itself, and the researchers would be able to report great results even if their algorithm reduced BOTH the speech and noise above 4 kHz.

Once this unusual bandwidth was uncovered, the remainder of the investigation was refocused on finding whether this "surgical" spectral subtraction approach could improve intelligibility in random noise in the situation of more typical communications channels. The DRT tests found that there was a small improvement in highway noise (−5-dB SNR), but that the algorithm actually degraded intelligibility for a white-noise channel with better quality (0-dB SNR).

Table 1 shows that our test results did not approach the improvements originally reported (table 2), particularly the nearly doubling for the −5-dB SNR enhancement.

Table 1. ILIR DRT test results, 1999.

Degraded/Enhanced	Score (%)	Error (%)
FWN 0 dB	77.241	9.707
FWN 0 dB enhanced	73.793	9.553
HWY −5 dB	88.275	7.456
HWY −5 dB enhanced	90.345	6.520

Table 2. Tsoukalas, Mourjopoulos, and Kokkinakis (1997) DRT scores.

Degraded/Enhanced	Score (%)	Error (%)
Pink 0 dB	72.22	18.5
Pink 0 dB enhanced	77.78	14.8
Pink –5 dB	33.33	16.7
Pink –5 dB enhanced	61.11	22.2

CONCLUSIONS

The results of this investigation show that the new algorithm does not perform significantly better than the traditional methods. Most of the originally reported improvement appears to be due to the reduction in high-frequency noise that is not present in typical noisy voice communication channels, which do not include such frequencies.

There is a growing interest in perceptual-based processing in the speech community, so this approach may yet yield the hoped-for result if some of the technical problems can be solved. Already, the problems and potentials of this approach have intrigued Ruhi Sarikaya, a graduate student at the University of Colorado. He published a paper at EuroSpeech '99 that included a clever codebook scheme as one approach to more consistent perceptual threshold calculations. There are difficult noise-floor estimation problems that are still unresolved. These estimation errors result in inappropriate spectral subtraction processing and can actually add distortion to signals that are already marginally intelligible. For signals with one type of noise, the current algorithms' processing helped more than hindered, but the improvement was minor.

REFERENCES

1. Tsoukalas, D. E., J. Mourjopoulos, and G. Kokkinakis. 1997. "Improving the Intelligibility of Noisy Speech Using an Audible Noise Suppression Technique," *EuroSpeech '97*, pp. 1415–1418.

2. Tsoukalas, D. E., J. Mourjopoulos, and G. Kokkinakis. 1997. "Speech Enhancement Based on Audible Noise Suppression," *IEEE Transactions on Speech and Audio Processing*, vol. 5, no.6, pp. 497–514.

3. Boll, S. F. 1979. "Suppression of Acoustic Noise in Speech Using Spectral Subtraction," *IEEE Transactions on Acoustics, Speech and Signal Processing,* vol. 27, pp. 113–120.

4. Viers, W. D. 1977a. "Diagnostic Evaluation of Speech Intelligibility," *Speech Intelligibility and Speaker Recognition* (M. Hawley, ed.), *Benchmark Papers in Acoustics*, Dowden, Hutincton, and Ross, Stroudsberg, vol. 11, pp. 374–387.

5. Voiers, W. D. 1977b. "Diagnostic Accepability Measure for Speech Communications Systems," *Proceedings of the IEEE International Conference on Acoustics, Speech, and Signal Processing (ICASSP)*, pp. 204–207.

6. Fairbanks, G. 1958. "Test of Phonemic Differentiation: The Rhyme Test," *Journal of the Acoustical Society of America*, vol. 30, no. 7, pp. 596–600.

7. Sarikaya, R. and J. H. L. Hansen. 1999. "Auditory Masking Threshold Estimation for Broadband Noise Sources with Application to Speech Enhancement," *EuroSpeech '99*, pp. 2571–2574.

Principal Investigator:
Ralph R. Johnson
D44213
(619) 553–3653
rjohnson@spawar.navy.mil

ZU84

COMMUNICATIONS

Telesonar Channel Models

Objective(s): Understand undersea acoustic communication channels via theoretical and numerical modeling of the propagation physics.

Accomplishment(s): A physics-based numerical propagation model that includes the effects of multipath spread and Doppler spread has been developed as a prediction and analysis tool for underwater acoustic communication problems. The model uses three-dimensional Gaussian beams and quadrature detection to obtain the channel response for finite-duration, constant-wavelength tones. By using a very short pulse, the output of the quadrature detector provides an estimate of the channel impulse response, which may be used to determine the multipath spread. In addition, the Doppler shifts associated with source/receiver motion can be accumulated for the individual beams, providing Doppler spread. The model has been productively used in experiment planning and channel data analysis for several telesonar sea tests. A statistics-based, real-time channel emulator has also been developed. The use of the physics-based, impulse-response predictions with the emulator provides a powerful tool for testing and developing underwater acoustic modems and sonar systems.

SUMMARY

Telesonar is undersea acoustic signaling for data telemetry, wireless networks, remote control, feedback links, ranging, and beaconing. Telesonar technology incorporates modern digital signal processors (DSPs) and digital communications theory to combat the deleterious aspects of the physical channel and to exploit advantageous channel features. Acoustic communication signals propagating through a shallow-water environment may be adversely affected by the phenomena of multipath spread and Doppler spread (see figure 1). The multipath spread is caused by the complex multipath propagation characteristic of shallow-water waveguides, including such effects as refraction, multiple reflections from boundaries, and scattering from inhomogeneities. The Doppler spread results from the time-variability of the acoustic medium, arising primarily from source/receiver motion or surface boundary motion. These phenomena can significantly disperse and distort the signal as it propagates through the channel. A numerical propagation model that simulates these effects is desired for the systematic study of these phenomena. Such a model is also a useful tool for environment-dependence assessment, performance prediction, and mission planning of telesonar systems.

In this project, the modeling philosophy is based on a three-stage approach. Stage-1 is a physics-based numerical propagation model built upon the construct of multiple Gaussian beams radiating from the mobile transmitter in three dimensions, refracting through the layered medium, and interacting with channel boundaries. Stage-1 output is a representative time-variant, quadrature-detector (QD) (an analog of the discrete Fourier transform) response of the nonstationary channel, along with inferred channel characteristics such as coherence time, coherence bandwidth, multipath spread, and Doppler spread. Stage-2 is a time-dependent simulation implemented as a Markov process. The QD response and underlying channel characteristics obtained from Stage-1 initiate and statistically govern Stage-2. Stage-3 involves superposition of measured or simulated channel noise, including co-channel network multiple-access interference (MAI) and jammers.
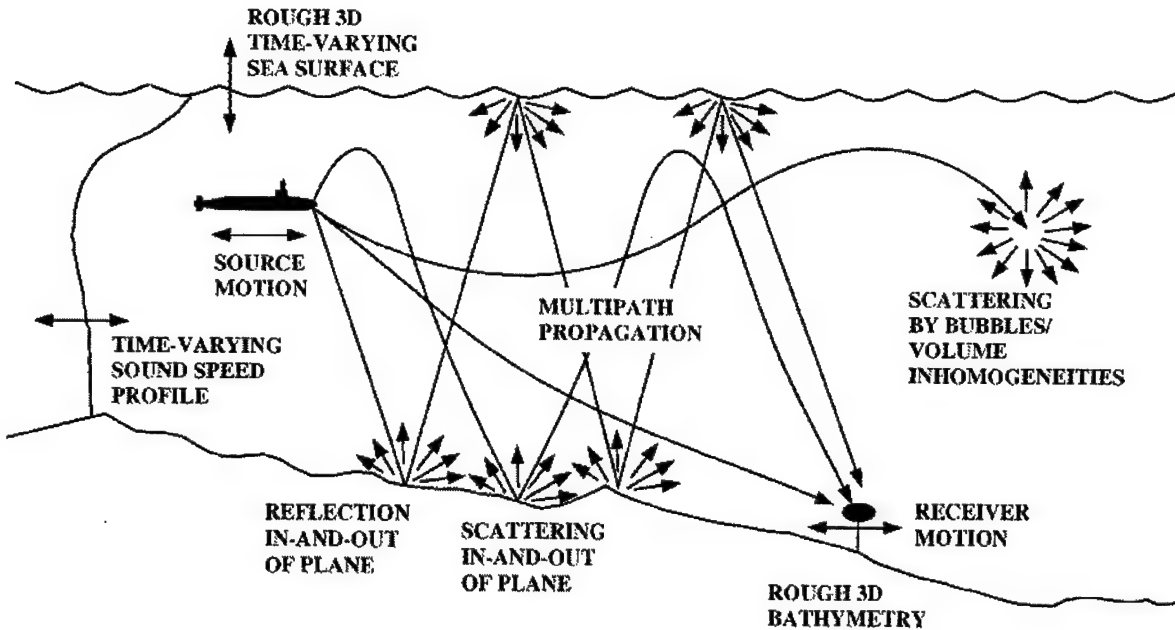
Figure 1. Important physical processes affecting underwater acoustic communications signals.

The approach for Stage-1 is to trace, in three dimensions, closely spaced microbeams of a finite-duration, constant-wavelength pulse from source to receiver, accumulating travel-time, level, phase-shift, and Doppler-shift information for each microbeam [1]. This information is used to construct the QD response for each microbeam. The QD response provides a prediction of the levels and arrival times associated with the various propagation paths from the source to the receiver. The total QD response is then obtained by summing the QD responses of all component microbeams. By using a very short pulse, the output of the QD represents an estimate of the channel impulse response, which may be used to determine the multipath spread. Three-dimensional Gaussian beam tracing [2] is used so that out-of-plane reflections from rough surfaces or sloping bathymetry can be adequately modeled. The use of a dense fan of Gaussian microbeams allows direct modeling of scattering from arbitrarily rough surfaces. Currently, the model includes multipath spread associated with the propagation through a refractive medium and the reflection and scattering of energy from an arbitrarily rough three-dimensional seafloor. Doppler spread resulting from source-receiver motion is included at present, and future implementations will include the effects of a time-varying sea surface.

The Stage-1 model has been successfully used to predict multipath spread, thus aiding in the design of recent experimental configurations (Sublink '99 [3], ModemEx '99 [4], Seaweb '99 [3], Modem-Demo-'99, FRONT-1, and a Swedish Defense Research Establishment (FOA) experiment in the Baltic Sea [5]). For Sublink '99, ModemDemo '99, and the Baltic experiment, simulated impulse responses agreed well with measured impulse responses in most cases, although loss assumptions had to be adjusted because of inadequate knowledge of bottom properties.

An example of the agreement between modeled and measured impulse responses is provided for ModemEx '99, which occurred in April 1999 in a shallow water region (~200 m) 6 km southwest of San Diego. The data considered here were linear frequency modulated (LFM) chirps emitted from a source deployed at a depth of 30 m and recorded on a receiver mounted 6.7 m above the seafloor.

34

The source was deployed from a freely drifting ship, resulting in measurements as a function of time along a fairly constant track. The water depth at the receiver was 210 m, while the water depth decreased in a near linear fashion along the track to a depth of approximately 170 m at a range of 3.8 km from the receiver. The LFM chirps were transmitted sweeping the 8- to 16-kHz band over a 1-second period. Theoretically, the impulse response is a combination of these chirps delayed in time according to their path length and attenuated according to volume absorption and reflection loss at the boundaries. The impulse reponse can be estimated experimentally by correlating the received pulses with the original transmitted pulse. Figure 2 presents the resulting correlogram, which plots the replica correlation for consecutive LFM chirps (the 10-min gap starting at approximately 12.7 hours is a period where no datum was collected). A strong first path followed by a pair of later paths are clearly observed. A faint outline of later higher order multipaths is also observed. As the ship drifts to greater ranges, the groups of paths become less separated in time.
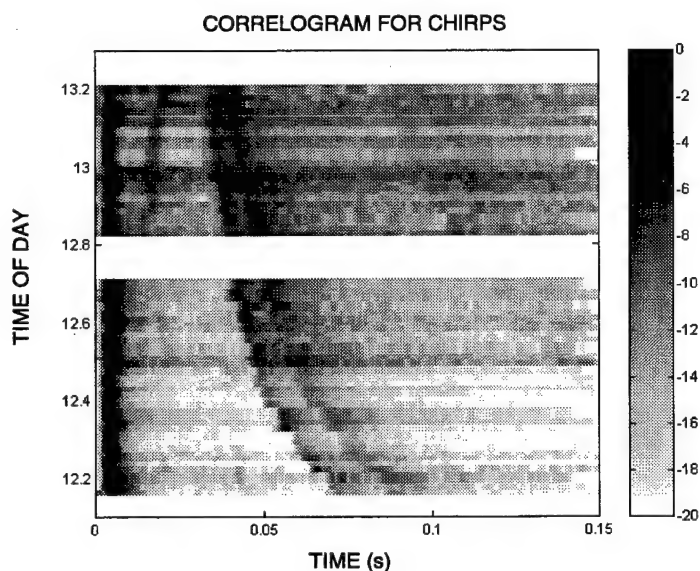
Figure 2. Correlogram showing the impulse response over a period of 1 hour.

Figure 3 compares the measured impulse response at a time of day of 12.5 hours (ping number 34) to a simluated response obtained via the Stage-1 model for the same source-receiver configuration. The source range at this time was 2.2 km. The simulation was performed assuming a flat bottom at a water depth of 210 m, and ignoring the effects of rough-surface scattering and time-variability. The measured impulse response has been normalized relative to the maximum, and the arbitrary time scale has been shifted to facilitate comparison with the modeled result. Note that the predicted arrivals agree well with the measured arrivals, indicating that refraction and reflection from boundaries are well-modeled. Any time dicrepancies between arrival paths may be caused by the neglect of the varying bathymetry or errors in the assumed sound-speed profile. The higher resolution of the model results indicates that the first arrival is actually a combination of several arrivals; namely, the direct path, the one-bottom-reflected path, the one-surface-reflected path, and the one-surface-reflected/one-bottom-reflected path. Likewise, the later arrivals are actually a combination of several higher order paths. Note also that the data exhibit a gradual rolloff after the arrival of the
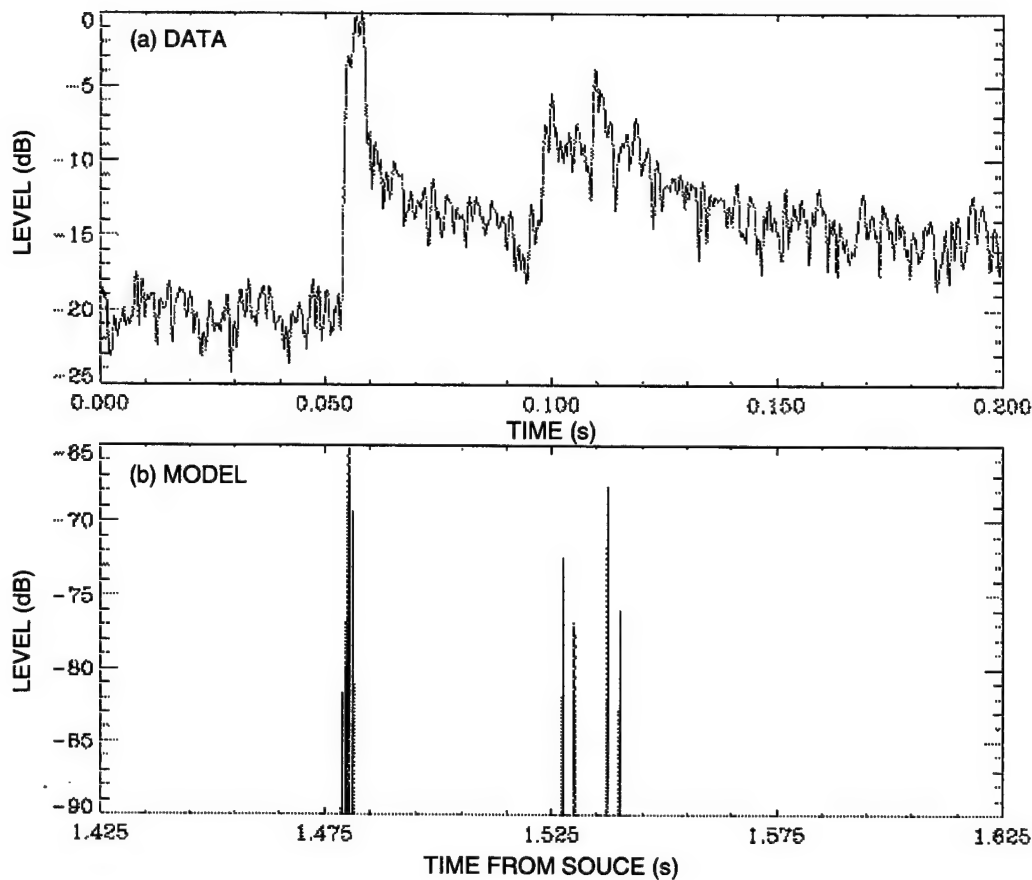
*Figure 3. Comparison between (a) measured and (b) modeled impulse responses.
Time of day = 12.5 hours. Source range = 2.2 km.*

pulses, suggesting a reverberant environment. The likely cause of this behavior is the scattering of energy in three-dimensions caused by the interaction of rays with the boundaries. Future work will attempt to model these interactions.

The Stage-2 model [6], developed by Dale Green of Benthos, Inc., in association with this project but under independent ONR sponsorship, is currently operational and has been used to simulate the performance of several underwater communications channels. Modeled impulse responses obtained by the Stage-1 model are supplied as input to this statistics-based, real-time channel emulator. The use of realistic physics-based, impulse-response predictions in conjunction with the emulator has greatly augmented at-sea data for the testing and development of underwater acoustic modems and sonar systems.

REFERENCES

1. Baxley, P. A., H. P. Bucker, and J. A. Rice. 1998. "Shallow-Water Acoustic Communications Channel Modeling Using Three-Dimensional Gaussian Beams," *Proceedings of MTS Ocean Community Conference*, vol. 2, pp. 1022–1026.

2. Bucker, H. P. 1994. "A Simple 3-D Gaussian Beam Sound Propagation Model for Shallow Water," *Journal of Acoustical Society of America*, vol. 95, no. 5 (May), pp. 2437–2440.

3. Baxley, P. A., H. P. Bucker, and J. A. Rice. 1999. "First Results from an Acoustic-Communications Transmission Model Using 3D Gaussian Beams and Quadrature Detection," *Journal of the Acoustical Society of America*, vol. 105, no. 2 (February), part 2, p. 1364.

4. McDonald, V. K., J. A. Rice, M. B. Porter, and P. A. Baxley. 1999. "Performance Measurements of a Diverse Collection of Undersea Acoustic Communication Signals," *Proceedings of the IEEE Oceans '99 Conference*, Seattle, WA, CD-ROM, Session 3F.

5. Baxley, P. A., H. P. Bucker, J. A. Rice, and M. D. Green. 1999. "Acoustic Communication Channel Modeling for the Baltic," *Proceedings of the IEEE Oceans '99 Conference*, CD-ROM, Poster Session.

6. Green, M. D. and J. A. Rice. 1999. "Statistics-Governed Channel Simulator," *Journal of the Acoustical Society of America*, vol. 105, no. 2 (February), part 2, p. 1365.

Co-Principal Investigators:

Paul Baxley
D857
(619) 553–5634
baxley@spawar.navy.mil

Joseph A. Rice
D857
(619) 553–3107
rice@spawar.navy.mil

ZU61

Co-Investigators:

Dr. Homer P. Bucker
D857
(619) 553–3093
bucker@spawar.navy.mil

Vincent K. McDonald
D857
(619) 553–3094
vmcdonal@spawar.navy.mil

Associates:
Professors John Prokias and Melica Stojanovic, Northeastern University; Professor Michael Porter, New Jersey Institute of Technology; Dale Green, Benthos, Inc.

Public-Key Cryptosystems Based on Groups on Elliptic Curves

Objective(s): Improve the capability to design Elliptic Curve Cryptosystems (ECCs) and attack them, based on new analysis of and cryptanalytic attacks on the Discrete Logarithm Problem for Elliptic Curves.

Accomplishment(s): We developed a software implementation of Finite Field and Elliptic Curve arithmetic in an extensible language interpreter. We outlined a seemingly new attack on the Discrete Log Problem that equaled but did not improve on the asymptotic complexity of the current best attack. We outlined an approach for a cryptanalytic attack on a slight generalization of the Discrete Log Problem that translates the number theory formulation into the arena of symmetric cryptosystems, where linear cryptanalysis or differential cryptanalysis may be brought to bear. We promoted local knowledge of Elliptic Curve Cryptography and awareness of its importance with a series of distinguished guest lectures.

BACKGROUND AND NAVAL SIGNIFICANCE

The Navy's move toward Network-Centric Warfare is making the security of communications more difficult and more critical, especially with the advent of mobile Internet Protocol (IP) networking, use of more commercial-off-the-shelf (COTS) hardware and software on desktops ashore and afloat, and pervasive interfacing of Navy networks with the global Internet. All communications systems from which the users expect traffic to be authenticated and/or confidential must protect that traffic either with a cryptosystem or with physical isolation. Conventional symmetric cryptosystems have properties that are problematic in a Navy context (e.g., there is need for a highly reliable, highly available authentication server that is a Trusted Third Party). RSA* public-key cryptosystems have some good properties but are handicapped by large key sizes and very slow performance. Elliptic Curve (EC) public-key cryptosystems have the desirable properties of RSA, are subject to fewer known attacks, and enjoy substantial advantages in speed and in small key size—issues that can be critical in implementing embedded systems such as smart cards and cell phones. In many cases, an RSA design will have too large a gate-count to be implementable in the space available. Even in desktop systems, reducing a response time from a few seconds to a fraction of a second can make an unacceptable user-interface usable.

The modern theory of public-key cryptography is based on the concept of the trap-door, one-way function, i.e., it involves a computation that is relatively easy to go through one-way but practically infeasible to reverse. For example, RSA is based on the ease of multiplying two large prime numbers and the difficulty of finding those prime factors given only the product. The El Gamal cipher is based on the discrete logarithm problem: Computing the value of an exponential in a finite group is easy, but reversing the process to find an exact logarithm can be difficult. For the group of whole numbers multiplied modulo some prime (the original setup for El Gamal), there are some subexponential algorithms to compute discrete logs, but for groups defined on Elliptic Curves, given some simple conditions, there is no such subexponential algorithm known. The attack of Menezes et al. [1] on

---

* RSA is an Internet encryption and authentication system that uses an algorithm developed in 1977 by Ron Rivset, Adi Shamin, and Leonard Adleman.

supersingular curves and the recently published attacks on anomalous curves by Smart [2], Satoh [3], and others all suggest that analysis of special cases of group order may be a fruitful source of further attacks on Elliptic Curve Cryptosystems (ECCs).

ECCs are a hot area of research in recent years, and once they become sufficiently studied so as to win the confidence of system designers, they are likely to replace symmetric systems and RSA in many technology areas. For instance, when the Global Positioning System (GPS) moves to over-the-air keying, if a public-key system such as an ECC is used for broadcasting new keys, then successful tampering with the tamper-resistant box in a GPS receiver would disclose the military-accuracy signal, but would not enable an enemy to spoof another receiver into accepting a jammer's signal.

There is a DoD-wide movement to create a Public-Key Infrastructure (PKI) on which an IP-network-based messaging system can be based. This is related to the recent DoD/Netscape contract and some pilot efforts at SSC San Diego and elsewhere to work with the Netscape tools and their recently published sources. While RSA is the current algorithm, the choice can vary because the formats support multiple cryptosystems. An ECC is a possibility, especially since smart cards are expected to be a critical part of the procurement.

APPROACH

Our goal was to develop an improved capability to choose good parameters for the large and diverse family of ECCs—based on an increased understanding of which ECCs are more or less secure. We determine this by finding one or more attacks on some systems and identifying associated classes of weak keys or weak systems.

Based on current knowledge of number-theory-based cryptography and assisted by consultation with some leading elliptic-curve theorists in academia, we planned to analyze the discrete logarithm problem for some classes of groups on Elliptic Curves. Through applied imagination and analogy with known attacks on ECCs, we hoped to find new attacks, identify the classes of weak systems or weak keys that result, and characterize the level of computational effort required to effect the attack. Software implementation of our ideas inside one of the free-ware frameworks was expected, but our product was to be a mathematical paper presenting our analytical results.

While ECC analogs exist for many different cryptographic algorithms defined earlier on finite fields (e.g., ciphers, signature algorithms, key exchange protocols), we focused mainly on the ciphers related to El Gamal.

RESULTS

We developed a software implementation of Finite Field and Elliptic Curve arithmetic in an extensible language interpreter; the language is Python. This implementation enables one to do both interactive and batch experimentation with the EC arithmetic at a reasonable speed without recompilations.

We outlined a seemingly new attack on the Discrete Log Problem for EC arithmetic. This used a meet-in-the-middle approach based on an algorithm for computing 2-divisors in Elliptic Curves of even order. Since the computational complexity required was of the same order as that of the baby-step-giant-step algorithm, which is the best currently known attack, this was not pursued further.

One of the discoveries made during this investigation was the possibility of applying cryptanalytic techniques from the world of symmetric cryptosystems to asymmetric ciphers, based on the discrete log problem in number theory such as El Gamal with Elliptic Curve arithmetic. The approach we were able to outline attempts to apply linear or differential cryptanalysis in a known-plain-text attack on the cipher. This would not provide a solution to a simple discrete log problem since it is usually formulated, but it could provide a solution to a family of discrete log problems all having the same unknown exponent.

The basis of this approach was a startling analogy between an iterated block cipher, such as those that linear and differential cryptanalysis can be applied to, and the usual algorithm for computing exponentials by shifting and squaring. In each stage of the iterated block cipher, a power of the base and an accumulated product are acted on by one or more bits of the key to compute the next appropriate power of the base and the next accumulated product. A linear relation that applies to each stage with probability ¾ is not hard to find, but the following questions remain unanswered. What other linear and differential relations can be found, and are they significant enough to provide a fast attack on the cipher? We did not have enough time to answer these questions.

During the work year, we did promote local knowledge of Elliptic Curve Cryptography [4] and raised awareness of its importance by means of a series of distinguished guest lectures with presentations made by Neil Koblitz, Harold Stark, Jesus Jimenez, and SSC San Diego's Wendy Miller.

REFERENCES

1. Menezes, A. J., T. Okamoto, and S. A. Vanstone. 1993. "Reducing Elliptic Curve Logarithms to Logarithms in Finite Fields," *IEEE Transactions on Information Theory*, vol. 39, pp. 1639–1646.

2. Smart, N. P. 1999. "The Discrete Logarithm Problem on Elliptic Curves of Trace 1," HP-Labs Technical Report #HPL-97-128, Hewlett-Packard; also *Journal of Cryptology*, to appear.

3. Satoh, T. and K. Araki. 1997. "Fermat Quotients and the Polynomial Time Discrete Log Algorithm for Anomalous Elliptic Curves," preprint, contact V. Broman.

4. Broman, V. and J. Jimenez. 1999. "Elliptic Curve Cryptography and Cryptanalysis." unpublished paper, SSC San Diego (contact author).

BIBLIOGRAPHY

1. Blake, I. G. Seroussi, and N. Samrt. 1999. *Elliptic Curves in Cryptography*, Cambridge University Press, New York, NY.

2. Diffie, W. and M. Hellman. 1976. "New Directions in Cryptography," *IEEE Transactions on Information Theory*, vol. 22, pp. 644–654.

3. IEEE P1363. "Standard Specifications for Public Key Cryptography," http://grouper.ieee.org/groups/1363/.

4. Koblitz, N. 1987. "Elliptic Curve Cryptosystems," *Mathematics of Computation*, vol. 48, pp. 203–209.

5. Menezes, A. J. 1993. *Elliptic Curve Public Key Cryptosystems*, Kluwer Academic Publishers, Dordrecht, the Netherlands.

6. Menezes, A. J., P. C. van Oorschot, and S. A. Vanstone. 1996. *Handbook of Applied Cryptography*, CRC Press, Boca Raton, FL.

7. Miller, V. 1986. "Uses of Elliptic Curves in Cryptography," *Advances in Cryptology, CRYPTO '85: Lecture Notes in Computer Science*, Springer–Verlag, vol. 218, pp. 417–426.

8. te Riele, H. 1999. "Security of E-Commerce Threatened by 512-Bit Number Factorization," http://www.cwi.nl/~kik/persb-UK.html (August 26).

9. Rivest, R., A. Shamir, and L. Adleman. 1978. "A Method for Obtaining Digital Signatures and Public-Key Cryptosystems," *Communications of the Association for Computing Machinery (ACM)*, vol. 21, pp. 120–126.

10. Schoof, R. 1995. "Counting Points on Elliptic Curves over Finite Fields," *J. Théorie des Nombres de Bordeaux*, vol. 7, pp. 219–254.

11. Silverman, J. H. 1986. *The Arithmetic of Elliptic Curves*, Springer–Verlag, New York, NY, GTM series, vol. 106.

Principal Investigator: ZU69
Vincent P. Broman
D712
(619) 553–1641
broman@spawar.navy.mil

Wireless Network Resource Allocation with QoS Guarantees

Objective(s): Develop resource-allocation mechanisms for network elements that are optimal with respect to Quality of Service (QoS) objectives.

Accomplishment(s): For the individual network node, the problem of resource allocation is one of packet scheduling. In this work, we characterized packet-scheduling objectives in terms of fundamental QoS parameters and developed packet schedulers that are optimal with respect to these objectives. This task involved placing the packet-scheduling problem in the context of stochastic control theory. An appropriate state space was formulated, and a natural indexing scheme for this space was developed. Appropriate cost and objective functions were identified. The discounted control problem was formulated and then solved for the optimal packet schedulers. Finally, performance results for specific examples were computed and comparisons with existing scheduling mechanisms were made.

Most current military networks, both wired and wireless, are based on Internet Protocol (IP) technology, and it is anticipated that this will continue to be the case in the future. Currently fielded and/or planned systems such as the Integrated Shipboard Network Systems (ISNS), the Automated Digital Network System (ADNS), and the Navy/Marine Corps Intranet (N/MCI) are IP-based. Traditional IP networks offer an unreliable connectionless service with no sophisticated Quality of Service (QoS) guarantees. In such networks, packets may experience excessive delivery delay, be dropped, or experience other detrimental behaviors. The next generation of networks for military applications will carry a variety of traffic types with greatly diverse delivery requirements. The traditional IP QoS will not be sufficient. SSC San Diego has developed expertise in providing QoS enhancements to IP networks.

There are a number of fundamental QoS parameters, e.g., delivery delay, delay variation, packet loss, and throughput. Of these, delivery delay is the most important to service quality. There are a number of resources available to the network that it can allocate to meet the QoS needs of the traffic it is carrying. These include bandwidth, buffer space, and the intelligence it brings to resource allocation. The resource-allocation protocols are crucial. At individual network node level, resource allocation is treated by the packet service discipline. This is the protocol by which each node determines which of its buffered packets to transmit, which to save for possible later transmission, and which to drop. The transmission scheduling mechanism is central to network performance.

A number of packet-scheduling protocols are in use today. In traditional IP networks, no distinction is made between traffic of different types, and the oldest packet buffered at a network node is transmitted first. This is the default first-in/first-out (FIFO) scheduling. An alternative is to distinguish between classes of different types and then prioritize the classes; at a transmission opportunity, the oldest packet of the highest priority class buffered is sent. A number of other schemes are based on assigning deadlines to packets and then servicing the packets in order of increasing deadline. Finally, a number of scheduling protocols are based on the allocation of transmission bandwidth to different traffic classes. Among these schemes, the most popular is weighted fair queuing (WFQ), which assigns bandwidth to each of its traffic classes and allocates excess bandwidth in proportion to these assignments.

None of these packet schedulers is known to be optimal in meeting QoS requirements. The goal of this research is to develop packet-scheduling techniques that are optimal.

An optimal packet scheduler is developed using the tools of stochastic control theory. To apply these tools, it is necessary to specify (1) a system state space, (2) a set of admissible controls, (3) the dynamics of the controlled system, and (4) cost and objective functions to be minimized. We consider a single network node servicing M traffic streams (figure 1). The system is time-slotted with one time slot being equal to the time required to transmit one fixed-size packet. We assume that the packets from stream i will be held in their buffer for at most N_i time slots before being dropped. We also assume that no more than one packet from each stream arrives in any given time slot. Under these assumptions, there are a finite number of possible configurations S_i for the stream i buffer, and these are conveniently indexed with a binary expansion. The overall system state is $S = S_1 \times \cdots \times S_M$.

Given the system is in state $x = (x(1), \ldots, x(M)) \in S$ at time n, a control u_n is a rule for deciding which stream to service at that time. This is, therefore, a function $u_n: S \rightarrow \{1, \ldots, M\}$. A control policy is a sequence $(u_0, u_1, u_2 \ldots)$. Since we are interested only in time-homogeneous problems, we will consider only ergodic controls, i.e., policies of the form $(u, u, u, \ldots)$. The system dynamics are determined once the controls and the arrival processes are specified.
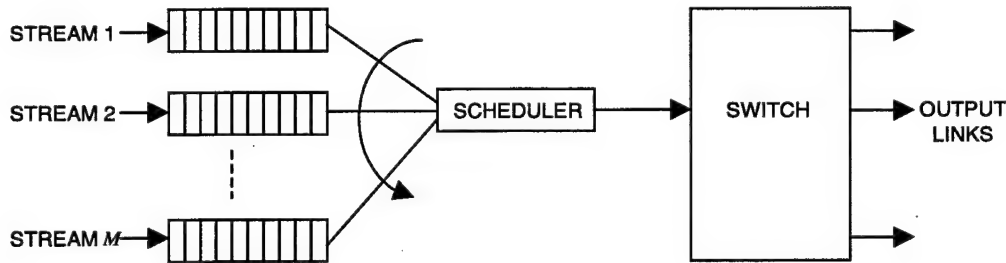
Figure 1. A packet scheduler.

Costs arise from two sources: the delay of packets at the network element and the process of discarding packets whose age exceeds the thresholds set for the streams. For each stream i, a cost function K_i is specified. The value $K_i(\alpha)$ is the contribution to the total cost when a packet from stream i is delayed α time units in the network element while $K_i(\infty)$ is the cost of discarding a stream i packet. If the system is in state x at time n and the control used is $u(x) = i$, then the one-time cost associated with this use of the control is

$$K(x,i) = K_i(\alpha(x(i)) + \sum_{j \neq i} K_j(\infty)\, 1(\alpha(x(j)) \geq N_j)$$

where $\alpha(x(i))$ is the age of the oldest packet in a buffer in state $x(i)$ and $1(.)$ is the indicator function.

Two infinite time-horizon objective functions can be considered. These are the ergodic control objective function

$$J_e(x,u) = \lim_{N \to \infty} \mathrm{E}[\frac{1}{N} \sum_{n=0}^{N-1} K(X_n, u(X_n)) \mid X_0 = x]$$

43

and the discounted control objective function

$$J_\rho(x,u) = E[\sum_{n=0}^{\infty} \rho^n K(X_n, u(X_n)) \mid X_0 = x]$$

where $\rho \in (0,1)$ is the discount factor and X_n is the state of the system at time n. The goal of the control problem is to find the control u that makes these two objective functions as small as possible. This optimal control is the optimal scheduler.

The ergodic control problem is the more natural of the two control problems (in that it does not involve a discounting factor). However, the discounted control problem is more easily treated analytically. Moreover, the discounted control problem is known to be an approximation to the ergodic control problem as ρ approaches 1. The approach we take is to treat the discounted control problem with ρ close to 1, viewing this as an approximation to ergodic control. The dynamic programming equation for the discounted control problem can now be found and solutions obtained via iterative techniques. In this way, the desired optimal scheduler is obtained.

The results are illustrated with a fundamental example. In this example, a network node is servicing two competing streams. The set-up is illustrated in figure 2. Figure 2 also shows the cost functions for each of the streams. Stream 1 represents a time-critical application such as voice. For this application, costs accrue linearly with delay to a maximum cost of 1 at $N_1 = 4$ time slots. Stream 1 packets delayed longer than 4 time slots are dropped. Stream 2 represents an application that is somewhat more tolerant of delivery delay but less tolerant of packet dropping, such as a data file transfer application. No costs accumulate from delaying stream 2 packets, but when these packets are dropped due to their age exceeding $N_2 = 5$ time slots, a cost of 2 is accrued. Thus, it is twice as expensive to drop a stream 2 packet as a stream 1 packet.
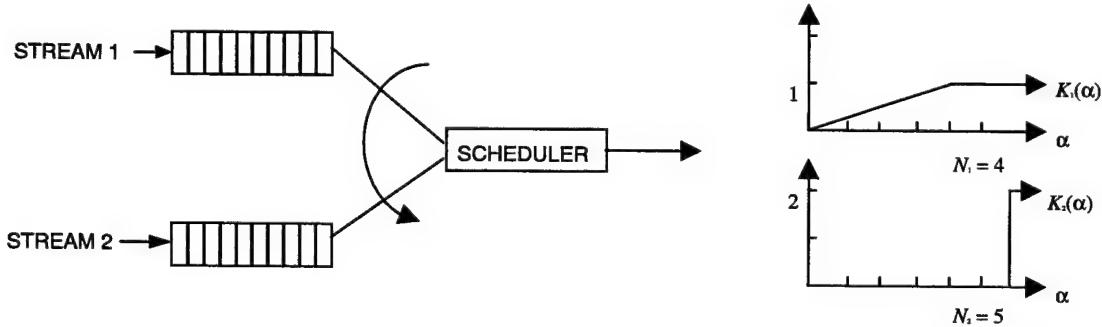
Figure 2. A two-stream example showing cost functions.

The arrival intensities of the streams are denoted p_1 and p_2, respectively. The intensity p_i denotes the probability that a packet from stream i will arrive at the scheduler in any given time slot. Since at most one packet is output in any time slot, the scheduler utilization is $p_1 + p_2$. For this example, $p_1 = p_2$.

In figure 3, we show results from running this scheduler for a 10,000 time-slot simulation. In figure 3, the average aggregate cost observed over the simulation is plotted against scheduler utilization $p_1 + p_2$. Each of the several curves appearing in figure 3 represents the average cost obtained when a different scheduling algorithm is used. The bottom curve is the one obtained using optimal scheduling.

The average cost is indeed minimized (among the schedulers represented) by the optimal scheme developed here. Note also that the effect of using optimal scheduling becomes more pronounced as the scheduler utilization increases. The effect of intelligence resource allocation becomes more significant as the demands on system resources increase.
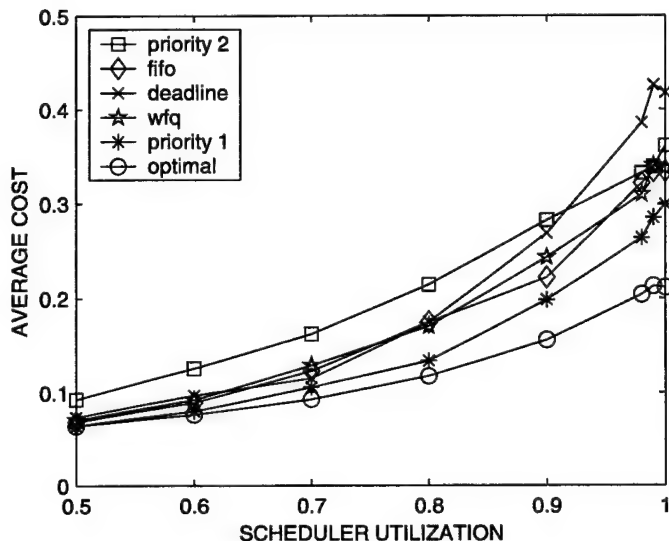
Figure 3. An example of scheduling performance results.

The other curves in figure 3 include those obtained with traditional FIFO scheduling (with ties going to traffic from stream 1, in this case), and two strict priority schedulers, one with priority to packets from stream 1 and one with priority to packets from stream 2. Also shown are results from a deadline-based scheduler in which the packets from stream i are assigned a deadline of N_i time slots from their arrival time, and packets are serviced in order of increasing deadlines (with ties to stream 1). Finally, in figure 3, a WFQ scheduler is considered. In this implementation of WFQ, as is typical, the bandwidth allocations are proportional to the arrival intensities p_i and so are equal.

Note that, at high utilization, the optimal scheduler has a lower average cost on the order of 0.1 for the second best scheduler for this example (the one giving priority to traffic from stream 1) and on the order of 0.2 and higher for the others. In terms of the cost functions specified, this is a savings of 5 to 10 packets dropped and 0.5 to 1 time slot in terms of delay.

Principal Investigator: ZU70
Stephan K. Lapic
D822
(619) 553–3073
lapic@spawar.navy.mil

Applications of Stochastic Nonlinear Dynamics to Communications Arrays

Objective(s): Apply recent advances in nonlinear dynamics to coupled-oscillator and phase locked loop (PLL) systems to develop dynamic nonlinear antennas.

Accomplishment(s): The project leverages recent advances in active antenna design and the theory of non-identical oscillators to generate beam steering and beam forming across an array of nonlinear oscillators. Additionally, compact arrays, antennas with element spacing significantly smaller than a half-wavelength, are possible by *directly* coupling nonlinear elements. Recent results in the design of compact multi-element antenna arrays demonstrate the importance of the mutual coupling effects between elements upon array performance. This research merges nonlinear dynamics and radio frequency (RF) microelectronics to create an antenna design that may provide a significant level of directivity in a small volume. By employing non-identical oscillator theory (the "tuning" of the *spatial* disorder), the signal-to-noise ratio of an array of PLLs improves as well as the frequency and phase locking across the array. Beam steering is accomplished simply by adjusting the spatial disorder. Theoretical advances in this research include analytical conditions for the beam steering, complete stability analysis for general uniform phase gradients and coupling, and the exact solutions of dynamic beam steering of one- and two-dimensional nonlinear arrays. Complementing the analytical and numerical studies of disorder in nonlinear arrays is a series of experiments on microelectronic coupled dynamic elements.

The signal transmission from a Global Positioning Satellite (GPS) is composed of two spread-spectrum signals in quadrature. The transmitted signal level from the satellites provides approximately −160 dBw at the surface of the earth. Consequently, the signal is below the inherent thermal noise level. Such weak signals broadcast on known frequencies leave GPS navigation systems vulnerable to jamming. This vulnerability is well documented by the Naval Research Advisory Council. GPS countermeasures fall into two categories: a relatively small number of high-power ($\sim 10^4$ to 10^5 W) jammers and a large number of low-power (~ 1 to 100 W) jammers distributed across the battlefield. Compounding the problem, highly mobile vehicles mounting GPS receivers preclude the use of strongly directive, large-aperture antennas to mitigate the effects of jamming. Current antenna technology provides no ready solution to numerous low-power jammers. Subsequently, the objective is to obtain increased immunity to jamming and interference.

Nonlinear antenna technology relies on dynamic array processing at microwave and millimeter-wave frequencies. Active antenna design employs diodes, transistors, or nonlinear circuits distributed over a plain surface that interact with the free-space beams at the plane of radiation collection. Combining free-space beams, rather than waveguide modes or transmission-line voltages, results in lower insertion losses. The dynamic range of the array improves because the signal power (transmit or receive) is distributed across many devices. Active antennas differ fundamentally from passive antennas in two ways: the unit cells are nonlinear, and signal processing (dynamic interactions between cells) is done via mutual coupling. In passive antenna arrays, which employ some multi-pole as the unit cell, the radiation pattern is controlled by prescribing the geometry of the array. Due to superposition

interacting, non-identical *linear* oscillators can only produce beats, not a single frequency, making it impossible to synchronize a linear array.

Active antennas are inherently nonlinear dynamic systems that can generate a number of unusual nonlinear phenomena. Over the last several years, an explosion of new analysis and control techniques for manipulating nonlinear dynamics has emerged. Active antenna design is ripe for the application of these new nonlinear techniques. Current array-design practice strives to suppress any inter-element coupling while minimizing noise. However, the interplay between coupling and noise can be "tuned" to achieve optimal performance. This is done in a variety of ways in nonlinear devices, including adjusting the coupling strength, changing the number elements in the array, dynamically controlling the device potential, introducing spatial disorder into the array, or optimizing the input noise. These nontraditional design approaches have already been experimentally verified in prototype antennas.

Generically, any active antenna design is an ensemble of coupled nonlinear devices. The dynamics of such arrays have been the subject of intense study in the last decade—with a particular focus on superconducting oscillator arrays. Fortuitously, the equation that governs the motion of exotic superconducting oscillators also describes the analog phase locked loop (PLL)—one of the building blocks in active antennas. Therefore, all the advances in understanding the dynamics of superconducting oscillator arrays may transfer to active antenna design. As a first step toward applying these results to the beam-steering problem, a one-dimensional chain of analog PLLs is simulated. Figure 1 dramatically illustrates this point. This is a numerical simulation of a one-dimensional array of seven analog PLLs. The PLLs are coupled via linear nearest neighbor with each element receiving a globally applied signal $A\sin(\omega_D t)$: The equation of motion is

$$\ddot{\theta}_n + \gamma\dot{\theta}_n \cos\theta_n = -\omega_{0_n}^2 \sin\theta_n + A\sin(\omega_D t) + k(\theta_{n+1} - \theta_n) - k(\theta_n - \theta_{n-1}) \qquad (1)$$

where θ_n is the phase error of the nth PLL in the chain, ω_{0_n} is the natural frequency of the nth PLL, and ω_D is the frequency of the global alternating current (AC) driving. Spatial disorder is introduced through variations in the natural frequency (ω_o) of each PLL. To understand this phenomenon, the PLL equation is reduced to a simplified model of the array dynamics (equation 2).
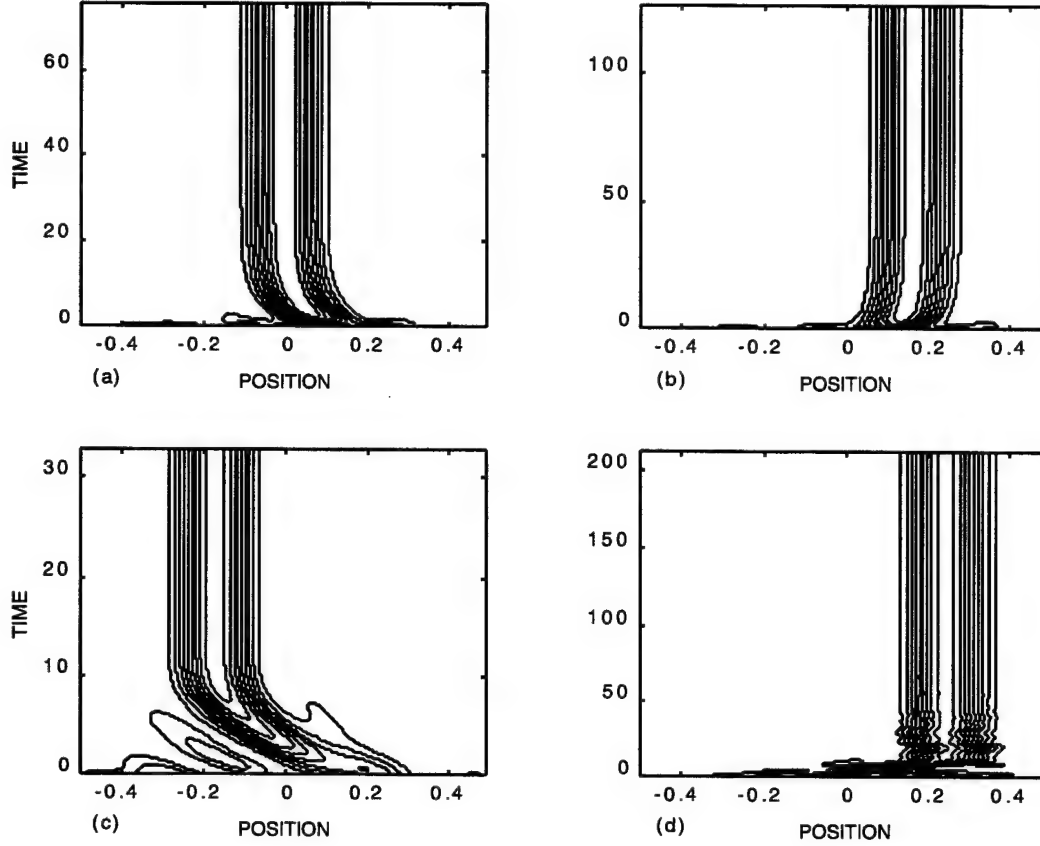
Figure 1. Numerical simulations of nonlinear active antenna array with spatially uniform time-*independent* solutions. Four contour plots demonstrate the static beam steering of a seven-element, one-dimensional array. For each plot, the free-space wavelength and inter-element spacing are 10^3; the perpendicular distance between the array and far-field screen is 1; the same random initial conditions were used in each simulation. Plots (a) and (b) correspond to zero coupling phase ($\Phi = 0$), while plots (c) and (d) represent a non-zero coupling phase ($\Phi = \pi/4$). The phase gradients are: (a) $\theta = 0$, (b) $\theta = \pi/3$, (c) $\theta = -\pi/3$, (d) $\theta = \pi/2$. These figures conclusively demonstrate beam steering for various coupling and phase-gradient values. The transient times are explained by Floquet stability analysis. Limitations of time-independent solutions (limited beam-steering range and loss of stability as array size increases) were overcome by employing time-*dependent*, spatially uniform phase gradients across the array. Exact analytical results were obtained for beam steering one- and two-dimensional arrays.

This model makes three key assumptions: first, the voltage-controlled oscillators (VCOs) possess a weakly nonlinear conductance; second, a given element is only influenced by its nearest neighbors; and third, each element possesses identical amplitude dynamics. Under these assumptions, the array dynamics can be described by a set of coupled-phase equations:

$$\dot{\phi}_j = \omega_j + k \left\{ \sin\left(\phi_{j+1} - \phi_j + \Phi \right) + \sin\left(\phi_{j-1} - \phi_j + \Phi \right) \right\} \tag{2}$$

where ω_j is the natural frequency of the jth element, and k and Φ are the coupling strength and coupling phase, respectively. Interestingly, this type of phase model has appeared in models of coupled solid-state lasers, Josephson junction arrays, Van der Pol oscillators, as well as biological systems such as eel locomotion and the synchronized flashing of fireflies. The extension of this

48

model to two-dimensional rectangular arrays is straightforward: In that case, a typical element would be influenced by its four nearest neighbors, leading to four coupling terms instead of the two shown previously. In accordance with experiments, the natural frequencies were taken as the accessible parameters. Two distinct problems were addressed: static and dynamic beam steering. In static beam steering, the array output is to be directed toward a fixed location, whereas dynamic beam steering seeks to continuously scan the array output. In both cases, one desires a uniform phase gradient whose value is controlled through manipulation of the natural frequencies.

The ultimate objective is the formulation of design rules that incorporate active elements, noise-induced synchronization, non-identical oscillator theory, and novel coupling architectures to produce a new generation of antennas. These new design rules stem from nonlinear coupled differential equation analysis.

Principal Investigator:
Dr. Brian K. Meadows   ZU71
D364
(619) 553–2823
bmeadows@spawar.navy.mil

Co-Principal Investigator:
Dr. Mario Inchiosa
D364
(619) 553–1255
inchiosa@spawar.navy.mil

High-Isolation Fiber-Optic Add/Drop Multiplexers for Shipboard Networking Applications

Objective(s): Demonstrate a novel method for producing high-isolation add/drop (A/D) multiplexers that may be used in fiber-optic systems employing multiple wavelengths of light to carry information.

Accomplishment(s): The technology for producing add/drop multiplexers by writing fiber Bragg gratings in the coupling region of fused-fiber couplers has been demonstrated. Gratings have been written in couplers made from standard photosensitive optical fiber with a drop efficiency of better than 60%. Fused-fiber-coupler-fabrication-process variables were shown to have a significant effect on the strength of grating formation in the couplers.

SSC San Diego has an established expertise in the area of fused-fiber biconical tapered couplers and has used this technology to demonstrate a variety of wavelength division multiplexers (WDMs), which are devices capable of combining multiple wavelengths of light onto a single optical fiber. Narrow-channel, fused-fiber WDMs have very low loss (typically <0.2 dB), are environmentally stable (~0.01 nm/degree C channel shift), exhibit polarization insensitivity leading to low channel cross-talk with unpolarized light (>20-dB isolation), have been packaged to tolerate high pressures (tested to 10 kpsi), and have a small size (1/8 in diameter, <2.5 inches long). However, these devices cannot be made with arbitrarily close wavelength spacings, and due to the condition for maintaining polarization independence, they are limited in the number of channels with which they can be used. In addition, higher channel counts require multiple WDMs to be cascaded together, even if one wishes to separate only a single wavelength of light from the fiber link. This becomes important for most naval systems that will use such devices since cost, component count, and packaged size are all-important issues. Thus, it is highly desirable to develop a more compact, inexpensive device.

The add/drop (A/D) WDMs being developed in this project are based on a combination of tapered fused optical fiber and fiber-optic Bragg grating technologies. Fused-fiber couplers are produced such that light that was originally in one fiber is transferred entirely into a second fiber. This is done by laying two optical fibers side by side, heating and fusing them together. The ends are then pulled so that the fibers form a tapered region in which light can transfer from the guiding region of one optical fiber to the other. Fused couplers can be made from a variety of different types of optical fibers such that the light in a very broad wavelength band in the 1550-nm region will undergo 100% coupling. A reflective region is then created in the center of the fused coupler, which will reflect a single narrow band of light of a given wavelength. Light that has been shifted from the original optical fiber into the second one will have undergone a phase shift of 90 degrees. If the reflective region is placed in the center of the fused coupler, then light will accumulate a phase shift of 45 degrees as it travels through the coupler to the reflective region. Another 45-degree phase shift will accrue as the light is reflected and travels backwards through the fiber coupler. Thus, the reflected light will also be coupled over 100% into the second optical fiber, only this time emerging from the input side of the device. Thus, if many wavelengths of light are input to the coupler on one optical fiber, most of the wavelengths will be coupled over to the second optical fiber on the output end. However, the one wavelength that is reflected will end up emerging from the input side of the second fiber. This will

provide a mechanism for dropping a single wavelength of light off a fiber link that is carrying multiple wavelengths of light. If the grating is properly designed, it is conceivable that the device could be capable of operating similarly with light traveling in the opposite direction as well. In this way, a signal can be added to a fiber link. Thus, a single device may be capable of providing both the add and drop functions simultaneously. Figure 1 depicts the operation of the A/D WDM.
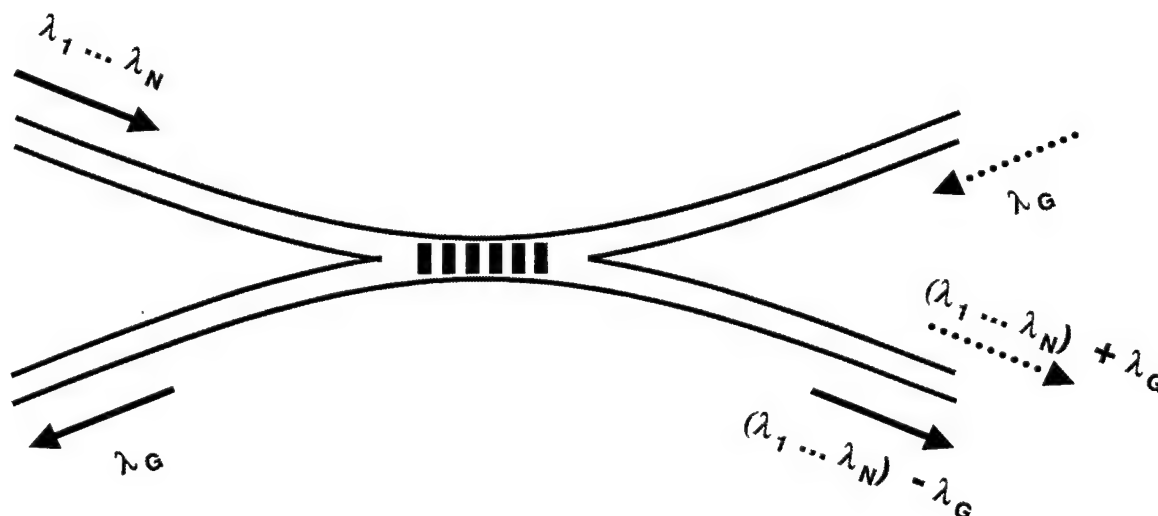
Figure 1. Operation of the multiplexer in both the add (dotted arrow) and drop (solid arrow) configurations.

Key to the success of this task is the ability to create the narrowband reflective region in the center of the fused region of the coupler. In recent years, a technique for creating periodic changes in the index of refraction of an optical fiber has been developed. This technique causes light traveling though a fiber to be reflected when it hits this region of index modulation only if the wavelength is correct relative to the period of the index modulation. These devices, known as fiber Bragg gratings, are created by exposing periodic regions of the fiber to high-intensity ultraviolet light, which has the effect of raising the index of refraction of the exposed region. In this effort, an excimer laser, emitting at a wavelength of 248 or 193 nm, is used to create the grating. In past work with fused-fiber WDMs, such a laser has been used to tune the wavelength response of WDMs, and index of refraction changes on the order of 10^{-3} have been achieved in the fused region of couplers without damaging them. This result is more than adequate to produce a Bragg grating. Of the various possible methods for creating the periodic exposure of the glass, the phase-mask technique has been chosen due to the more relaxed fabrication requirements. Technical issues to be explored in this work included: the strength and duration of the ultraviolet (UV) beam, length and placement of the Bragg grating within the fused region, the effect of the grating writing process on the optical properties of the fused-fiber WDM, and mechanical/alignment issues regarding the placement of a phase mask close to a fused coupler.

Early work on this task was geared toward developing the capability of creating fiber Bragg gratings. Bragg gratings have been demonstrated with reflective grating strengths of better than 10% in standard telecom optical fibers and up to 99.5% in specially developed photosensitive optical fibers. Once high-quality Bragg gratings were demonstrated, investigations into writing them in the fused region of fiber couplers were begun. The Bragg grating facility was altered to allow the writing of

51

gratings on pre-packaged, tapered, fused-fiber couplers. Low-loss 100% coupled fused-fiber couplers were produced with both standard photosensitive core fiber and an experimental photosensitive clad fiber. Experiments on couplers made with standard telecom fibers indicated that no significant gratings formation occurred. Although photosensitive cladding fibers were expected to produce strong reflectivities, once again gratings of appreciable reflectivities were not observed in couplers made with this fiber. Since it was also observed that this fiber was not capable of producing strong gratings outside of a coupler, it is assumed that the fiber itself had design flaws, and that an optimized photosensitive cladding fiber would still be expected to produce high-quality add/drop filters.

Couplers produced from fibers with a photosensitive core did show significant grating formation. The degree of reflectivity was shown to be strongly dependent on the length of the coupling region of the device. Highly fused devices with shorter fused regions had significantly lower grating strengths than longer, less well-fused devices. It is thought that a high degree of fusion results in a larger diffusion of the photosensitive core dopants into the cladding, and this lowers the doping levels below the critical amounts necessary for strong grating formation. A drop-efficiency of greater 60% was observed from couplers with a low degree of fusion while using a 4-mm grating length, with a total change in excess loss of less than 0.3 dB. Sidebands were down by at least 15 dB in the drop port, although significant loss peaks in the throughput port at wavelengths lower than the grating wavelength were observed, which is consistent with strong Bragg gratings produced outside of couplers. Both observations are expected to be improved with the introduction of proper grating apodization and well-designed cladding doped fiber. The capability for hydrogen loading of both optical fibers and 100% fused couplers has recently been established. This capability is expected to significantly increase the photosensitivity of the fused couplers and thus lead to even greater drop-port efficiency.

Principal Investigator:
Richard J. Orazi
D825
(619) 553–1065
orazi@spawar.navy.mil

ZU59

52

Development and Analysis of Turbo Codes for Navy Applications

Objective(s): Develop turbo-coding techniques and evaluate their performance in digital radio communications channels common to Navy environments.

Accomplishments(s): This research investigated the use of the powerful turbo-coding technique combined with the bandwidth-efficient methods known as trellis-coded modulation (TCM) and continuous-phase modulation (CPM), with appli-cations including the 5- and 25-kHz UHF SATCOM channels. See Wahlen and Mai [1] for a description of our turbo-coded TCM (TC-TCM) results obtained during FY 98. During FY 99, our research investigated coded CPM, obtained by precoding the digital symbol inputs to the CPM modulator using Reed–Solomon (RS), convolutional, and turbo codes. Our simulation results of coded CPM demon-strated gain of up to 7.5 dB relative to minimum shift keying (MSK) at a bit error rate (BER) of 10^{-6}. Further gains might be realized with the development of a soft-decision CPM demodulator rather than the hard-decision one used in this study.

SUMMARY

SSC San Diego and the Defense Information Systems Agency (DISA) Joint Interoperability and Engineering Organization (JIEO) have been investigating methods to increase data-throughput rates to 12 kbps and 64 kbps over the 5- and 25-kHz UHF SATCOM channels, respectively. There are, however, many challenges to bandwidth-efficient communication over the UHF SATCOM channel. For example, the hard-limiting transponder on DoD UHF satellites and the nonlinear amplifiers often used in earth station and satellite high-power amplifiers have the effect of removing all amplitude modulation from the transmitted signal and producing spectral re-growth.

In view of these challenges, two well-known bandwidth-efficient techniques, trellis-coded modula-tion (TCM) and continuous-phase modulation (CPM), were proposed as methods to increase UHF SATCOM data rates. TCM achieves coding gain and, therefore, higher data rates, without increasing transmitted power or required bandwidth by combining convolutional coding with higher order modulation schemes. During FY 98, our research investigated turbo-coded TCM (TC-TCM), that is, the application of turbo codes to TCM, in which the standard convolutional codes typically used in TCM are replaced with more powerful turbo codes; see Wahlen and Mai [1] for a description of our methods and results.

CPM is a constant amplitude, phase-modulated technique in which the phase is constrained to be continuous everywhere, particularly at symbol transitions. The phase continuity constraint forces the phase process to have a memory, which leads to an improvement in energy efficiency, or coding gain, much like in traditional coding schemes. Also, the smoothing out of phase discontinuities at symbol transitions reduces spectral spreading relative to other constant amplitude techniques that have phase discontinuities at symbol transitions. During FY 99, our research investigated coded CPM, obtained by precoding the digital symbol inputs to the CPM modulator while using Reed–Solomon (RS), convolutional, and turbo codes.

Our research focused on the CPM waveforms defined in MIL-STD-188-181B [2], which have a full-response rectangular frequency pulse (1REC), a 4-ary symbol alphabet, and two modulation indices given by {4/16,5/16}, {5/16,6/16}, {6/16,7/16}, {7/16,10/16}, or {12/16,13/16}. We completed a comparison, assuming synchronization, of uncoded CPM, convolutionally encoded CPM, RS-encoded CPM, interleaved RS-encoded CPM, and turbo-encoded CPM. We began an investigation of maximum likelihood and other methods of synchronization that continues in FY 00.

We performed simulations of uncoded and coded CPM using the five sets of modulation indices listed above and assuming an additive white Gaussian noise channel. We report the results only for the lowest and highest sets of modulation indices, {4/16,5/16} and {12/16,13/16}, since results from the other three sets vary between these extremes. In the progression from uncoded {4/16,5/16}-CPM to convolutionally encoded {4/16,5/16}-CPM, to RS-encoded {4/16,5/16}-CPM, and finally to interleaved RS-encoded {4/16,5/16}-CPM, simulated gains relative to minimum shift keying (MSK) at a bit error rate (BER) of 10^{-6} increased monotonically from approximately 1.5 dB to 5 dB. A similar progression of even larger gains up to approximately 7.5 dB was achieved in the case of {12/16,13/16}-CPM at the cost of greater spectral occupancy than {4/16,5/16}-CPM. Because the slopes of the turbo-encoded CPM (TC-CPM) performance curves were shallower than the interleaved RS-encoded CPM (IRS-CPM) performance curves, the small positive gain realized by TC-CPM over IRS-CPM at high BERs became a negative gain at low BERs. Development of a soft-decision CPM demodulator rather than a hard-decision one might allow the more powerful TC-CPM to realize positive gain over IRS-CPM at lower BERs.

Unpublished documentation of our research effort is presented in Wahlen, Graser, Mai, and Burr [3], which includes a description of the uncoded and coded CPM waveform, the baseband correlation receiver, synchronization techniques, simulation methods and software, and simulation results. It is hoped that, after publication, our results will be useful in setting UHF and SHF SATCOM follow-on standards.

REFERENCES

1. Wahlen, B. E. and C. Y. Mai. 2000. "Turbo Coding Applied to Pragmatic Trellis-Coded Modulation," *IEEE Communications Letters*, vol. 4, no. 2, pp. 65–67.

2. Department of Defense. 1999. "Interoperability Standard for Single-Access 5-kHz and 25-kHz UHF Satellite Communications Channels," MIL-STD-188-181B, 20 March.

3. Wahlen, B. E., S. J. Graser, C. Y. Mai, and T. A. Burr. "Continuous-Phase Modulation Waveform Simulation," in preparation.

Principal Investigator:
Dr. Bruce E. Wahlen
D841
(619) 553–5622
wahlen@spawar.navy.mil

Co-Investigator:
Calvin Y. Mai
D841
(619) 553–6220
cmai@spawar.navy.mil

ZU63

INTELLIGENCE, SURVEILLANCE, AND RECONNAISSANCE

3-D Propagation in Shallow Water Overlaying an Elastic Bottom

Objective(s): Provide a numerically efficient and robust acoustic model for the propagation of waves in a three-dimensional (3-D) ocean overlaying an elastic bottom.

Accomplishment(s): A propagation model based on the normal mode theory was developed for use in a range-dependent elastic waveguide. A method for computing the elastic modes was developed and used in the model to compute the acoustic field propagating in an elastic wedge. During FY 98, the equations of motion in an elastic waveguide were used to derive coupled mode equations for the propagation of waves in a range-dependent elastic waveguide [1, 2]. A set of first-order, coupled differential equations as a function of range were obtained for the mode amplitudes [3, 4]. The coupling between modes, which results in a range-dependent waveguide, is expressed in terms of the mode coupling matrix. An accurate computation of the acoustic field requires that the coupling matrix be computed accurately. This makes it necessary to express the integrals appearing in the coupling matrix in terms of local modes and their depth derivatives. In addition to yielding a set of first-order differential equations for the mode amplitudes, which can easily be integrated in range, the use of the equations of motion, as opposed to the wave equation, also made it possible to express the coupling matrix in terms of local modes.

During FY 99, the above model was used to compute the propagation of acoustic waves in an elastic waveguide. Computation of the acoustic field using this model requires the normal modes of an elastic waveguide. To accurately compute the acoustic field without relying on the use of other models, we constructed an analytic normal mode solution of the wave equation in an elastic waveguide consisting of a water layer over an elastic layer.* To obtain this solution, the scalar potential in the water and the scalar and the shear potentials in the elastic layer were expressed in terms of up and down waves.

These potentials were used to derive all other components of the field, such as the compressional and shear components of the stress tensor and the components of the displacement vector. The eigenvalue equation was obtained by applying the boundary and interface conditions to each of the field components. Once the eigenvalues were obtained, the eigenfunctions were computed for each component of the field. Figure 1 shows the first 10 eigenfunctions of an elastic waveguide where the water depth is 200 meters, the elastic layer depth is 1000 meters, the bottom compressional speed is 1700 m/s and its shear speed is 700 m/s. The compressional wave attenuation is 0.5 dB per wavelength, and the shear wave attenuation is 1.5 dB per wavelength. The right panel in figure 1 shows the compressional pressure field throughout the waveguide.

After the algorithm for computing the eigenvalues and eigenfunctions was developed, the model was applied to the propagation of acoustic waves in a range-dependent elastic waveguide.

---

* An elastic layer supports shear waves as well as compressional waves.
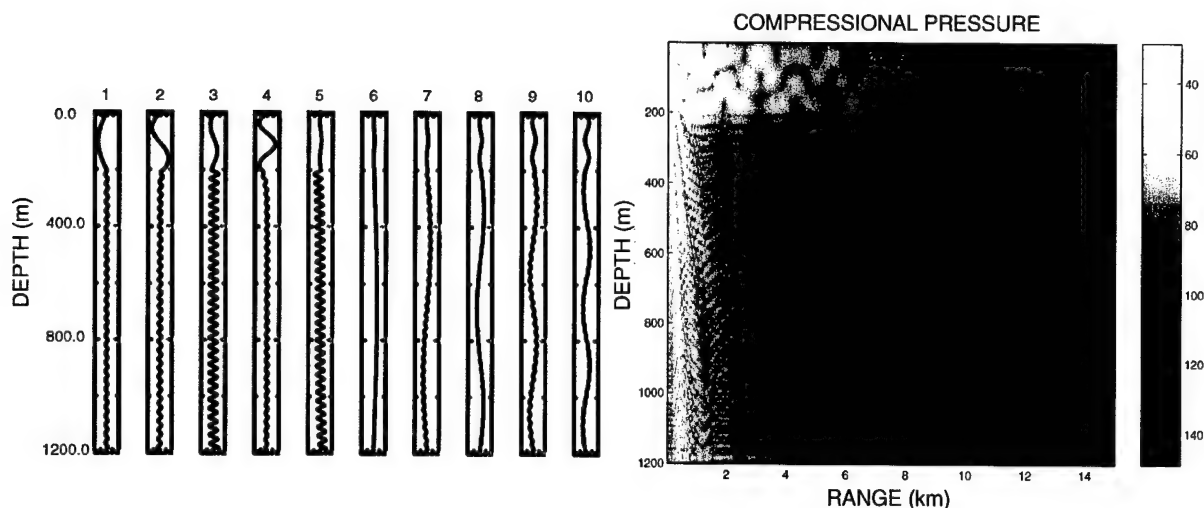
Figure 1. The first 10 eigenfunctions of an elastic waveguide where the water depth is 200 meters, the elastic layer thickness is 1000 meters, the bottom compressional speed is 1700 m/s and its shear speed is 700 m/s. The right panel shows the compressional pressure field level in dB in the waveguide for a 25-Hz source placed at 180 meters.

The waveguide, which was 15 km long, consisted of a water layer over an elastic layer. The water depth was constant at 200 meters for the first 5 km, and at a range of 5 km, it started to decrease at a rate of 1 meter for every 50 meters. The water depth decreased to 60 meters at a range of 12 km and stayed at this depth to a range of 15 km.

A 25-Hz source was placed at a depth of 180 meters, and the acoustic field was computed by dividing the wedge into smaller, range-independent sections. A separate set of modes and mode amplitudes were computed for each section, and the one-way coupled mode model was used to propagate the solution from one section to the next, and thus, through the waveguide. Figure 2 shows the acoustic field in the waveguide described above. The top panel shows the compressional field, and the bottom panel shows the shear field. Figure 2 also shows the geometry of the wedge.

REFERENCES

1. Pierce, A. D. 1965. "Extension of the Method of Normal Modes to Sound Propagation in Almost-Stratified Medium," *Journal of the Acoustical Society of America*, vol. 37, pp. 19–27.

2. Abawi, A. T., W. A. Kuperman, and M. D. Collins. 1997. "The Coupled Mode Parabolic Equation," *Journal of the Acoustical Society of America*, vol. 102, no. 1, pp. 233–238.

3. Tromp, Jeroen. 1994. "A Coupled Local-Mode Analysis of Surface-Wave Propagation in a Laterally Hetrogeneous Waveguide," *Geophysics Journal International*, vol. 117, pp. 153–161.

4. Odom, R. I. 1986. "A Coupled Mode Examination of Irregular Waveguides Including the Continuum Spectrum," *Geophysical Journal of the Royal Astronomical Society*, vol. 86, pp. 425–453.

COMPRESSIONAL PRESSURE

SHEAR PRESSURE
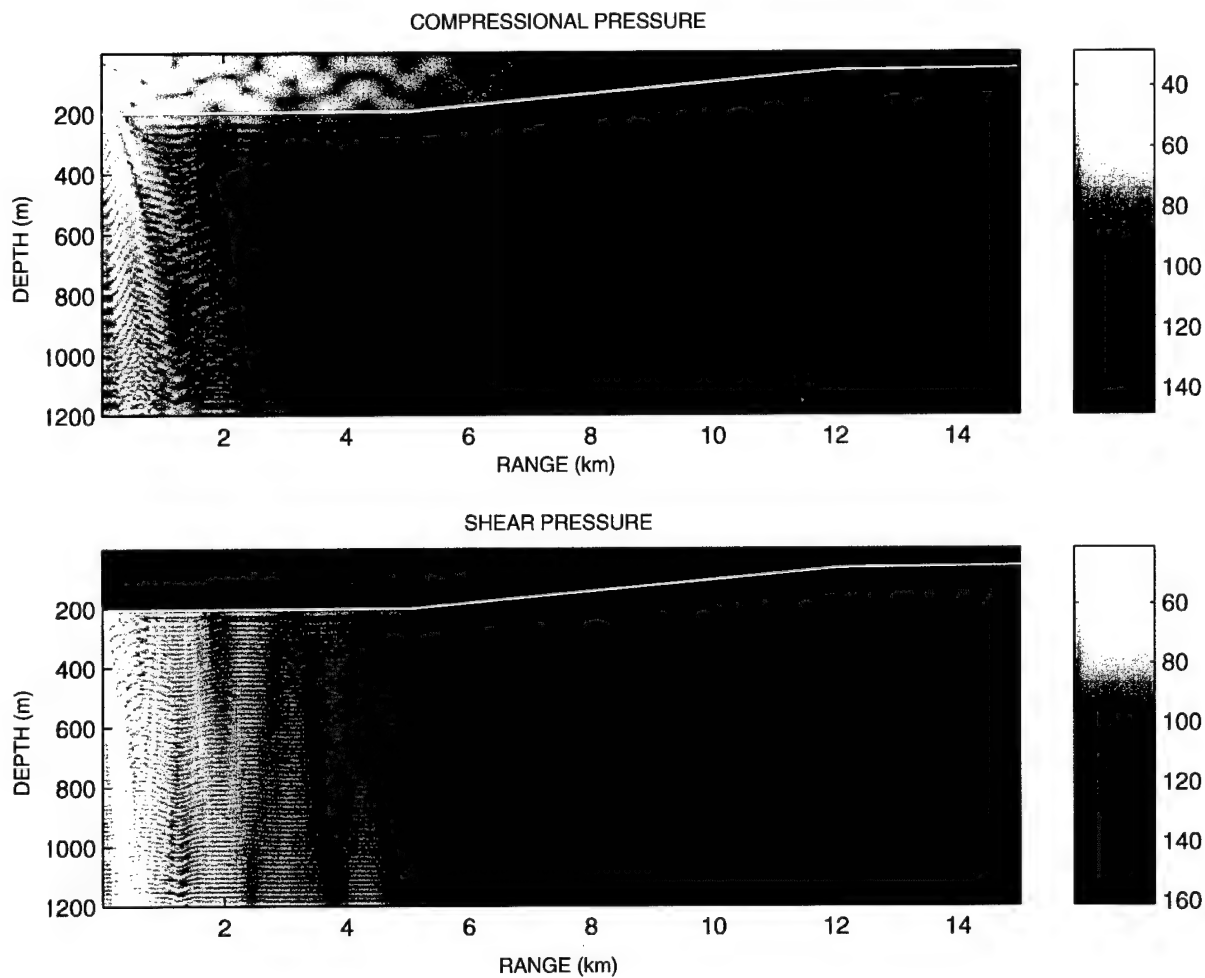
Figure 2. Acoustic propagation in a range-dependent elastic waveguide (wedge). A 25-Hz acoustic source is placed at 180 meters. The bottom compressional sound speed is 1700 m/s, and its shear sound speed is 700 m/s. The compressional wave attenuation is 0.5 dB/wavelength, and the shear wave attenuation is 1.5 dB/wavelength. The top panel shows the compressional pressure field level, and the bottom panel shows the shear pressure field level in dB.

Principal Investigator:
Dr. Ahmad T. Abawi
D857
(619) 553–3101
abawi@spawar.navy.mil

Automatic Matched-Field Tracking

Objective(s): Demonstrate automatic detection of an underwater target by using matched-field tracking.

Accomplishment(s): Real-time automatic detection of an underwater target was accomplished by using data collected on the Shallow-Water Environmental Cell Experiment, 1996 (SwellEX-96) sea test. The process involved calculating the correlation between the fast Fourier transform (FFT) data collected on six hydrophones of a vertical line array and predicting the results for a hypothetical track. Normal mode theory was used to calculate the expected complex sound pressure at different points along the track.

BACKGROUND

The detection of diesel submarines operating in shallow water is a serious Navy problem. Since sound attenuates rapidly in shallow water because of bottom interaction, sonar systems (active or passive) will have limited range (typically 10 km or less). Therefore, an effective antisubmarine warfare (ASW) detection system will consist of a large number of inexpensive units. By use of matched-field tracking algorithms, an automatic submarine detection can be made in each unit, thus providing an economical means of surveillance. Since the shallow-water sound field is a complicated mixture of multipath signals, conventional signal-processing methods (which assume a single plane-wave signal radiated by the submarine) will have degraded detection capability. In contrast, matched-field processing (MFP) [1], which matches the received signal to that calculated for a unique target location in the shallow-water environment, uses the complexity of the field to obtain the target depth.

APPROACH

The basic concept of matched-field tracking was first proposed in a paper by Bucker [2]. Consider that a submarine travels from point A to point B during a period of 3 to 5 minutes. A point in seven-dimensional space represents the path (A,B). Three coordinates (x_A, y_A, z_A) define the starting point; three more coordinates (x_B, y_B, z_B) set the end point; and track curvature is the seventh coordinate. For convenience, it is initially assumed that z_A is the same as z_B and that the curvature is zero. During the time period, acoustic data are collected from an array of hydrophones, and elements of the covariance matrix $g_{jkft} = <F_{jf} \bullet F^*_{kf}>$ are formed. Here, F_{jf} is the complex Fourier transform of the signal from sensor j, in frequency bin f, for the time interval t. The symbol * denotes a complex conjugate and $<\bullet>$ represents a time average. For example, if a fast Fourier transform (FFT) is used to generate 1-Hz output each second and f represents the frequency band from 80 to 90 Hz and t represents the time period from 30 to 40 s, then there will be 100 terms in the time average $<\bullet>$. During FY 98, it was shown that MFT worked well processing data collected during the Shallow-Water Environmental Cell Experiment, 1996 (SwellEX-96) [3]. The effort in FY 99 was in two phases. The first was to automate the selection of which FFT frequency bins to process. This was done by using constant false alarm rate (CFAR) [4] processing. In the second phase, normal mode code was used to generate range-demodulated tables of the complex pressure field (figure 1). The top part of figure 1 shows a plot of a typical sound pressure field. The lower part of the figure shows the complex pressure field after range demodulation. Values from this curve are stored in lookup tables. This

allows real-time matched-field tracking. This work has recently been published in the *Journal of the Acoustical Society of America* [5].
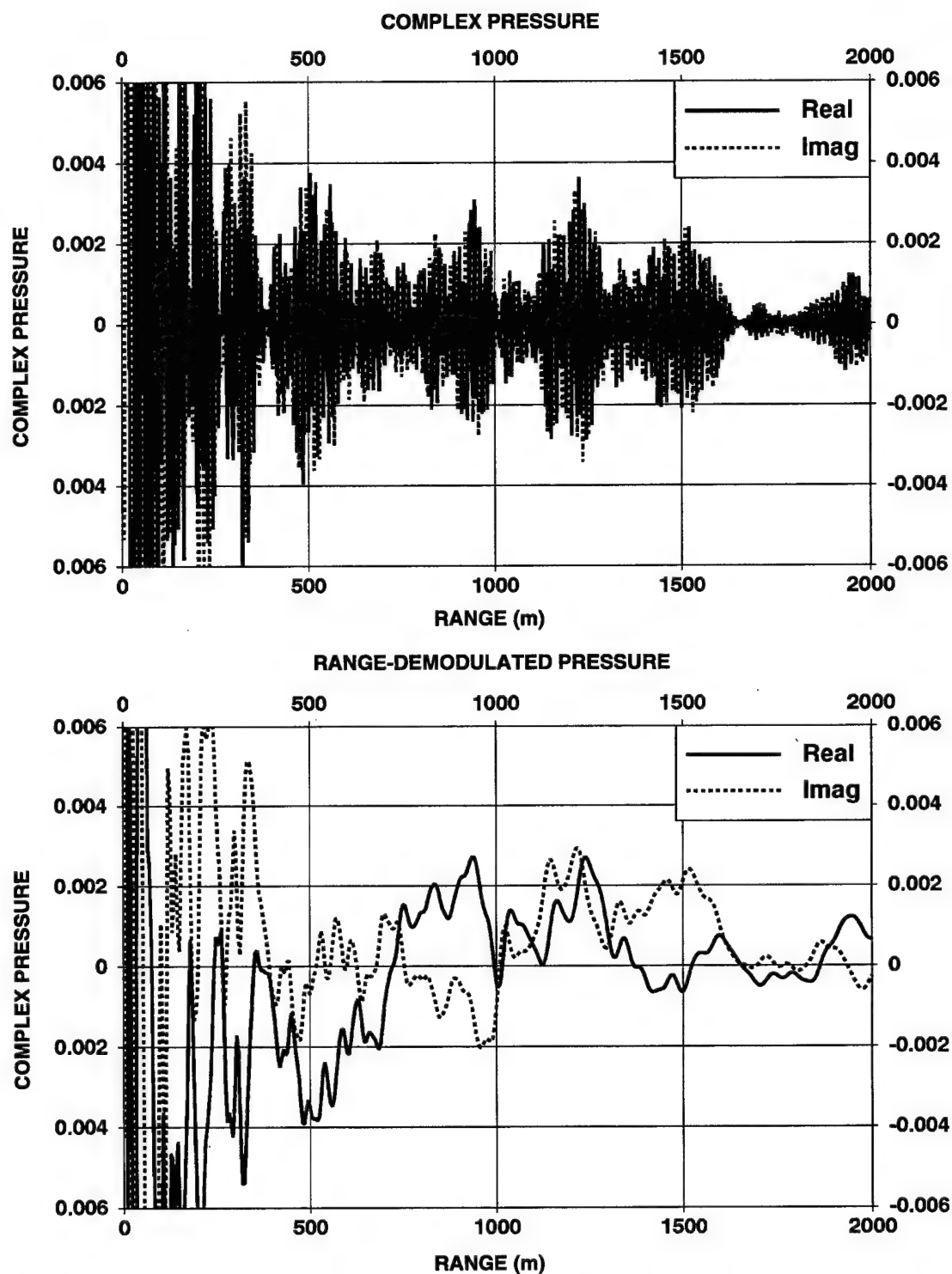
Figure 1. *Plots of a typical sound pressure field and of the complex pressure field after range demodulation.*

REFERENCES

1. Bucker, H. 1976. "Use of Calculated Sound Fields and Matched-Field Detection to Locate Sound Sources in Shallow Water," *Journal of the Acoustical Society of America*, vol. 59, p. 368ff.

2. Bucker, H. 1994. "Use of Matched-Field Tracking for Shallow Water Detection," *Journal of the Acoustical Society of America,* vol. 96, p. 3809–3811.

3. D'Spain, D. L. et. al. 1999. "Mirages in Matched-Field Processing," *Journal of the Acoustical Society of America,* vol. 105, p. 3245.

4. Hassab, J. C. 1989. *Underwater Signal and Data Processing,* CRC, Boca Raton, FL.

5. Bucker, H. and P. A. Baxley. 2000. "Automatic Matched-Field Tracking with Table Lookup," *Journal of the Acoustical Society of America,* vol. 106, no. 6 pp. 3226–3230.

Principal Investigator:
Dr. Homer Bucker
D857
(619) 553–3093
bucker@spawar.navy.mil

ZU55

A Time Difference of Arrival (TDOA) Geolocation Error Model for a Moving Sensor Pair

Objective(s): Improve geolocation error models that use time difference of arrival (TDOA) measurements by addressing aspects that are either not dealt with or are incorrectly dealt with in the literature.

Accomplishment(s): An analytical performance model for geolocation using TDOA measurements has been developed for qualitative and conceptual understanding. The model uses simplest modeling to understand analytically how geolocation's circular and elliptical error performance depends on geometry and error budget. The key is to understand the effects of correlation of TDOA measurements on geolocation errors. A working paper entitled "Effects of Correlation of Measurements on TDOA Geolocation" was prepared. The development used results from Tim Pattison and S. I. Chou's (this investigator's) paper on "Sensitivity Analysis of Dual-Satellite Geolocation"[1].

ERROR ELLIPSES INSCRIBED IN A FIXED PARALLELOGRAM

For geolocation using time difference of arrival (TDOA) measurements, three types of geometric angles determine the sensor-emitter configuration:

1. the angles between the sensors' line-of-sight (LOS) vectors relative to an emitter, θ,
2. the angles between the hyperboloid surfaces and the earth or given altitude, ψ, and
3. the angle between intersecting isochrones, β.

The first two geometric angles decide the uncertainty widths of the isochrones, which are the lines of position (LOP) for each TDOA measurement. The isochrone crossing angle completes the description of a parallelogram, but not the error ellipse. The shape and size of the error ellipse is governed by the isochrone correlation coefficient.

The first two angles individually and geometrically amplify the isochrone widths in the final error expression, whether in the covariance matrix or circular-probable-error expressions. The amplification factor by isochrone crossing angle also depends on the relative error budget ratio of bias/random.

In figure 1, a family of nine ellipses with correlation coefficients -1, $-3/4$, $-1/2$, $-1/4$, 0, $1/4$, $1/2$, $3/4$, and 1 are plotted where -1 corresponds to the vertical line-ellipse and $+1$ corresponds to the horizontal line-ellipse. The fixed parallelogram inscribes the error ellipses no matter what the correlation is between two TDOA measurements.

Both the size and shape of the inscribed ellipse change as the normalized correlation coefficient value (in the off-diagonal element) varies. For the unity correlation coefficient cases, two line-ellipses emerge when the parallelogram is a diamond. The left–right and right–left lock steps between LOP errors sweep out a vertical line-ellipse. Similarly, the left–left and right–right lock steps sweep out a horizontal-line ellipse.

The characterization for the parallelogram and ellipses is a graphic demonstration of the new discovery stated for parallelepiped and ellipsoid by Pattison. The parallelogram is independent of the

correlation coefficient, while the ellipses are sensitive to it. Still there is the inscription relation between the parallelogram and ellipses.

Two line-ellipses emerge from 100% correlated LOP cases (e.g., when random errors are small to start with or are variance-reduced through an extended period of linear smoothing). For small isochrone rotations, the two LOPs are nearly parallel. A line-ellipse emerges along the short diagonal of the diamond, regardless of how slender the diamond or parallelogram is. The points of tangency occur at the ends of the short diagonal of the diamond.

DEPENDENCE OF CIRCULAR ERROR ON RELATIVE ERROR BUDGET AND ISOCHRONE ROTATION FROM A MOVING SENSOR PAIR

The circular probable error is found as the Pythagorean sum of two components from random- and bias-error sources. Specialization is made to simplify the expressions for the circular error performance from a moving sensor pair's isochrone rotation.

$$(CEP95)^2 = \frac{16}{\left(2\sin\frac{\theta}{2}\sin\psi\right)^2}\left(\frac{\sigma^2_{toa\_random}}{\sin^2\beta}+\frac{\sigma^2_{sys}}{2}\right) \text{ where } \sigma^2_{sys} = \sigma^2_{toa\_bias} + 2\sigma^2_{position}.$$

The time of arrival (TOA) random error is subject to isochrone rotation amplification, while the measurement-bias and sensor-uncertainty errors are not. Figure 2 is used to show the dependence of circular error on relative error budget and isochrone rotation from a moving sensor pair.
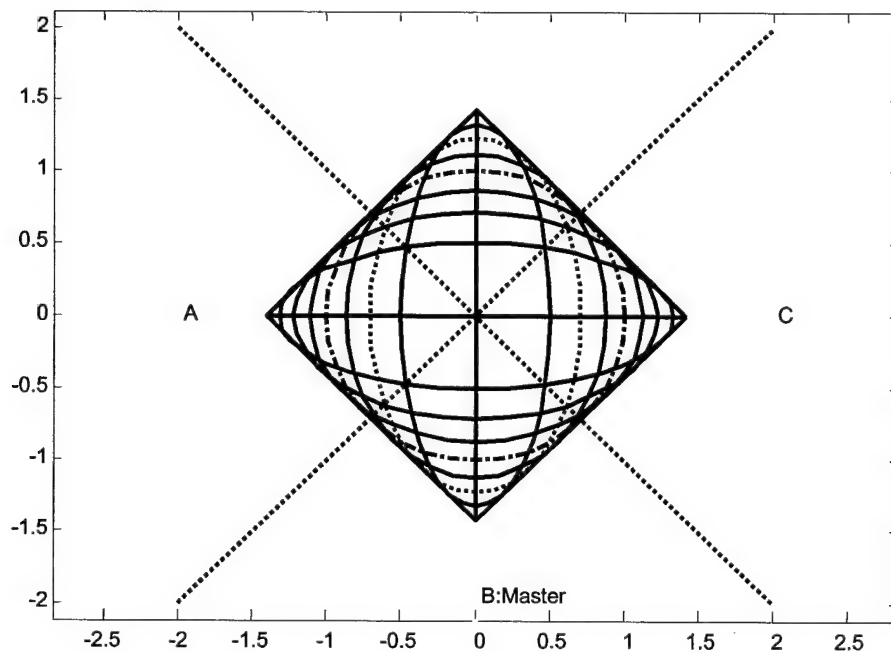
Figure 1. Error ellipses inscribed in a fixed parallelogram.

log-log-log SUM(1:10,:)
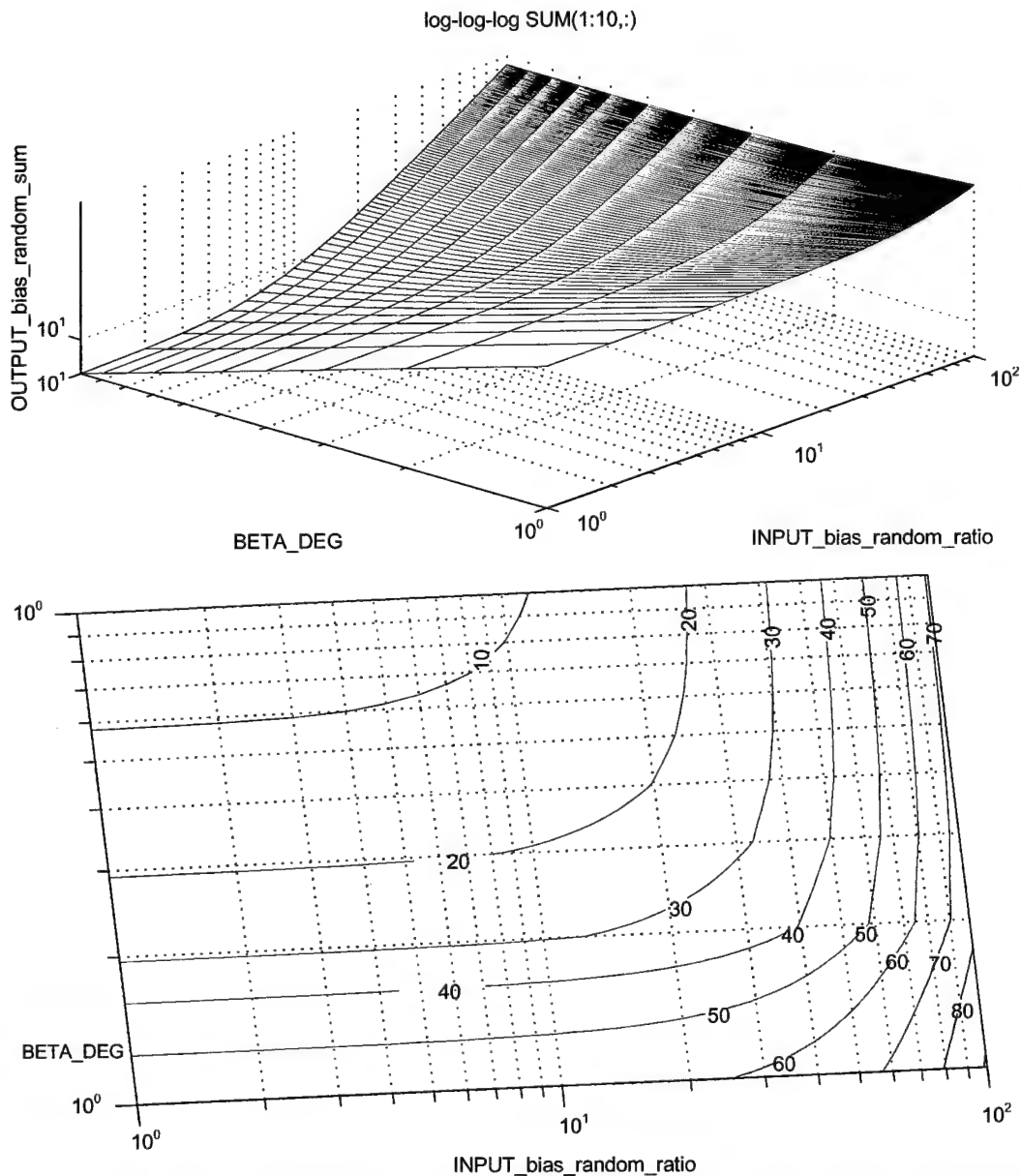
Figure 2. Random error dominates in the lower left region; the triple sine product approximation is valid.

For relative error budget ratio bias/random = 1, the random-error component of CEP95[*] dominates the geolocation error as shown by a linear left edge in the log-log-log plots (figure 2). This is in the random-error dominant region with horizontal contour lines, and the CEP95 is inversely proportional to the isochrone rotation angles, β. Inside the random-error dominant region, an inverse triple sine-product characterization is valid for the circular error description. Even for the input bias/random ratio up to 10, CEP95 is still dominated mainly by the random errors.

For bias/random ratio = 100, the bias error component of CEP95 dominates the geolocation error as shown by a flat right edge. Inside this bias-error dominant region with vertical contour lines, the right

---

[*] CEP95 is the radius of a circle that catches 95% of the error distribution when centered at the correct location.

edge of the mesh or contour plots for the log-log-log sum indicates a flat right edge for the sum. Here, the bias-error term of the CEP95 expressions dominates the random term. This means the circular error statistics are independent of the isochrone rotation angles. At these large bias errors, the triple sine product characterization of the circular error statistics is no longer valid. The bias-error dominant region is intuitively explainable with a lockstep of right–right or left–left bias input errors, as explained earlier, with positional error constrained to isochrone width.

The dividing line of the two dominance regions is a –45-degree slope line in the log-log contour plot. The TOA random error is subject to isochrone rotation amplification, while the bias errors are not. Circular probable error in both regions is amplified by $1/(\sin\theta/2 \sin\psi)$ and hence is used as part of the normalizing factor for the plotted circular probable error.

REFERENCE

1. Pattison, T. and S. I. Chou. 2000. "Sensitivity Analysis of Dual-Satellite Geolocation," *IEEE Transactions on Aerospace and Electronic Systems*, vol. 36, no. 1, pp. 56–71.

Principal Investigator:
Dr. S. I. Chou
D73A
(619) 553–2541
chou@spawar.navy.mil

ZU72

In-Fiber Polarizers Using Blazed Fiber Gratings

Objective(s): Produce highly polarizing structures with minimal restorative volume in surveillance-array optical fiber by using in-fiber Bragg gratings.

Accomplishment(s): We explored the production of minimum-volume polarization filters in surveillance-array fiber by using the tilted, or blazed, in-fiber Bragg gratings. A set of analytical tools was produced to guide the design of the grating. Gratings were produced in array-type fiber with a polarization extinction ratio of 15.8 dB on radiation and 0.5 dB on transmission. Dual-fiber grating cross-coupled devices were then produced to take advantage of higher extinction on radiation while maintaining a minimal volume. Characterizations of these devices support a predicted polarization extinction of 32 dB. The efficiency of the devices fabricated is quite low, although this may be partially due to the low coherence of the particular laser used for device fabrication.

BACKGROUND

All-optical sensing schemes based on optical fiber provide lightweight, compact, and sensitive solutions for undersea-surveillance applications. Naval designs minimize sensing-array volume by excluding batteries and powered cables and by minimizing the size of "lumps" and devices.

This work examined the possibility of using tilted, or blazed, in-fiber Bragg gratings as optical polarization filters, or polarizers. By fabricating devices directly into low bending-loss or "pay-out" fibers used in surveillance arrays, the volume committed to the usual service loops and splice potting can be excluded. The fact that low-bending loss surveillance-type fibers have a greater photosensitive dopant concentration than conventional telecommunications fiber favors success when combined with a high photon-energy 193-nm-excimer-laser grating writing source. The hope is to produce useful devices that are mechanically flexible, that add no additional size to the array, and that can be fabricated directly into the fiber of the sensing array during array manufacturing.

METHOD

Our first task was to develop a mathematical analysis for scattering light out of a fiber by using a tilted periodic refractive index perturbation, or blazed grating. Next, we determined the external phase-mask period and orientation and the laser-operating conditions needed to create the optimal grating as derived from the analysis. This process was complicated by the curvature of the fiber's cladding-air interface, which is encountered by the write beam in passing to the core. Finally, the above analysis was used to guide the production of an optimal polarizing in-fiber Bragg grating, and then its polarization properties were characterized through experiment.

APPROACH

The fiber types determined to be used in existing naval undersea surveillance arrays are Corning Payout, 3M CS-98-3523, 3M CS1550, and Lucent Acutether. These low bend-loss, small-mode fibers have a high germanium concentration in the core, which increases the likelihood of useful device production in otherwise unenhanced fiber while using a 193-nm-writing-laser wavelength.

Samples of Payout, CS-98-3523, and Acutether fibers were obtained in addition to Truewave and Lucent depressed-clad telecommunications, Spectran Specialty, and INO photosensitized fiber. The CS-98-3523 fiber was discarded because the small cladding diameter was not compatible with existing fixtures. Gratings could only be written in Corning Payout fiber after a hazardous HF-acid etch removed the titanium-oxide outer layer, so work with that fiber was discontinued. Acutether, Spectran Specialty, INO, Truewave, and Lucent depressed-clad fibers were used to fabricate the gratings.

A perturbation analysis was developed to predict the fraction of light radiated from a given fiber as a function of input polarization and grating parameters. This formalism is analogous to the First-Born treatment of Schrodinger's Equation in quantum mechanics. This treatment involves the determination of the guided mode's electric-field profile. The mode profile is determined analytically for step-profile fibers, such as Accutether, and numerically for linear-profile fibers. Key parameters such as the mode's effective index and refractive index perturbation depth were determined from the experimental measurements of the spectrum reflected from an unblazed Bragg grating written into a given fiber.

The period of the grating written into the core was assumed to be that at the air-cladding interface, or one-half the phase-mask period used to make the grating divided by the cosine of its angle. This relationship was found to agree with the experiment. The tangent of the grating blaze angle was found to be the tangent of the phase-mask tilt angle scaled by the index of refraction of the fiber at the 193-nm writing wavelength. This relationship was derived through a ray-tracing analysis of an interference fringe from the cladding/air interface to the core region.

These write-distortion expressions and the Bragg grating law, which comes from the perturbation analysis, were combined to give a series of expressions defining the optimal mask parameters. An optimal mask was purchased and production parameters defined.

RESULTS AND POTENTIAL NAVAL SIGNIFICANCE

Blazed in-fiber Bragg gratings of 3-mm length were fabricated in Acutether, Spectran Specialty, INO, Lucent depressed-clad, and Truewave fibers. Measurements show the polarization extinction of radiation that increases as the grating blaze in the fiber approached its optimum of 45 degrees.

The magnitude of this extinction ratio in radiation for unenhanced Accutether fiber is 15.8 dB. On transmission, this extinction ratio is much smaller (0.5 dB) due to the low grating radiation efficiency. It is the transmission-polarization extinction ratio that is of practical importance because the transmission configuration allows devices to be made with essentially no increase in size over the original fiber. The perturbation analysis shows the radiation efficiency to increase linearly with grating length and as the square of the peak index changes. Photosensitive fibers are known to have a maximum index change of 10^{-3}, compared to the 6.25×10^{-5} measured for the Accutether samples, although there are some indications that this index change could be increased to as high as 5×10^{-4} with increased write-laser coherence and set-up improvements. Gratings were fabricated in Spectran photosensitized fiber with a measured extinction ratio on radiation of 18.4 dB, a maximum radiation of 4.8%, while the extinction ratio on transmission is 0.35 to 0.55 dB depending on wavelength. Knowing in the ideal case that the sum of transmission and radiation is unity, it was determined that a 20-dB extinction ratio on transmission requires a maximum radiation over all polarization of 99.01% for an 18-dB extinction ratio on radiation. For the Spectran fiber, the required grating length would

be almost 70 mm, while for Accutether, the required grating length is almost 1 meter. Measurements on untilted gratings indicate that the efficiency can be increased up to 64 times with increases in coherence of the laser used to fabricate the devices, resulting in a significant reduction in these lengths. The stated lengths are greater than the useful beam dimension of the excimer laser in our laboratory. The polarization wander inherent in these symmetric-core fibers rules out using a serial combination of smaller gratings. Thus, the strength of the grating written in surveillance-type fiber is insufficient to produce useful single-grating devices in a transmission configuration.

An alternate approach is to use the much stronger polarization extinction on radiation. Collecting the radiated light with lenses would produce a package volume larger than desired. A more compact arrangement is to use two identical fibers placed in parallel, both with in-fiber gratings providing cross-coupling. Ideally, the device volume could still be quite small at twice a fiber's diameter and could be flexible and similar in appearance to the single grating device. This two-fiber coupler arrangement has resulted in several patent applications being filed under this project. From reciprocity, it seems that both the polarization extinction ratio and the radiation loss would double in dB. Single and double-parallel grating devices were fabricated with the following polarization extinction ratios. The INO sample has 4.4 dB for single and 9.2 dB for double at 30.3-degree blaze. The depressed-clad has 3.85 dB for single and 7.85 dB for double at 26-degree blaze. The Spectran Specialty sample has 18 dB for single and 23.6 dB for double at the optimal 45-degree blaze, where there is some chance that the polarization controller used in the experiment may have been the limitation. The Accutether double-grating sample did not couple, probably due to fiber misalignment. Note that the extinction ratio did double in going from single to double grating devices for all but the Spectran case. It should be noted that although the polarization extinction ratio can be quite high in these devices, the fiber-to-fiber coupling efficiency of the two-fiber polarizer is small with our fabrication set-up.

Results show that although the possibility of creating useful, small, and flexible polarization filters in the fiber already present in a surveillance array using blazed Bragg gratings is low, there are many indications that this probability can be increased significantly with writing-laser coherence and set-up improvements. One type of application where weak in-line polarizers may be useful is inside a fiber laser cavity, where the dynamics of the laser action will amplify the weak polarizing effects. An example of a naval application would be a fiber version of an intercavity laser sensor (ILS). These conclusions do not preclude the possibility of fabricating useful unblazed devices, such as optical filters, into existing sensor fiber.

Principal Investigator: ZU73
Douglass C. Evans
D746
(619) 553–1978
evansd@spawar.navy.mil

Evaporation-Duct Assessment from Meteorological Buoys

Objective(s): Evaluate the capability of oceanographic buoys to provide real-time assessments of evaporation-duct effects on radio propagation and validate evaporation-duct and radio-propagation models.

Accomplishments(s): A 2.4-GHz-radio-propagation link was established between the Scripps Institution of Oceanography (SIO) Point La Jolla buoy and a suitable SSC San Diego Seaside location. Commercial digital radio transceivers operating in the license-free industrial, scientific, and medical (ISM) band were used. The path length was 18.2 km, and the terminal heights were 7 and 21.5 meters. Radio propagation loss was measured during a period in April 1999 and compared to radio-propagation predictions based on the sea temperature, air temperature, humidity, and wind speed measured on the buoy. Two methods were used to compute the evaporation-duct height and corresponding vertical-refractivity profiles. Both methods gave generally good results, but one method was slightly better. To analyze the horizontal variability of the assessments, concurrent meteorological data were also used from an identical SIO buoy located west of San Clemente Island. The distance between the buoys was 128 km. The assessments based on the distant buoy were only slightly worse than assessments based on the nearby buoy. Twelve months of meteorological measurements were also analyzed to assess the long-term horizontal variability of propagation conditions between the two buoys.

BACKGROUND

The evaporation duct is a nearly permanent propagation mechanism over the sea that can substantially enhance radio and radar signal levels near and beyond the horizon at frequencies generally above a few GHz. The long-term statistical agreement of meteorological and propagation models to measurements at radar frequencies is remarkably close, often within 1 or 2 dB at median levels. However, comparisons of the same models to measurements in a time series, although good, have often shown significant errors. We believe that these discrepancies have been due to a lack of sufficient quality meteorological data collected near the air–sea boundary. Recently, the Scripps Institution of Oceanography (SIO) has placed an oceanographic buoy a few kilometers west of Point La Jolla to provide real-time, high-quality oceanographic and meteorological data. SIO has also placed an identical buoy a few kilometers west of San Clemente Island. We believe that data from these two buoys can establish the validity of real-time propagation assessments and the horizontal applicability of such assessments, provided a suitable radio-propagation link can be established from or near the Point La Jolla buoy.

METHOD

We established a 2.4-GHz radio link between the Point La Jolla buoy and SSC San Diego Seaside. We collected radio-propagation-loss data versus time and compared the data to modeled loss based on meteorological data collected on the buoy. We also compared the same radio-propagation-loss data to models based on meteorological data from the San Clemente Island buoy to assess horizontal variability. We then compared long-term meteorological measurements and radio propagation

assessments at both buoys to evaluate the long-term horizontal variability of propagation assessments.

APPROACH

We used two commercial digital radio transceivers (Utilicom model 2020) that operate in the 2.4-GHz license-free industrial, scientific, and medical (ISM) band to establish a radio-propagation link between the Point La Jolla buoy and SSC San Diego Seaside. We developed a PC logging program to monitor and log the observed propagation loss versus time. We obtained meteorological data from the two buoys and compared modeled propagation loss to observed propagation loss. We also performed a long-term (12-month) statistical study of propagation conditions at each buoy to help evaluate horizontal variability.

RESULTS

The propagation link was tested and calibrated on land between November 1998 and February 1999. The link was installed on the Point La Jolla buoy in March 1999 (while the buoy was in San Diego harbor for repairs) and was deployed in April 1999. Data were collected during April. Two popular methods to compute the evaporation-duct height and the vertical-refractivity profile are the Paulus method and the LKB method. These methods were used with the SSC San Diego waveguide propagation program MLAYER to produce propagation assessments for hourly time periods over several days. The Paulus method resulted in a median error of 1.4 dB, and the LKB method resulted in a median error of 0.9 dB over all samples for the Point La Jolla buoy meteorological data. For the San Clemente Island buoy data, both methods resulted in a median error of 1.3 dB over all samples. The San Clemente Island buoy did almost as well as the Point La Jolla buoy, so the horizontal variability over this sample was small. The LKB method did appear to be slightly better than the Paulus method for this sample. The conclusion of the long-term study was that for frequencies of 3 GHz and below, horizontal homogeneity over ranges in excess of 100 km is reasonable, at least in the Southern California offshore area. A paper title "Evaporation-Duct Assessment from Meteorological Buoys" has been submitted to *Radio Science*.

Principal Investigator: ZU74
Herbert V. Hitney
D858
(619) 553–1428
herb@spawar.navy.mil

Near Sea-Surface Propagation Vector Anomalous Effects on Vertically Polarized Electrically Small Floating Antennas

Objective(s): For the case of floating ("bobbing") electrically small antennas, determine the RF propagation vector perturbation statistics as a function of RF wavelength, sea-surface wavelengths, and the relative propagation direction of RF and sea-surface structure vectors.

Accomplishment(s): Due to funding problems and the departure of the principal co-investigator (Dr. M. Pollock), the goals have been de-scoped and the instrumentation simplified.

SUMMARY

The initial goal of this effort was to measure the time-varying distortion of electromagnetic wave fronts propagating parallel to and near the sea surface over the frequency range of 1 MHz to 1.5 GHz while using three coherently digitized RF channels. Furthermore, the transmitter was to simultaneously transmit vertical and horizontal polarization on the same frequency through the use of orthogonal bi-phase coding. Given the funding problems and disrupted schedule, the goals have been reduced to a single frequency (150-MHz nominal) and a two-channel system. It is now expected that a minimum amount of experimental data will be collected and analyzed by midsummer 2000.

Principal Investigator:
Barry R. Hunt
D7303
(619) 553–5345
brhunt@spawar.navy.mil

ZU75

Parallel Symbolic Sparse Factorizations through Recursive Bordered Block Diagonalization

Objective(s): Develop a parallel sparse matrix ordering and symbolic factorization method and a computer code to speed up computations in a class of problems arising in signal and image processing, computational electromagnetics, nonlinear acoustics, and target strength.

Accomplishment(s): Developed a new sparse matrix ordering and symbolic factorization method that applies to general systems, in which the matrix may be symmetric or unsymmetric, positive definite or indefinite. In principle, the approach is designed for symmetric matrices, but more general systems may be cast in symmetric form. Furthermore, we have completed a C computer code that will soon be transitioned to the computers at the shared resource centers of the DoD High Performance Computing Modernization Program (HPCMP).

Large sparse problems arise throughout DoD applications, and their effective solution is of critical importance to DoD. Many problems encountered in diverse disciplines of DoD such as computational electromagnetics, nonlinear acoustics, nonlinear transducers, structural mechanics, and fluid dynamics are systems governed by partial differential equations whose analysis by finite-element and finite difference methods leads to sparse symmetric systems of equations $Mx = b$, in which the coefficient matrix M is either positive definite or indefinite. Also, a large class of command and control decision problems, as well as least-squares data-fitting problems such as encountered in bistatic target strength models [1], can be formulated as constrained optimization problems [2] that, in turn, lead to a sequence of sparse indefinite symmetric systems. In all these critical DoD applications, the effective exploitation of sparsity is crucial for the efficient solution of the problem on scalable parallel computers.

For a general n-by-n sparse symmetric matrix M (positive definite or indefinite), we have completed the implementation (in C language) of a graph-theoretic work [3 to 7] that exploits the sparsity in M to compute a permutation matrix P so that the Cholesky factor of PMP^T has a sparse recursive bordered block diagonal (bbd) form. The structuring of problems into recursive bbd form allows the organization of the computational tasks into a sequence of hierarchic layers so that all tasks within each layer are completely independent of each other. The independence of computational tasks within a hierarchic layer suggests that all tasks within the layer can be solved in parallel on different processors of a scalable parallel machine. We have applied our computer program to problems of varied sizes from diverse disciplines [8, 9], and observed the following: (a) sparse matrices generally possess hidden structures well-suited for recursive bbd form; (b) the sparsity of the recursive bbd Cholesky factor competes favorably with reputable sparse matrix ordering methods available in MATLAB [10, 11]; and (c) while our method is subjected to the additional task to find parallelism in sparse matrices, the overall compute time of our C implementation to generate the symbolic factor of PMP^T is noticeably faster [5] than the methods adopted in MATLAB.

REFERENCES

1. Schenck, H. A., G. W. Benthien, and D. Barach. 1995. "A Hybrid Method for Predicting the Complete Scattering Function from Limited Data," *Journal of the Acoustical Society of America*, vol. 98, pp. 3469–3481.

2. Saunders, M. A. 1996. "Cholesky-Based Methods for Sparse Least Squares: The Benefits of Regularization," *Linear and Nonlinear Conjugate Gradient-Related Methods* (L. Adams and J. L. Nazareth, eds.), Society of Industrial and Applied Mathematics (SIAM), Philadelphia, pp. 92–100.

3. Kevorkian, A. K. 1995. "Method and Apparatus for Pre-Processing Inputs to Parallel Architecture Computers," United States Patent Number 5,446,908.

4. Kevorkian, A. K. 1997. "Method and Apparatus for Pre-Processing Inputs to Parallel Architecture Computers," United States Patent Number 5,655,137.

5. Kevorkian, A. K. "Symbolic Factorization of Sparse Symmetric Matrices into Recursive Bordered Block Diagonal Form," SSC San Diego Technical Report (in preparation; contact author).

6. Kevorkian, A. K. "A Computer Program for the Symbolic Factorization of Sparse Symmetric Matrices into Recursive BBD Form," SSC San Diego Technical Report (in preparation; contact author).

7. Saunders, M. A. 1995 to 1999. Private communication.

8. Duff, I. S., R. G. Grimes, and J. G. Lewis. 1989. "Sparse Matrix Test Problems," *Association for Computing Machinery (ACM) Transactions on Mathematical Software*, vol. 15, no. 1, pp. 70–76.

9. George, A., and Joseph Liu. 1981. *Computer Solution of Large Sparse Positive Definite Systems*, Prentice-Hall, Saddle River, N.J.

10. Gilbert, J. R., C. Moler, and R. Schriber. 1992. "Sparse Matrices in MATLAB: Design and Implementation," *SIAM Journal on Matrix Analysis and Applications*, vol. 13, pp. 333–356.

Principal Investigator:
Dr. Aram K. Kevorkian
D712
(619) 553–2058
kevork@spawar.navy.mil

ZU35

Adaptive Stochastic Mixture Processing for Hyperspectral Imaging

Objective(s): Enhance the capability of hyperspectral data-processing systems to more accurately identify materials in image scenes. Develop an algorithm to accomplish spectral-mixture analysis that takes into account the natural variation in material spectra due to sensor noise, illumination conditions, and other factors. Couple this algorithm to a formal detection algorithm to detect anomalous materials or predefined spectral signatures.

Accomplishment(s): Project tasks accomplished during FY 99 were all vital to the formulation of a Stochastic Mixture Processing (SMP) algorithm. The SMP algorithm will be an effective hybrid of two existing approaches to hyperspectral processing: Linear Unmixing (LUM) and Stochastic Expectation Maximization (SEM). We compared these two approaches and found interesting similarities and contrasts that will guide the mathematical development of SMP. Dimensionality reduction may be an important step in SMP for efficient computation and improved performance. We considered two dimensionality-reducing transforms: the Principal Component (PC) and Maximum Noise Fraction (MNF) transforms and found they do not preserve signature signal-to-noise ratio (SNR). We developed a transform that preserves SNR for all spectral signatures lying within a given subspace (the signal subspace), such that the dimensionality of the data is reduced to the dimension of the signal subspace. We have shown the performance of detection algorithms to be improved when the data are preprocessed with this algorithm. We have laid out the general mathematical approach to SMP, and the basic equations have been developed.

BACKGROUND

The availability of spectral-imaging sensors and advanced methods for processing spectral-sensor data have made it possible to accomplish passive remote-material identification (ID) over large areas. However, except for pixels filled entirely with a single material under ideal lighting conditions with low sensor and environmental clutter noise, material ID is difficult and prone to error. Processing techniques have been developed to deal either with mixtures of materials in a single pixel Linear Unmixing (LUM) or with variations in sample spectra from a single material Stochastic Expectation Maximization (SEM), but no processing algorithm as yet deals with both conditions simultaneously. Part of this project's objective was to develop such an algorithm.

Often the purpose of processing image data is to detect the presence and position of a particular target material or anomalous material in the scene. The LUM algorithms and SEM typically do not incorporate target detection as part of the algorithm. LUM algorithms find a basis set of spectra (end-members) and determine the fractional abundance of each end-member in each scene pixel. SEM determines a set of spectral classes contained in a scene and assigns each scene pixel to a class. Target detection in spectral-image data has often been accomplished with spectral-anomaly detectors such as the Reed–Xioali (RX) algorithm or with spectral matched filters, but these detectors often fail because they are based on assumptions of local Gaussian statistics or pure deterministic spectra in the image pixels. This project integrates appropriate formal detection methods with the SMP algorithm developed.

APPROACH

LUM algorithms are based on the linear mixture model of spectral data, and SEM is based on the Gaussian mixture model. Since the underlying model for the SMP algorithm may be considered a hybrid of these two existing models, a good understanding of the strengths and weaknesses of each is vital in our development of the SMP approach. Thus, the first project task was to undertake a thorough investigation and comparison of both models. The next task was to lay out the basic mathematical approach to achieve SMP and write down the basic equations. In the process of accomplishing this task, we realized that a reduction in the dimension (number of information channels) of the spectral data to be processed was going to be an important part of an efficient SMP algorithm. We then sought a transform that would reduce the dimensionality of the data while preserving target signature signal-to-noise ratio (SNR). The remaining tasks would be to work out the details of the mathematical approach described below, implement the algorithm in computer code, and test the algorithm against SEM, RX, and LUM algorithms on actual sensor data.

COMPARISON OF LINEAR MIXTURE AND GAUSSIAN MIXTURE MODELS

The similarities between Gaussian-mixture and linear-mixture models for spectral data are surprising. We demonstrated that mathematical parallels exist between a Gaussian-mixture model and a linear-mixture model for characterization and classification of hyperspectral imagery. Although the underlying models are based on very different assumptions, we found several conditions under which the results from each had very similar qualities in a global sense. The mathematical parallels show that statistics estimated for fitting spectral data with stochastic models are analogous to some properties estimated with deterministic linear-mixture models. We have also empirically demonstrated the similarity obtained through examination of hyperspectral data (figure 1). These results indicate that the similarities are quite striking. Additionally, we observed cases where there was not a one-to-one correspondence between the analogous parameters for a given portion of actual data. Further examination of these differences and similarities may lead to a better understanding of the applicability of each model and will guide the development of techniques based on the generalized SMP model.
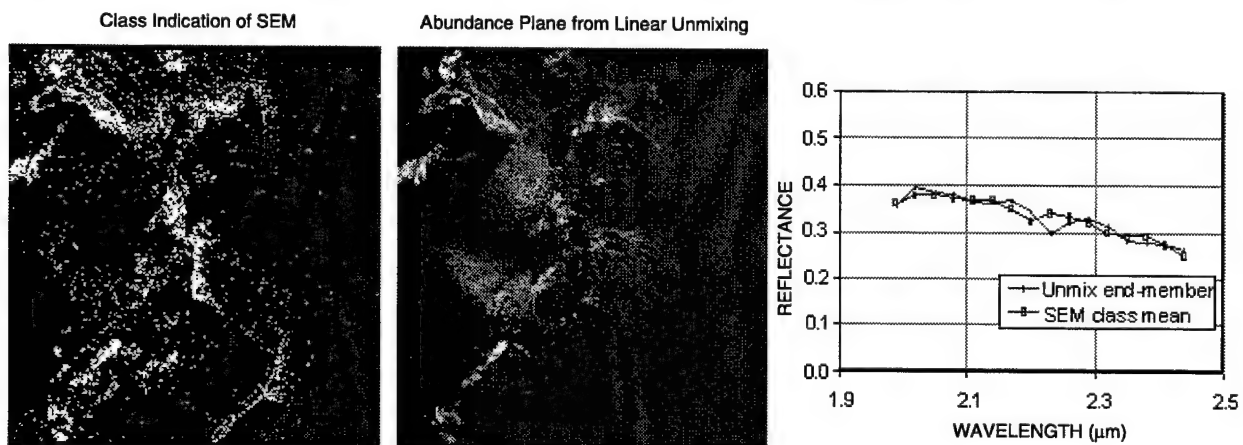

Figure 1. *Comparison of the class map from the Gaussian-mixture model (left) with the end-member fractional abundance (center) for class pair C. The mean spectrum and end-member spectrum for this pair (right) had a spectral angle difference of 2.7°.*

76

DIMENSIONALITY REDUCTION

The Principal Component (PC) and Maximum Noise Fraction (MNF) transforms are commonly used in analysis of hyperspectral data to reduce the dimension of the data and to determine an appropriate subspace for further analysis. The PC transform projects the original data onto the subspace spanned by the k eigenvectors of the data covariance matrix having the k-largest eigenvalues. The mean-square difference between the original image and the transformed image is the sum of the eigenvalues of the eigenvectors in the kernel of the transform. The PC transform defines the reduction to a given dimension having minimal mean-square error. The MNF transform is a generalization of the PC transform that was developed to separate sensor noise from image variance. Using the solution to a generalized eigenvector problem, a linear transform is defined that separates the hyperspectral or multispectral image cube into uncorrelated planes sorted in order of decreasing noise-to-signal-plus-noise ratio, defined in this context to be the ratio of the variance of the sensor noise to the variance of the observations. The MNF transform projects the data onto the subspace spanned by the k-generalized eigenvectors for which this ratio is smallest. These transforms have been used to reduce the dimension of hyperspectral data to simplify subsequent processing such as end-member selection.

A principal military use of hyperspectral data is the identification of anomalous materials and the determination of the presence or absence within a scene of a predefined set of materials. For these applications, mean-square error may not be an appropriate measure of the effect of data-reduction methods on image quality. For algorithms based on an additive signal model, such as the RX algorithm and the spectral matched filter that are widely used in the processing of hyperspectral and multispectral data, the SNR ratio is an appropriate metric. We determined the effect of linear transforms on the SNR ratio, and we showed that losses in SNR could result from the application of the PC and MNF transforms. However, dimensionality reduction may be an important step in many hyperspectral-processing algorithms. Therefore, we developed a transform using a generalized eigenvector (GEV) approach that preserves SNR for all spectral signatures lying within a given subspace (the signal subspace), such that the dimensionality of the data is reduced to the dimension of the signal subspace. The performance of the RX algorithm, given by a probability of detection, increases with SNR and decreases as the number of bands, i.e., the number of degrees of freedom increases. Thus, if the signatures of interest are contained within a lower dimensional subspace, performance of the RX algorithm can be improved by preprocessing with this transform.

To evaluate the relative performance gains due to dimensionality reduction and the significance of an SNR-preserving transform, a spectral matched filter was applied to hyperspectral data containing a target of interest after the application of various transforms to reduce the dimension of the data. The PC and MNF transforms, each retaining 5 bands, and the GEV transform with both 2 and 5 bands were applied. Additionally, the RX algorithm was applied to the original 48-band data and to the data reduced to 5 and 2 dimensions using the GEV transform. The SNR of the output image was computed and compared with the SNR of a full 48-band spectral matched filter, and the results are presented in figure 2. The PC and MNF transforms reduce the SNR by 5 and 2.5 standard deviations, respectively, whereas the generalized-eigenvector transform produces less than 0.5 reduction in SNR. One can also see the improvement in the performance of RX when the dimension of the data is reduced by using the GEV technique.
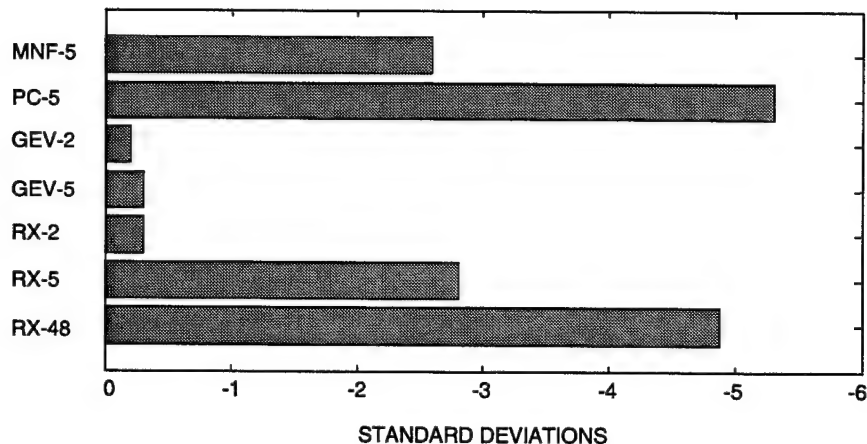
Figure 2. Relative performance of detector algorithms after dimensionality reduction by various transforms.

MATHEMATICAL APPROACH

The stochastic unmixing algorithm models the signature from each pixel as a convex combination of spectra such that each signature emanates from a class having a multivariate normal distribution and such that the coefficients have a logistic normal mixture distribution. Unmixing is then a matter of determining the contribution from each class and the corresponding coefficients. This will be achieved by constructing an iterative solution of the maximum likelihood equations. Matched-filter and anomaly-detection algorithms will be readily constructed from this formulation. The anomaly detector will be constructed by comparing the probability of the unmixing solution to a threshold. The matched filter will be obtained by computing the probability of the unmixing solution under H_0, i.e., by using the background classes estimated from the data, and under H_1, i.e., by using the background classes and a set of classes of targets of interest, forming the likelihood ratio, and comparing it with a threshold.

A stochastic unmixing algorithm will be very interesting to hyperspectral-data-exploitation programs that involve identification of materials. Follow-on work would include tailoring the SMP algorithm to specific applications and incorporating the algorithm into standard hyperspectral-data-processing software packages or workbenches.

Principal Investigator:
Dr. Stephen E. Stewart
D743
(619) 553–2546
stewart@spawar.navy.mil

Co-Investigators:
Dr. David W. Stein
D743
(619) 553–2533
stein@spawar.navy.mil

Dr. Scott G. Beaven
D855
(619) 553–4186
sbeaven@spawar.navy.mil

ZU76

78

Super-Composite Slotted-Cylinder Projector

Objective(s): Explore and demonstrate the bending-extension (b-e) coupling effect of (graphite/epoxy) two-layered cross-ply laminates for potentially substantial improvements (e.g., substantial reductions in fundamental frequencies) of low-frequency, wall-driven composite projectors, such as the slotted cylinder projector.

Accomplishment(s): Vibration tests have been conducted on the flat and the curved bare-beam and actuator-beam specimens (mainly fabricated in FY 96) with two-layered and near-symmetric graphite/epoxy cross-ply laminated composites. All flat specimens have been tested in both the simply supported and the free-free boundary conditions, whereas all curved specimens have been tested in only the free-free boundary conditions because they cannot be tested in the current testing fixtures for simple supports. For all bare-beam specimens, excellent data have been obtained: (a) With the simple supports, the average experimental data on the fundamental (resonant) frequency and the relative fundamental frequency obtained from the flat specimens are within 2% of the predictions by the available analytical solutions. (b) With the free-free supports, the average experimental data on the relative fundamental frequency obtained from the flat and curved specimens are identical; either is almost the same (with a difference of 1.15%) as that obtained from the simply supported flat specimens. For the actuator-beam specimens, only a few have yielded good data, whereas the others may need to be refabricated and retested due to suspected loss of bonds between the actuator and the composite for specimens fabricated in FY 96.

This project is an outgrowth of our research on developing super-performance low-frequency, wall-driven composite projectors, which use piezoelectric translator (PZT) or high-energy density active materials as actuators and fiber-reinforced composites with bending-extension (b-e) coupling properties as radiator materials. The technical focus has been on exploring and demonstrating the b-e coupling effects for potential substantial (up to 20 to 40%) improvement in either resonant frequency or size reductions of the low-frequency, wall-driven composite projectors currently used in mobile and deployed ocean-surveillance systems. Obviously, the size-reduction improvement is particularly desirable for the Navy because it would reduce platform limitations and drag limitations in the case of towed sources, and it would reduce the costs of making and operating these projectors.

As is well known, the basic acoustic radiation mechanism for all wall-driven projectors is the conversion of the extensionally actuated deformation of the actuator into the bending motion of the radiator (thereby radiating acoustic waves through water for detecting targets such as submarines). In light of this, it seems beneficial to study the use of a radiator material with inherent b-e coupling properties, such as the N-layered regular (equal-thickness layers) anti-symmetric cross-ply laminate. For such a b-e coupled composite, the largest coupling occurs at N = 2 (two-layered cross-ply laminate), whereas the coupling vanishes as N (even number) approaches infinity (homogenized or near-symmetric cross-ply laminate).

Exploratory theoretical studies [1, 2, 3] were sponsored by ONR in FY 94 and SSC San Diego in FY 95. The studies covered the (in-air) free-vibration and induced-strain actuation of b-e coupled

composite beams bonded to one side or both sides with actuator(s) as well as split cylindrical shells bonded to their concave side with an actuator. These studies favorably concluded that substantial bending-deformation increases and fundamental frequency reductions of the simply supported composite beams and split cylinders can be achieved with graphite/epoxy, Kevlar 49/epoxy, and s-glass/epoxy two-layered cross-ply laminates, as compared with near-symmetric cross-ply laminates.

In FY 96, to confirm the theoretical discoveries, SSC San Diego sponsored experimental investigations on the static bending and free vibration of simply supported graphite/epoxy two-layered (i.e., b-e coupled) and near-symmetric cross-ply laminated beams and split cylinders. We also studied the induced strain actuation and free vibration of the above-mentioned beams and split cylinders bonded with a PZT actuator to one side of the beams and to the concave side of the cylinders. We planned a program of controlled experiments. San Diego State University (SDSU) was then contracted to fabricate specified test specimens and to conduct planned static and dynamic tests to obtain the data required for comparisons with theoretical predictions.

In FY 97 and FY 98, both SSC San Diego and SDSU struggled to make progress under the constraints of no funding. SDSU completed fabrication of most of the specified flat and curved (i.e., half-circular cylindrical) specimens and started to run a limited number of free-vibration tests on beam specimens. SDSU found that these test specimens were easier to test in the free-free boundary conditions than in the planned, simply supported boundary conditions. Interestingly, these free-free boundary conditions were exactly those used for an operating slotted-cylinder projector. Moreover, in an FY 98 planning meeting, this research was identified by Scott Littlefield for ONR 6.2 transition, and the "Innovative Composite Shell Project" formed the basis for improving the ONR-favored slotted-cylinder projector.

In FY 99, mindful of the specific application of the slotted-cylinder projector, we proposed to conduct beam-vibration experiments with not only the simply supported composite-beam conditions, but also with the free-free boundary conditions. In these experiments, we found that: (a) Fundamental frequency data were unattainable from the curved specimens in the simply supported boundary conditions with the current specimen geometry of a half-circular cylindrical shell and the fixed-distance-apart supporting roller and sharp edge. (b) For all bare-beam (i.e., without actuator) specimens, excellent fundamental frequency and relative fundamental frequency (the ratio of the fundamental frequency of the two-layered composite and the near-symmetric composite) data were obtained from free-vibration tests with five different ways of mechanical excitation: fingernail flick, soft/hard hit with a large rubber mallet, and soft/hard hit with a small modal hammer. (c) For most of the actuator-beam specimens, erroneous data were obtained, probably resulting from the loss of bonds between the actuator and the composite since most of these bonds had been made in FY 96; these specimens might need to be refabricated and retested.

The excellent data obtained for all bare-beam specimens are highlighted in the following tables. Table 1 shows the consistency of the fundamental frequency data obtained by five different ways of mechanical excitation of the flat specimens with simple supports. Table 2 shows the remarkable (i.e., 2%) difference between the (specimen) average experimental data and the theoretical predictions in the fundamental frequency and the relative fundamental frequency of flat specimens with simple supports. Remarkably, table 3 shows that the average experimental data on the relative fundamental

frequency obtained from the free-free supported flat and curved specimens are identical; either of them is almost the same (with a difference of 1.15%) as the flat specimens with simple supports.

Table 1. Fundamental frequency (Hz) of flat bare-beam specimens with simple supports.

Mechanical Excitation	Two-Layered		Near-Symmetric	
	Specimen 1A	Specimen 1B	Specimen 2A	Specimen 2B
Nail Hit	148	150	246	244
Hammer (Soft)	148	152	244	246
Hammer (Hard)	148	152	244	242
Small Hammer (Soft)	148	150	246	246
Small Hammer (Hard)	148	150	244	244
Average	149.4		244.6	

Table 2. Comparison of the (average) experimental data with the theoretical predictions in the fundamental frequency and the relative fundamental frequency of flat bare-beam specimens with simple supports.

		Experiment	Prediction	Difference
Fundamental Frequency	Two-Layered	149.4 Hz	150 Hz	−0.40%
	Near-Symmetric	244.6 Hz	241 Hz	1.49%
Relative Fundamental Frequency		(149.4 / 244.6 =) 0.610	(150/241=) 0.6224	−1.99%

Table 3. Comparison of the (average) experimental data on the relative fundamental frequency of free-free supported flat and curved bare-beam specimens with that of simply supported flat ones.

	Fundamental Frequency (Hz)		Relative Fundamental Frequency	
	Two-Layered	Near Symmetric	Free-Free Supported	Difference (vs. 0.610 for Simply Supported, Flat Bare-Beam)
Flat Bare-Beam	331.2	536.8	(331.2/536.8 =) 0.617	1.15 %
Curved Bare-Beam	238.0	386.0	(238.0/386.0 =) 0.617	1.15 %

REFERERENCES

1. Tang, P. Y. 1995. "Bending Deformation Increase of Bending-Extension Coupled Composite Beams Bonded with Actuator(s)," *Proceedings of the Second International Conference on Composite Engineering (ICCE/2)*, 21 to 24 August, New Orleans, LA, pp.743–744.

2. Tang, P. Y. 1995. "Fundamental Frequency Reduction of Bending-Extension Coupled Composite Beams Bonded with Actuator(s)," *Proceedings of the* Coupled Composite Beams Bonded with Actuator(s)," *Proceedings of the Society of Engineering Science 32nd Annual Technical Meeting*, 29 October to 1 November, New Orleans, LA, pp. 609–610.

3. Tang, P. Y. 1996. "Induced Strain Actuation of Bending-Extension Coupled Composite Split Cylinders," *Proceedings of the International Society of Optical Engineering (SPIE) 1996 Symposium on Smart Structures and Materials*, 26 to 29 February, San Diego, CA, vol. 2715, pp. 670–681.

Principal Investigator:
Dr. Po-Yun Tang
D746
(619) 553–1938
tang@spawar.navy.mil

ZU77

OTHER RESEARCH

Detection of Ionic Nutrients in Aqueous Environments Using Surface-Enhanced Raman Spectroscopy (SERS)

Objective(s): Develop thiol-coated Surface-Enhanced Raman Spectroscopy (SERS) substrates to detect ionic nutrients, particularly nitrates, sulfates, and phosphates, in aqueous environments.

Accomplishments(s): We demonstrated that cationic-coated, SERS substrates could be used to detect nitrate and sulfate. The adsorption of these anions onto these coatings is described by a Frumkin isotherm. In the linear regions of the concentration curves, the limits of detection for nitrate and sulfate were in the ppm range. Using longer integration times, ppb detection was possible. We also developed a means of adhering thin gold and silver films onto glass while retaining the SERS response.

For the Navy, information on nutrient dynamics is useful to understand chemical reactions that impact marine environmental quality and to predict the distribution, growth, and community structure of biota in the coastal ocean. When waste waters that contain anionic nutrients are discharged into surface waters, they can promote the unnatural growth of blue-green algae that crowd out other plant and animal life. The decay of dead algae causes a reduction in the amount of dissolved oxygen available in the water. Eventually, the excess concentration of nutrients in the body of water results in the inability to support any other life forms (eutrophication). These ionic pollutants have also been blamed for the increased incidences of red tide—blooms of toxic, single-celled organisms that have caused die-offs of fish, dolphins, manatees, and other aquatic animals. While these ionic pollutants can enter the water supply by a number of natural means, the significant sources are the result of man-made processes: fertilizers used in agriculture and effluents from sewage treatment plants. A need exists to monitor these ionic pollutants continuously, simultaneously, in real time, *in situ*, and with little or no sample preparation. Such a sensor needs to be able to differentiate the ionic species, not suffer from interferents, be able to detect ppm concentrations of pollutants, and be reversible.

We are developing cationic-coated, silver substrates to detect anionic nutrients in aqueous environments by surface-enhanced Raman spectroscopy (SERS). The following cationic thiols are commercially available: cysteamine (CY) hydrochloride, 2-dimethylamino-ethanethiol (DMA) hydrochloride, diethylamino-ethanethiol (DEA) hydrochloride, L-cysteine ethyl ester (CYE) hydrochloride, and 2-mercapto-4-methylpyrimidine (MMP) hydrochloride. We have prepared silver electrodes which, after electrochemical roughening, have been reacted with the cationic thiols to form a self-assembled monolayer (SAM). To date, the response of these cationic thiols to nitrate and sulfate in the absence of chloride ion has been characterized. Figure 1 shows SERS spectra obtained for Ag/CY in the presence of sulfate, and figure 2 shows the concentration response. The adsorption of these anions onto these coatings is described by a Frumkin isotherm: $\theta = \dfrac{cKe^{2g\theta}}{1+cKe^{2g\theta}}$ where θ is the fractional coverage of the analyte in the coating, c is the solution concentration of the analyte, K is the ion-pair formation constant, and g is the Frumkin parameter. Table 1 summarizes the values obtained for K and g as well as the limit of detection (LOD). For both nitrate and sulfate ions, it was found that g has a negative value, which indicates the presence of a repulsive force upon adsorption.

85

In the linear regions of the concentration curves, the limits of detection for nitrate and sulfate using these coatings were in the ppm range. Using longer integration times, ppb detection was possible. We have also examined means of adhering thin gold and silver films (< 50 nm) on glass while retaining
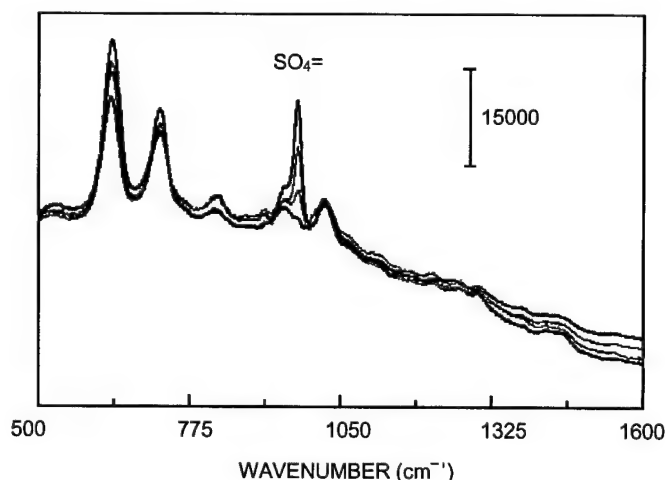
Figure 1. SERS response of cysteamine hydrochloride on silver as a function of sulfate concentration (0', 10', 100', and 2500-ppm sulfate).
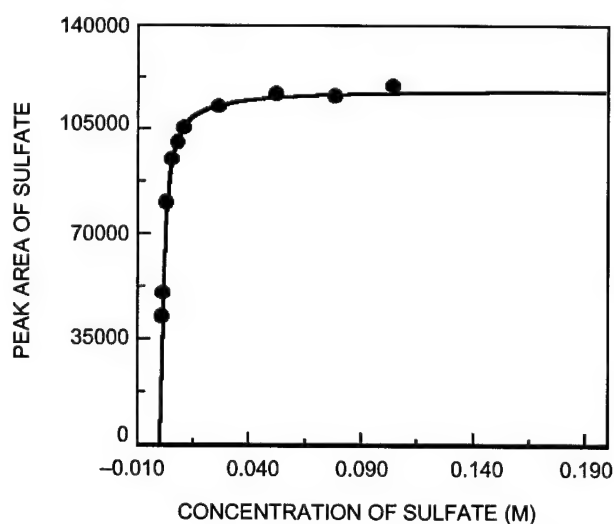
Figure 2. Sulfate peak area plotted as a function of sulfate concentration for cysteamine hydrochloride on silver.

the SERS response. Using thin metal films allows one to acquire data by using a "backside" configuration for data collection. This configuration is particularly advantageous for aqueous samples. In the backside configuration, the laser light is focused through the thin metal film onto the coated surface that is exposed to the sample. Since the laser light does not appreciably pass through a liquid film, any fluorescence interference is minimized as well as attenuation of the near infrared (IR) excitation by the water. Although thin island films of silver and gold exhibit large SERS response and, consequently, great sensitivity, they do not adhere well to glass, and significant exposure to water damages them. Three approaches were investigated to solve this problem. These methods included the use of

an adhesive metal (chromium (Cr) or titanium (Ti)) between the SERS-active metal film and the glass substrate; the use of (3-mercaptopropyl) trimethoxysilane (MCTMS); and the use of organo-metallic paints. Of the methods examined, the best film adherence and SERS response were obtained by using MCTMS to bind the metal film to a chemically etched glass slide.

Table 1. Summary of the ion-pair constants (K in M^{-1}), Frumkin parameters (g), and limits of detection (LOD) obtained for the interaction between the cationic thiols and either nitrate or sulfate ion.

Cationic Thiol	Nitrate Ion	Sulfate Ion
cysteamine (CY) hydrochloride	K = 350 ± 50 g = –0.33 ± 0.26 LOD = 4.2 ppm	K = 1000 ± 200 g = –0.27 ± 0.23 LOD = 4.7 ppm
dimethylamino-ethanethiol (DMA) hydrochloride	K = 330 ± 90 g = –0.82 ± 0.96 LOD = 6.0 ppm	K = 880 ± 140 g = –0.92 ± 0.22 LOD = 3.7 ppm
diethylamino-ethanethiol (DEA) hydrochloride	K = 190 ± 50 g = –0.66 ± 0.48 LOD = 5.3 ppm	K = 680 ± 50 g = 0.06 ± 0.08 LOD = 5.8 ppm
L-cysteine ethyl ester (CYE) hydrochloride	K = 350 ± 70 g = –0.43 ± 0.21 LOD = 14.0 ppm	No interaction was observed to occur
2-mercapto-4-methylpyrimidine (MMP) hydrochloride	K = 1780 ± 520 g = –1.66 ± 0.51 LOD = 9.8 ppm	Could not detect due to spectral interference

Principal Investigator:
Dr. Pamela A. Mosier–Boss   ZU55
D363
(619) 553-1603
bossp@spawar.navy.mil

Frequency Mixing in Nonlinear Dynamic Devices

Objective(s): To examine the response of a nonlinear dynamic system/sensor to a weak-target cyclic signal in noise, while introducing a known heterodyne cyclic signal to periodically modulate the system parameters; determine the conditions under which this procedure can lead to an enhancement (possibly in excess of "conventional" stochastic resonance (SR)) of the system response to the target signal, or, the conditions under which the device response to the cyclic signal can be annulled.

Accomplishment(s): We demonstrated a general nonfeedback control method that can both enhance the "classical" stochastic resonance effect and also suppress the response to a weak cyclic signal. Our experiments were carried out on a generic stochastic resonator (a modified Schmitt trigger as well as a potential system characterized by finite relaxation times in each stable state). The control was expected to be realizable, however, in a larger class of nonlinear dynamic systems in which internal parameters are externally accessible; it should be contrasted with the case of multiple cyclic signals applied additively at the input of a nonlinear device. In the latter case, the output contains "combination resonances" of the input frequencies. We believe that controlled SR may be useful in applications as diverse as the cancellation of power-line frequencies in very sensitive magnetic sensing applications with Superconducting Quantum Interference Devices (SQUIDs), vibration control in nonlinear mechanical devices, as well as in the context of electromagnetic field interactions with neuronal tissue where control of internal thresholds is possible and the selective suppression of specific frequencies could potentially be beneficial.

The basic idea behind "classical" stochastic resonance (SR) is the tuning, in a nonlinear device with a threshold or potential energy "barrier" separating stable states, of a deterministic time scale (the period of a weak *sub*threshold cyclic input or "target" signal) with a stochastic time scale (the mean exit time from a stable state of the device, in the presence of the noise). Such a tuning, aimed at optimizing the periodic character of the response, can be achieved either by changing the noise intensity or by adjusting the intrinsic system parameters such as barrier heights or thresholds. Hence, under the appropriate conditions, the background noise ceases to be a source of degradation better suppressed, and can actually become a part of the intrinsic system dynamics, leading to an enhancement in the response of the system to the signal of interest. In recent years, SR has gained widespread interest and has been observed in many different physical and biological systems. Variations and extensions of the classical definition of SR include aperiodic (e.g., dc or wideband) signals with the detector response quantified by various information-theoretic, or spectral cross-correlation measures. These approaches carry particular significance for neurophysiological applications.

Our work consisted of experiments wherein we demonstrated a *controlled SR* effect that is tantamount to an enhancement (or suppression) of the fundamental SR effect via the modulation of an internal system parameter. The experiments were carried out in a modified Schmitt trigger (ST) electronic circuit, which is one of the simplest threshold systems—a static hysteretic nonlinearity that is well-characterized. Concurrently with this work, a theoretical analysis of the ST response, via two-

state system dynamics, was carried out—the goal being to determine, analytically, the conditions under which a suppression of unwanted signal effects could be achieved. The experiments were conducted at the Applied Chaos Laboratory, Georgia Institute of Technology, with theoretical work conducted at SSC San Diego; Georgia Tech; University of Augsburg, Germany; and the University of Perugia, Italy.

The experiments (and supporting calculations) elucidated a very rich phenomenology created by the interplay of the two driving frequencies (applied externally, and to the threshold or energy barrier) as seen in the output power spectral densities (PSDs) of the driven ST, and the two-well potential system. Specifically, for relatively large barrier modulation amplitudes, digital simulations of the ST reveal "dips" and peaks in the power spectra at combination tones corresponding to the sum and difference frequencies generated by integer multiple combinations of the modulation and barrier frequencies. The phase offset between the signal and barrier frequencies, as well as the ratio of the frequencies, appeared to determine the locations of the peaks and dips. Note that the signal and barrier modulation amplitudes were always taken to be less than the barrier separation (the height of the potential "wall" or the separation of the levels in the ST). Shifting the phase to pi/2 resulted in strong peaks embedded within the same dips. For double frequency modulation (barrier frequency = twice signal frequency) and zero phase offset, the power spectrum displayed sharp peaks at odd multiples and dips at even multiples of the fundamental signal frequency (i.e., the dips occurred at integer multiples of the barrier frequency). For a pi/2 phase offset, the signal peaks were *suppressed*. An exploration of all the observed features in the output PSDs was beyond the scope of this effort. Instead, following a summarization of the experimental results, the remainder of the project was aimed at reproducing the experimental results for the signal output power at the fundamental frequency, for the special (and somewhat limited) case of small signal and barrier modulation amplitudes, via a perturbation development. Hence, the theory cannot reproduce all the features of the numerically generated results obtained by using relatively strong barrier modulation amplitudes.

Principal Investigator:
Dr. Adi R. Bulsara
D364
(619) 553–1595
bulsara@spawar.navy.mil

ZU79

Anti-Ice Coatings: New Low Surface Free Energy Coatings for Easy Ice-Release

Objective(s): Investigate new low surface free energy materials for easy ice-release applications (e.g., aircraft surfaces). These materials have the potential to replace or reduce the need for conventional chemical de-icing systems that are of environmental concern.

Accomplishment(s): The previous apparatus for measuring ice-release properties of candidate coatings was redesigned and computer-interfaced to accommodate the experimental methodology developed for screening potential materials and coatings in FY 98, and to more precisely measure the experimental parameters of interest.

This research was directed at providing an optimal coating surface upon which ice can adhere only weakly and be removed easily by minimal physical mechanisms (mechanical or thermal), rather than by environmentally unfriendly chemical processes (glycol-based freezing point depression). Chemical de-icing and anti-icing processes rely on the use of large quantities of chemicals that are subject to potential environmental regulation and treatment. Anti-ice coatings are an alternative to current chemical de-icing/anti-icing strategies and would result in a substantial decrease in chemical usage. Thus, this work addressed issues in wastewater treatment and hazardous materials management (minimization, reuse, and recycling) policies put forth by DoD agencies and the Environmental Protection Agency (EPA).

Recent advances in the area of new low surface energy materials for use in other coating applications has resulted in a range of new materials with low surface free energies. Low surface free energy materials are known for interacting only weakly with polar liquids, are generally robust, and are capable of withstanding harsh environmental conditions for extended periods of time. For many years, U.S. Navy efforts in this materials area have focused on using low surface free energy as a beneficial approach to preparing materials suitable for marine fouling environments. These low surface free energy materials are designed to work by minimizing the adhesion strength between marine organisms and their substrata (i.e., ship hulls, heat exchangers, power plant intakes, etc.)—an approach based on the thermodynamic work of adhesion between a solid and a liquid adherent (equation 1). The work of adhesion, or work required to separate the adherent from the solid (W_{sl}), is the sum of the surface free energies of adherent (γ_l) and solid (γ_s), minus the interfacial tension between the solid and adherent (γ_{sl}). A weaker adhesion results from lowering the surface free energy of the solid.

$$W_{sl} = \gamma_s + \gamma_l - \gamma_{sl} \qquad (1)$$

The hypothesis for ice-release is that if a liquid (water) does not wet a surface, it will not be able to adhere well when it becomes a solid (ice). An underlying mechanism for this theory may be related to a reduction of the actual contact area between the adherent and low energy surface.

Previous research at SSC San Diego was directed at preparing extremely low free energy surfaces for biofouling release. Useful chemistries were successfully demonstrated by preparation of comb-like polymers with siloxane, polyacrylate, and polymethacrylate backbones with perfluorinated sidechains.

Perfluorinated siloxanes exhibited excellent performance and properties but were considered too costly. Perfluorinated acrylate/methacrylate homopolymers exhibited low surface free energies but had undesirable physical properties. Perfluorinated acrylate/methacrylate copolymers showed low surface free energies, good physical properties, and economic feasibility.

The technical approach of this work was to use and transition existing knowledge, new materials, testing methods, and lessons learned from fouling-release coatings technologies into ice-release coatings. Initial efforts focused on new low surface free energy materials that were developed in-house for the fouling-release-coatings applications described above. Coatings prepared and evaluated for ice-release were screened for removal of ice under a minimal stress, or shear abhesion (release under shear due to low adhesion strength), by measuring the force required to remove ice from the coating. For this purpose, test instrumentation was designed and fabricated, and a protocol was developed for performing such measurements routinely. Ice-release screening to date has resulted in an initial down-selection of over 20 different coatings for materials previously prepared in this laboratory. Coatings prepared from these materials have been characterized and ice-adhesion measurements performed as a function of fluorine content, polymer structure and molecular weight, surface energy, coating crystallinity, and surface roughness. Figure 1 shows ice-release measurements for a representative series of materials differing only in fluorine content and coating type. Replicate samples of each type of coating were evaluated for initial ice-release. Additionally, each type of coating was subjected to repeated freeze-release-thaw cycles for evaluating physical toughness and release reproducibility. Homopolymer coatings did not appear as robust as copolymer coatings when subjected to multiple ice-release cycles. In general, and as illustrated by figure 1, those coatings prepared from materials that are nominally 50% fluorinated appear to exhibit the lowest ice-adhesion values.
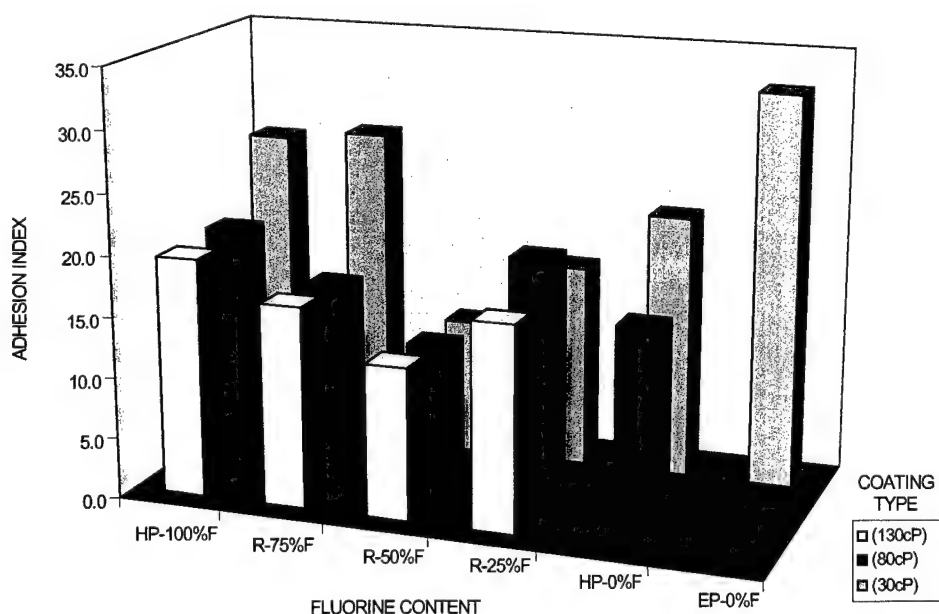
Figure 1. Ice-release properties of a low surface free energy coating series as a function of fluorine content (%F) for three types of coatings prepared with a design for varied coating crystallinity (30, 80, and 130 cP). A lower adhesion index indicates better ice-release.

Other preliminary work has focused on surface chemical/structural characterization for this type of coating and its interaction with water while using polarization-dependent surface infrared reflection spectroscopy.

Principal Investigator:
Dr. Robert D. George
D361
(619) 553–2776
george@spawar.navy.mil

ZU57

Propwash/Wake Resuspension in San Diego Bay (The Grand Plan III)

Objective(s): Reliably estimate the resuspension of bottom sediment due to the transit of vessels through San Diego Bay. This work is important because many water pollutants are attached to fine grain sediment, and sediment transport also has implications for planning of maintenance dredging operations.

Accomplishments(s): We built a well-characterized, closed-flow channel into which sampled sediments can be introduced and the critical shear stress and erosion rates measured. Also, we developed a method to automatically measure sediment erosion rate, and we took several representative sediment samples in San Diego Bay.

The problem of estimating sediment resuspension was divided into four parts:

1. Reliably estimate the ship-induced flow field. We used the Navy's most sophisticated, ship-wake numerical simulations (CFDSHIP-IOWA and TBWAKE) to calculate the shear stress on a flat bottom, produced by the passage of a ship. In the first year of this project, Dr. Mark Hyman, Naval Coastal Systems Center (NCSC), modified these codes to include a shallow bottom and ran them for an aircraft carrier and a frigate.

2. Determine the critical shear stress of the bottom sediment necessary to initiate resuspension. For cohesive sediments, such as those in San Diego Harbor, there is presently no way of predicting critical bed shear stress as a function of flow conditions. Consequently, we built an experimental flow channel to directly measure the onset of erosive shear stresses as a function of sediment depth. To obtain undisturbed samples of sediment, we designed and built a sampling tube that is used in a standard core sampler and then directly introduced to the flow channel. This flow channel has been used to measure the critical shear stress and rate of erosion of sediment core samples taken at selected locations in San Diego Bay.

3. Reliably estimate the response of the bottom sediment to the ship-induced flow field. Dr. Scott Jenkins and colleagues at Scripps Institution of Oceanography (SIO) developed a numerical simulation (SEDXPORT) to predict the transport of cohesive fine sediments, given the hydrodynamic forcing and critical shear stress. Output of the model included particle size and number distributions at each depth increment throughout the water column; bottom erosion and deposition patterns; and rates of change of these features. Over the last 2 years, Dr. Jenkins modified his code to accommodate the output of Dr. Hyman's simulation, which estimates the velocity field throughout the water column and the shear stress at the bottom. Work is in progress to take those critical shear stresses (measured in 2, above) and predict the fate of disturbed bottom sediment in selected locations in San Diego Bay.

4. We originally planned to perform field tests to validate the model. We were to use the Research Vessel (RV) ECOS (and associated capabilities, e.g., acoustic Doppler current profiler [ADCP]; conductivity, temperature, and depth [CTD]; transmissometers; and the global positioning system [GPS]) to identify and track the resuspended sediment footprint of an aircraft carrier, after it had passed through the shipping channel to San Diego Harbor. Preliminary experiments have shown that this is possible. However, incomplete funding prevented us from completing this task.

The portion of tasks directly funded by the ILIR program, in this and previous fiscal years, was the construction of the sediment flow channel (as previously described in 2).

Figure 1 shows the test section of the flow channel where the sediment is introduced. The working section of the channel is rectangular: 20 mm high, 254 mm wide, and 2.438 m long. The high aspect ratio (254/20) and long entrance length (2.057 m) ensures fully developed flow at the sediment measurement station. The channel is designed to use seawater as the working medium so as not to alter the chemical properties of cohesive sediments introduced into the working section. Wall shear stress on the channel is inferred from flow-induced pressure drop measurements inside the channel.
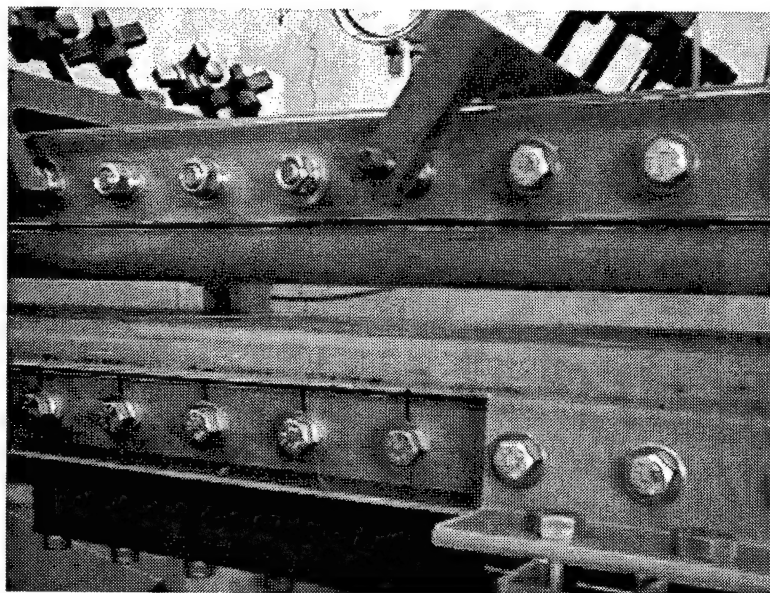
Figure 1. Side view of flow channel. Flow is from left to right. Sediment is introduced through the bottom of the channel through a 140- by 140-mm recess, and sediment height is automatically maintained by a laser displacement sensor coupled to a computer-controlled jacking system.

Figure 2 shows the friction factor of the channel as a function of the flow Reynolds' number (based on hydraulic diameter). The results are very close to traditional measurements of smooth pipe pressure drop (corrected to channel aspect ratio). The flow in the channel can be controlled from 0.035- to 1.73-m/s mean flow velocity, producing a shear stress range from 0.008 to 8.0 Pa (three orders of magnitude). This is adequate range to cover the critical shear stress for a huge range of sediment sizes and adhesion.

A measurement system was devised to automatically measure critical shear stress and the erosion rate of sediment introduced through the bottom of the flow channel. A laser displacement sensor measured the height of the sediment in relation to the bottom of the channel. A computer-controlled jacking system kept the top of the sediment even with the channel bottom.

After an erosion rate was determined, the data acquisition program adjusted the flow speed of the channel to another shear stress, such that a curve of erosion rate versus shear stress was generated. Figure 3 is an example of such a curve.
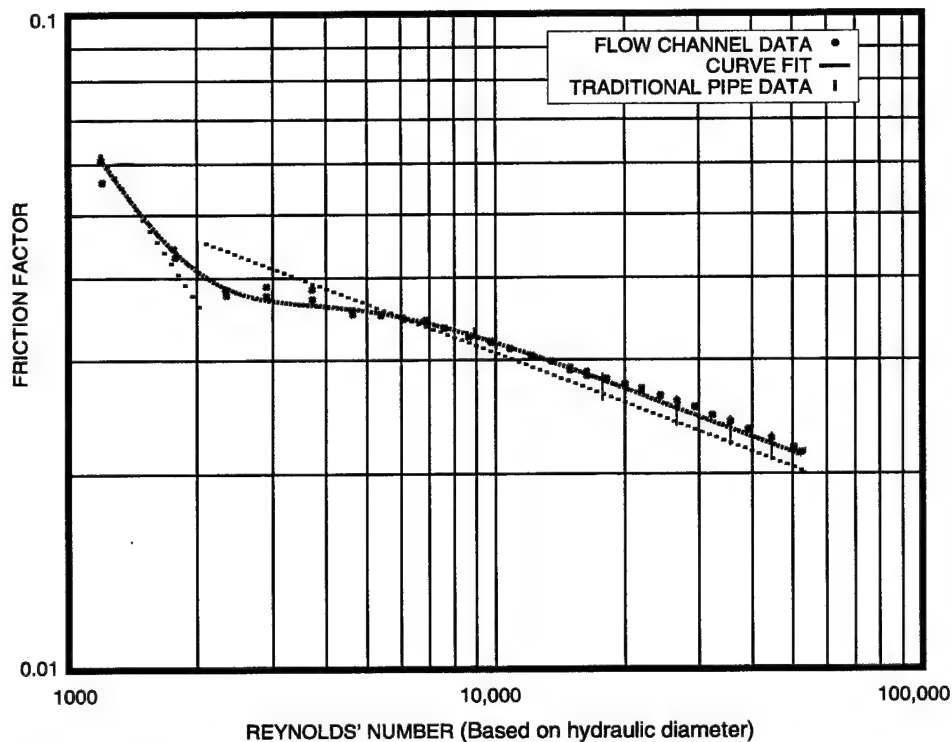
Figure 2. Darcy friction factor data for the flow channel. Curve "traditional pipe data" assumes instant transition from laminar to turbulent flow at Reynolds' number 2300. Actual flows have a smooth transition (as in the present data).
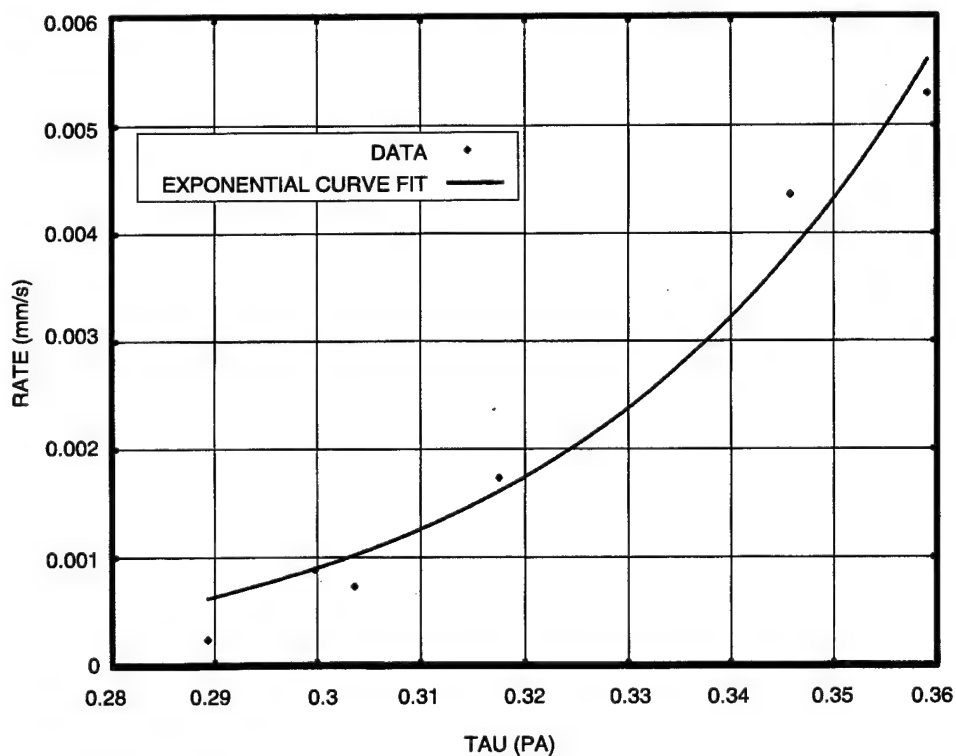
Figure 3. Erosion rate of 300-μm "Ottawa" test sand versus flow shear stress in channel.

95

Great care has been taken in the channel design to preserve the integrity of sediment samples, such that valid critical shear stresses are measured. The critical shear stress measurement is a small, but critical portion of the Grand Plan (from the project title) to track sediment transport in San Diego Bay. The ultimate prediction of the fate of bay sediments is crucial to implementation of Navy environmental policy and maintenance (e.g., dredging) plans for San Diego Bay.

Principal Investigator:
Daniel M. Ladd
D363
(619) 553–1617
ladd@spawar.navy.mil

ZU48

Coherent Mid-Infrared (IR) Optical Parametric Oscillator

Objective(s): Develop and characterize a coherent mid-IR source near 3.6 μm and demonstrate the potential for coherent laser radar applications, including micro-Doppler measurements of target vibration signatures.

Accomplishment(s): Extensive modeling of coherent laser radar performance in littoral environments of Navy interest was completed. The modeling was based on a large database of historical weather observations and included effects of visibility, cloud cover, humidity, and turbulence. In the majority of cases for three typical scenarios studied, it was found that a mid-IR system would give better performance than shorter or longer wavelength systems at equal power. A coherent optical parametric oscillator (OPO) based on periodically poled lithium niobate and a frequency-stable 1-μm pump source was built and demonstrated. This OPO was designed to achieve low continuous wave (cw)-pump threshold operation by resonating both signal (~1.5-μm) and idler (~3.6-μm) waves. However, we only were able to show transient operation due to the small but significant optical absorption of lithium niobate in the mid-IR, which affected the cavity stability. We concluded that an alternative approach using a pump-resonant and signal-resonant cavity design would have to be used. The design and fabrication of the new cavity were begun in late FY 99.

Laser radar techniques to measure small Doppler shifts from hard targets have been successfully demonstrated using laser sources at several wavelengths including 1 μm, 1.5 μm, 2 μm, and 9 μm. It has been shown that skin-vibration spectra due to the target power plant can be obtained and used to identify unknown targets. In many cases, there are no other alternative methods to identify targets at long range. However, in the majority of littoral environments where the Navy operates, atmospheric scattering, turbulence, and humidity can significantly degrade coherent laser radar performance. Scattering and turbulence have a more adverse effect at shorter wavelengths, whereas transmission at the 9- to 10-μm CO_2 laser wavelengths is severely limited by humidity. Performance modeling based on an extensive weather database has shown that, in expected Navy scenarios, coherent laser radar in the mid-IR near 3.8 μm would generally perform better than at shorter or longer wavelengths. Power levels of a few watts and coherence times of a few 100 μs would probably be required for such a laser radar to be useful in eventual fielded military systems. Up to now, sufficiently coherent sources have not been demonstrated in the laboratory at this wavelength.

The goal of this work has been to demonstrate the feasibility of making and operating a frequency-stable optical parametric oscillator (OPO) source at 3.5 to 4 μm with sufficient power for coherent laser radar applications. An OPO source offers wide frequency tunability and the use of the recently developed nonlinear material (periodically poled $LiNbO_3$ [PPLN]), and offers a much larger nonlinear gain than conventional bulk nonlinear materials. Double resonant OPO cavities where both the signal and idler waves are resonated have been demonstrated using PPLN and have shown excellent frequency stability and pump thresholds much less than 1 W. Our approach was similar. We built an OPO cavity using PPLN and a frequency stable 1-μm pump source (< 1 W) that resonated both signal and idler waves at ~1.5 μm and ~3.6 μm, respectively. However, there had not been any published reports of this type of OPO operation in the mid-IR near 3.6 μm.

We were able to show transient operation with this device as the cavity length was ramped through the discrete lengths that simultaneously satisfied the double-resonance conditions. However, we were unable to stabilize the cavity, even with active feedback, due to the small but significant optical absorption of lithium niobate in the mid-IR, which causes heating and a change in the optical path length. It was concluded that an alternative approach using a pump-resonant and signal-resonant cavity design would have to be used. The design and fabrication of the new cavity were begun in late FY 99.

Principal Investigator:
Dr. Frank E. Hanson
D853
(619) 553-2094
hansonfe@spawar.navy.mil

ZU80

Exact Diagonalization of Large Sparse Matrices

Objective(s): Develop computer code capable of diagonalizing large sparse matrices of physical interest and determine solutions other than the one associated with the lowest eigenvalue.

Accomplishment(s): The Density Matrix Renormalization Group (DMRG) method can provide approximate ground-state solutions for the quantum-mechanical, many-body problem for a variety of one- and two-dimensional systems with a high degree of accuracy. We have developed a technique for extending DMRG to investigate arbitrary excited states. As an example, we have applied our method to describe the properties of excitons (bound electron-hole pairs) that can occur during optical excitations of low-dimensional systems. Our results show that excited-state calculations within the standard DMRG procedure give results that are both quantitatively and qualitatively incorrect.

In the Density Matrix Renormalization Group (DMRG) method, a quantum-mechanical system of given size is divided into two pieces: a system block and an environment block. The system is chosen to be small enough so that an exact numerical solution of the ground state can be obtained. Then, the basis of this system can be represented as an outer product of the basis for the system block and the basis of the environment block. The density matrix for the system block is then formed by integrating out the basis of the environment block. This reduced-density matrix usually has dimensions that are on the order of the square root of the dimension of the original system. That allows us to completely diagonalize this matrix. The states with the lowest eigenvalues are then discarded, and only those states with the highest probably of configuration are kept. A reduced Hamiltonian for a system with two additional sites is then formed via an outer product of a complete basis for two new sites and the reduced basis of the system block. This process can be repeated over and over until the system reaches a size of interest.

With this technique, numerical solutions of the ground state of one-dimensional systems have been obtained with excellent accuracy to almost arbitrarily large system sizes. However, as the system size is increased, the repeated pruning of the system basis gradually removes information about excited states. Our work describes a technique whereby excited states, as well as the ground state, are targeted and additional density matrices representing the excited states are formed. All of the density matrices are added, and the resulting matrix is diagonalized, and again this basis is pruned. The eigenvalues do not converge as quickly, and typically more states must be kept to maintain the same level of accuracy, but the information describing the excited state is not lost.

Our technique for targeting excited states was worked out in some detail for a generic one-dimensional system. Optically excited states relevant to both optical absorption and third-order nonlinear optical coefficients were studied. This work is described in some detail in two recent articles [1, 2]. Figures in these references show the convergence of the energy level for states that are relevant for both optical absorption and third-order nonlinear optical processes.

REFERENCES

1. Chandross, M. and J. C. Hicks. 1999. "Density-Matrix Renormalization-Group Method for Excited States," *Physical Review B*, vol. 59, no. 15, pp. 9699–9702.

2. Chandross, M. and J. C. Hicks. 1999. "Low Lying Optically Excited States of Conjugated Polymers with DMRG," *Synthetic Metals*, vol. 102, pp. 928–929.

Principal Investigator:
Dr. Charles Hicks
D3604
(619) 553–1593
hicks@spawar.navy.mil

ZU53

Laser Optical Parametric Oscillator for Mid-Infrared (IR)

Objective(s): Demonstrate a laser-pumped optical parametric oscillator (OPO) tunable over the 2.5- to 5.0-µm-wavelength band.

Accomplishment(s): An intracavity laser-pumped OPO using Ti:Al$_2$O$_3$ (Ti:Sapphire) as the pump source and potassium tri-arsenate (KTA) as the OPO has been designed. The cavity, excluding KTA, has been demonstrated with continuous wave (cw) output to pump efficiencies of 20%. Present available pump sources include a Coherent 5-W Argon ion laser and a 20-W Spectra Physics Argon ion laser. All optics and the KTA have been coated and received. Performance evaluation of the laser is slated as part of the FY 00 research.

Optical parametric oscillators (OPOs) pumped by either continuous wave (cw) lasers such as Nd:YAG (Neodium: Yttrium Aluminum Garnet) [1] or self-mode locked lasers such as Ti:Sapphire [2] have produced outputs in the 1.0- to 5.0-µm-wavelength range with output conversion efficiencies of up to 30%. However, the nonlinear crystals used have poor resistance to damage and have high sensitivity to thermal loads. Although demonstrated in the past, laser-pumped OPOs have yet to be proven reliable in power and tunability. By nature, the nonlinear OPO crystal operates best at high temperatures—thus the need for a robust material. At present, much work is being done to manufacture materials that are both robust and broadly tunable. Various weapons use mid-infrared (IR) emissivity as a guide to their target. The intention of this program is to develop a directional mid-infrared source as an IR countermeasure.

The present configuration uses an intracavity laser-pumped OPO (figure 1). This design allows the OPO to see much higher energy densities than could be obtained with an external-cavity design. In the case of a Ti:Sapphire laser operating at 4.2 W with an output coupling of 10%, the intracavity circulating power is 40 W. This design should, therefore, produce outputs an order of magnitude greater than an external-cavity laser-pumped OPO. The laser pump source is a Ti:Sapphire laser pumped with an Ar$^+$ laser. Ti:Sapphire was selected as the pump source because of its broad tunability. A birefringent filter (BRF) is used to tune the output. It is important to note that by using a noncritically phase-matched OPO, tuning is accomplished by tuning the resonant frequency of the Ti:Sapphire crystal by rotating the BRF. Therefore, this design is not only unique in that the OPO exploits the circulating power, it is also unique because tuning is accomplished with the BRF. The FY 99 proposal stated that the OPO crystal would be Silver Gallium Sulfide (SGS). However, due to cost and availability issues, KTA has been substituted as a first step in demonstrating the concept. KTA is much less expensive and is widely available. The major issues to be addressed with this resonator design, including tunability, efficiency, and suitable output power, can be accomplished more cost effectively with KTA. When these issues have been resolved successfully, it will then be time to substitute SGS for KTA. SGS has the promise of obtaining the desired bandwidth and power requirements necessary to make it a viable candidate for mid-IR countermeasures. The original FY 99 proposal stated that a laser-pumped OPO would be demonstrable by the end of FY 99. Several setbacks have pushed this demonstration into FY 00.
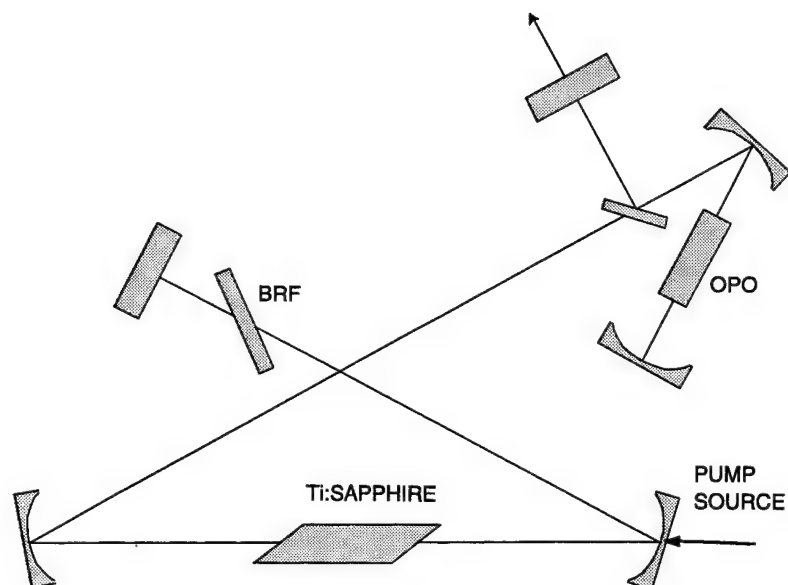
Figure 1. Configuration for intracavity laser-pumped OPO using Ti:Sapphire.

REFERENCES

1. Bosenberg, W. R., A. Drobshoff, and J. I. Alexander. 1996. "Continuous-Wave Singly Resonant Optical Parametric Oscillator Based on Periodically Poled LiNbO$_3$," *Optics Letters*, vol. 21, no.10, pp. 713–715.

2. Reid, D. T., M. Ebrahimzadeh, and W. Sibbett. 1995. "Noncritically Phase-Matched Ti:Sapphire-Pumped Femtosecond Optical Parametric Oscillator Based on RbTiOAsO$_4$," *Optics Letters*, vol. 20, no.1, pp. 55–57.

Principal Investigator:
Joeseph F. Myers
D743
(619) 553–2599
jfmyers@spawar.navy.mil

ZU82

Electronic Properties of Cubic Boron Nitride

Objective(s): Characterize the conductivity and carrier mobilities of semiconducting cubic boron-nitride thin films by using newly developed methods for making ohmic contact to this material.

Accomplishment(s): In preparation for depositing and characterizing metal contacts to cubic boron nitride films obtained from the University of Michigan, we completed a number of tasks, including refurbishment of an ultrahigh-vacuum deposition chamber, design of the required photolithographic masks and processes, and design and fabrication of a wide-temperature-range sample probe for sample transport measurements.

The cubic phase of boron nitride (c-BN) can be made semiconducting by doping with n- or p-type dopants. Because of its wide energy bandgap (approximately 6.4 eV), c-BN is a promising material for high-temperature/high-power electronic devices. Other wide bandgap semiconductors, such as diamond, silicon carbide (SiC), and gallium nitride (GaN), have received much research attention for these applications. However, these materials lack some of the important features of BN, such as stability at high temperatures in oxidizing atmospheres, or the ability to dope as either n- or p-type. One of the major impediments to using BN as a high-temperature semiconductor has been the lack of a good way to make ohmic electrical contact to the material. Since this problem has been overcome only recently, there have been essentially no measurements of the important electronic properties of c-BN, such as carrier mobility, and hence there has been no reliable basis for comparing BN to other semiconducting electronic materials. The first year of this project has focused on addressing the lack of basic materials' information, contacting techniques, and film-property measurement.

The BN contacting method employed in this research is similar to that developed here at SSC San Diego to make such contacts to semiconducting diamond. In that case, a metal such as molybdenum (Mo) is deposited onto the diamond substrate or film and then furnace-annealed, reacting with carbon to form conducting molybdenum carbide. The semiconducting-diamond/carbide combination forms an ohmic contact. For the case of boron nitride, titanium (Ti) metal (followed by diffusion barrier and contacting layers) is used to coat semiconducting c-BN, and the sample is then heated in an inert atmosphere. Ti reacts with BN to form titanium nitride and titanium boride, both of which are conducting.

The results of this project will help determine if c-BN is an appropriate and desirable material for making high-voltage/high-current switches and other solid-state devices to be used in such Navy/DoD/civilian areas of application as switching, control, and power conversion circuits for ships, aircraft, and other vehicles.

Principal Investigator: ZU81
Dr. Wayne C. McGinnis
D364
(619) 553–5610
mcginnis@spawar.navy.mil

Sensitivity of Marine Mammals to Low-Frequency Acoustic Pressure and Particle Motion

Objective(s): Determine the relative contributions of acoustic pressure and particle motion to the low-frequency, underwater hearing abilities of the bottlenose dolphin, white whale, and California sea lion.

Accomplishment(s): We assessed the relative contributions of acoustic pressure and particle velocity to the low-frequency, underwater hearing abilities of the bottlenose dolphin (*Tursiops truncatus*), white whale (*Delphinapterus leucas*), and California sea lion (*Zalophus californianus*). We measured hearing thresholds while manipulating the pressure to particle velocity (p/v) relationship by varying the distance within the nearfield of an underwater sound projector. Two bottlenose dolphins and one white whale were trained to station on an underwater platform and participate in hearing tests. Test subjects were trained to whistle in response to tone + noise trials and to remain silent during noise-only trials. Stimulus intensity was adjusted (while maintaining the p/v ratio) using a modified staircase procedure. Custom software was developed to calibrate the acoustic system, conduct hearing tests, and analyze the resulting data. A custom system was also developed to generate band-limited white noise whose frequency spectrum was compensated for projector response and acoustic standing waves. Masked hearing thresholds were measured at 300 and 400 Hz; measurements at 100 Hz are currently in progress. Future measurements will employ two sound projectors and an active sound control system to manipulate the p/v ratio.

BACKGROUND

Concern that man-made noise in the ocean may compromise the hearing or affect the behavior of marine mammals has given rise to legal actions that have resulted in costly delays and expensive modification to Navy projects. In addition, the discovery of dead whales often brings into question possible involvement of human activities, especially naval activities, in the event. At present, there is a critical lack of knowledge on which to base decisions concerning the effects of underwater sound on marine species, including whales, dolphins, and sea lions. There is also a near total lack of information concerning the possible effects of acoustic particle motion on marine mammals.

At present, there are only limited data on the sensitivity of marine mammals to acoustic particle motion. Johnson [1, 2] measured similar hearing thresholds for a dolphin while using two different source locations and concluded that the thresholds were not affected by nearfield particle motion. Turl [3] observed a decrease in sound-pressure thresholds in *Tursiops* between 50 and 150 Hz and suspected that the animals may have been detecting particle velocity (p/v). Kastak and Schusterman [4] measured aerial and underwater hearing thresholds in several species of pinnipeds and suspected a sensory modality shift (sound detection to vibration detection) below 100 Hz.

Our effort was to be the first systematic study of the relative contributions to marine mammal audition made by acoustic pressure and particle motion. The results would indicate, for the animals and frequencies studied, whether the ear is responding primarily to acoustic pressure, particle motion, or some combination. Such data would shed light on the basic principles of underwater hearing in the

species studied and would provide a basis for meaningful comparison of hearing thresholds in marine and terrestrial mammals. The information resulting from this study would also be important for the establishment of safe limits of low frequency, underwater noise exposure for marine mammals.

APPROACH

A behavioral-response paradigm was being used to measure underwater hearing thresholds while manipulating the particle velocity relationship by (1) varying the distance within the nearfield of a single source and (2) using an active sound control system. Animals available for this study were trained to produce audible "whistles" in response to hearing test tones. The source levels were varied, while maintaining the proper p/v relationship, in a staircase procedure until the threshold was determined. The approach was similar to previous research conducted on teleost (bony) fish in which the sound field's p/v ratio was varied to determine whether the subject was sensitive to acoustic particle motion or acoustic pressure.

RESULTS

Two bottlenose dolphins and one white whale were trained to station on an underwater platform and participate in hearing tests. Trials were delineated using a 3.5-s burst of white noise (0.5-s rise/fall time), which did or did not contain a hearing test tone (1-s duration, 0.25-s rise/fall time). Test subjects were trained to whistle in response to tone + noise trials and to remain silent during noise-only trials. Stimulus intensity was adjusted (while maintaining the p/v ratio) using a modified staircase procedure. Hearing thresholds were based on 10 response/no-response reversal points. Custom software was developed to calibrate the acoustic system, conduct hearing tests, and analyze the resulting data. A custom system was also developed to generate band-limited white noise whose frequency spectrum was compensated for projector response and acoustic standing waves [5].

Masked hearing thresholds were measured at 300 and 400 Hz for the dolphin "NIN" and the whale "MUK." No significant differences were observed in the thresholds at these frequencies with the subjects at distances of 1.0 and 2.4 m. This result was probably caused by the negligible differences between the acoustic impedance ratios at 1.0 and 2.4 m at frequencies of 300 Hz and above (e.g., at 300 Hz, the impedance ratio is approximately 0.92 at 1.0 m and 0.97 at 2.4 m).

Data collection at 100 Hz is currently in progress at source positions designed to yield larger acoustic impedance variations (approximate range of 0.25 to 1.0). Future measurements will employ two sound projectors and an active sound control system to manipulate the p/v ratio to any desired value.

REFERENCES

1. Johnson, C. S. 1966. "Auditory Thresholds of the Bottlenosed Porpoise (*Tursiops truncatus*, Montagu)," U.S. Naval Ordnance Test Station Technical Publication 4178, China Lake, CA.

2. Johnson, C. S. 1967. "Sound Detection Thresholds in Marine Mammals," *Marine Bioacoustics II*, (W. N. Tavolga, ed.), Pergamon Press, Oxford, pp. 247–260.

3. Turl, C. W. 1993. "Low-Frequency Sound Detection by a Bottlenose Dolphin," *Journal of the Acoustical Society of America*, vol. 94, pp. 3006–3008.

4. Kastak, D. and R. J. Schusterman. 1998. "Low-Frequency Amphibious Hearing in Pinnipeds: Methods, Measurements, Noise, and Ecology," *Journal of the Acoustical Society of America*, vol. 103, pp. 2216–2228.

5. Finneran, J. J., D. A. Carder, S. H. Ridgway, and C. E. Schlundt. 1999. "Technique for the Generation and Frequency Compensation of Bandlimited White Noise and Its Application in Studies of Masked Hearing Thresholds," *Journal of the Acoustical Society of America*, vol. 106, no. 4, p. 2130.

Principal Investigator:
Dr. Samuel H. Ridgway
D3503
(619) 553–1374
ridgway@spawar.navy.mil

ZU83

ACCOMPLISHMENTS AND IMPACTS

ACCOMPLISHMENTS AND IMPACTS

Telesonar Channel Models

Principal Investigators: Paul Baxley, (619) 553–5634, baxley@spawar.navy.mil and
Joseph Rice, (619) 553–3107, rice@spawar.navy.mil

SSC San Diego Co-Investigators: Dr. Homer Bucker and Vincent McDonald

Academic and Industry Associates: Professors John Proakis and Milica Stojanovic,
Northeastern University; Professor Michael Porter, New Jersey Institute of Technology; and Dale
Green, Benthos, Inc.

Background

"Telesonar" is undersea acoustic signaling for inexpensive, low-power, wireless networks of distributed sensors in shallow and very shallow water. Research on the adverse transmission channel is essential for developing, optimizing, and using telesonar technology. The physical channel is seawater—a refractive, nonhomogeneous medium. An absorptive, range-dependent seafloor and a reflective, time-varying sea-surface bound the channel. The transmitter broadcasts the signal, generally in an omnidirectional pattern. Signal propagation is via pressure waves and includes forward-scattering from the channel boundaries. Signal energy arrives at the receiver amidst a background of non-white noise, including jammers and co-channel interference. This ILIR project addresses the need for numerical propagation models in support of telesonar-link simulation, environment-dependence assessment, performance prediction, and mission planning. Basic research for these physics-based and statistics-based models has already aided signal design, sea-test planning, and data analysis for several 6.2 and 6.3 telesonar efforts.

The initial work on the telesonar-channel-models project began in FY 98, and work has continued through FY 99 and into FY 00. In general, the payoff from ILIR projects does not occur until many years after the project is concluded. This delay is the result of time required for basic research to be turned into practice and implemented in commercial products or military systems. The telesonar-channel-models project is an exception because the research results feed directly into ongoing 6.2 and 6.3 development efforts, resulting in almost immediate impacts on more advanced technology development.

Scientific Accomplishments

A physics-based numerical propagation model that includes the effects of multipath spread and Doppler spread has been developed as a prediction and analysis tool for underwater acoustic communication problems. The model uses three-dimensional Gaussian beams and quadrature detection to obtain the channel response for finite-duration, constant-wavelength tones. By using a very short pulse, the output of the quadrature detector provides an estimate of the channel impulse response, which may be used to determine the multipath spread. In addition, the Doppler shifts associated with source/receiver motion can be accumulated for the individual beams, providing Doppler spread. The model has been productively used in experiment planning and channel data analysis for several telesonar sea tests. A statistics-based, real-time channel emulator has also been developed. The use of the

physics-based impulse-response predictions with the emulator provides a powerful tool for the testing and development of underwater acoustic modems and sonar systems.

To date, there have been 30 presentations and 25 conference-proceedings publications resulting from work under this project.

Technology Impacts

1. The Stage-1 model developed under this ILIR project has been used extensively for experiment planning and data analysis associated with the SSC San Diego *Seaweb Science & Technology Capabilities Initiative*, an internally funded umbrella program to advance telesonar C4ISR concepts and to coordinate the various telesonar R&D projects.

2. The Stage-1 model has also been used extensively for experiment planning and data analysis associated with the SSC San Diego/ONR 321SS *Telesonar Technology Project* (6.2), which develops signaling techniques, networking philosophies, telesonar testbeds, digital-signal-processor (DSP)-based modems, link-layer handshake protocols, adaptive modulation, directional transducers, gateways to manned command centers, submarine installations, transmission-security strategies, and command-center user interfaces.

3. The Stage-1 model has also been used extensively for experiment planning and data analysis associated with the SSC San Diego/ONR 321 *Telesonar Surveillance Applications Project* (6.3), advancing communications infrastructure for future naval capabilities in littoral ASW. The Stage-1 model was instrumental in securing funding for this project, which began in FY 00.

4. The Stage-1 model developed under this ILIR project has been used extensively for experiment planning and data analysis associated with the SSC San Diego/ONR 322OM *Telesonar Signaling Measurements Project* (6.2), quantifying the relative performance of telesonar signaling techniques with respect to the probed channel response, observed ocean environment, and model predictions.

5. The Stage-1 model has also been used extensively for experiment planning and data analysis associated with the SSC San Diego/PD 18E Project X1933 *Telesonar Sublink Task* (6.3), integrating telesonar technology into submarine UQC-2 underwater telephone systems for digital data and digital voice links with other platforms and off-board systems.

6. Additionally, the Stage-1 model developed under this ILIR project has been used in support of the SSC San Diego/ONR 322BC *Telesonar Network for the Front-Resolving Observational Network with Telemetry (FRONT) Project*, which began in FY 99. FRONT is a major National Oceanographic Partnership Program (NOPP) initiative led by University of Connecticut scientists and involving several academic, government, and industrial partners. SSC San Diego is using telesonar technology for interconnecting remote undersea sensors on the continental shelf and linking this distributed ocean observatory with the terrestrial internet via cell-phone gateway buoys. The model has been used extensively for experiment planning and data analysis for experiments associated with this project.

7. The Swedish Navy contracted Benthos, Inc., to demonstrate second-generation telesonar modems and third-generation telesonar signaling in the Baltic Sea. SSC San Diego observed these tests and used the model developed under this ILIR project to perform channel analysis to help interpret performance in the Baltic waters.

8. Results from this project are being transitioned into a Small Business Innovation Research (SBIR) program initiated in FY 99. SBIR Topic N99-011, "Directional Underwater Acoustic Communications Transducer," is supported by ONR SBIR funds. The ONR SBIR program manager is Doug Harry, ONR 362, (703) 696–4286, harryd@onr.navy.mil.

Fleet Impacts

Because of the covert nature of telesonar, it is well-suited for autonomous surveillance systems in hostile littoral environments. Other potential applications include activating and deactivating mines, turning active sonar sources on and off, and communicating with autonomous robotic systems. The basic research performed under this ILIR project will help ensure that future Navy telesonar systems are optimized for the environments in which they are deployed.

Chief of Naval Research, RADM Gaffney, highlighted telesonar and Seaweb in his article titled, "Ocean Science and Technology at the Office of Naval Research," which appeared in the January 2000 issue of *Sea Technology*. Seaweb is the networked implementation of telesonar for underwater acoustic communications.

PROJECT TRANSITIONS

FY 99 TRANSITIONED PROJECTS

Acoustic 3-D Propagation in Shallow Water Overlaying an Elastic Bottom

Principal Investigator: Dr. Ahmad T. Abawi, (619) 553–3101, abawi@spawar.navy.mil

SSC San Diego ILIR project ZU54 was completed in FY 99. The objective of this 2-year task was to provide a numerically efficient and robust acoustic model for the propagation of waves in a three-dimensional ocean overlaying an elastic bottom.

The capability to detect and track submarine targets in shallow water is of great importance. Matched-field processing (MFP) and matched-field tracking (MFT) are acoustic processing techniques that have been experimentally demonstrated to enhance this capability by enabling the discrimination of acoustic signals according to the depth of the target source. Most of these experiments have been conducted in environments with high sound-speed bottoms that do not support elastic (shear) propagation. However, future experiments and operational situations are anticipated in environments with elastic bottoms. In addition, these environments will also have significant variations in depth. Therefore, it is very important to develop a theoretical understanding of acoustic propagation in these environments to facilitate application of MFP and MFT.

During the course of this investigation, a propagation model based on the normal mode theory was developed for use in a range-dependent elastic waveguide that simulates a variable-depth ocean environment. A method for computing the elastic modes was developed and used in the model to compute the acoustic field propagating in an elastic wedge.

This ILIR project was transitioned to direct ONR 6.1 funding under a continuing program titled "3-D Broadband Propagation in a Fluctuating Shallow-Water Environment." Program officer is Dr. Jeff Simmen, ONR 321, (703) 696–4204, simmenj@onr.navy.mil. The objective of the ONR project is to apply the model developed under ILIR ZU54 to the study of wave propagation in a random shallow-water environment. In addition, the model is particularly appropriate for use in tomography and for generating replica field vectors used in MFP work sponsored by ONR and DARPA.

Frequency-Mixing in Nonlinear Dynamic Devices

Principal Investigator: Dr. Adi Bulsara, (619) 553–1595, bulsara@spawar.navy.mil

SSC San Diego ILIR project ZU79, completed in FY 99, investigated the control of nonlinear phenomena to enhance signal detection in nonlinear systems. During the course of this work, a general nonfeedback control method was demonstrated that can both enhance the usual Stochastic Resonance (SR) effect and also suppress system response to a weak cyclic signal. Controlled SR may be useful in applications as diverse as the cancellation of cyclic noise in very sensitive magnetic-sensing applications and vibration control in nonlinear mechanical devices. Additionally, the phenomena discovered during this research may be useful in the context of electromagnetic field interactions with neurons where control of internal thresholds and the selective suppression of specific frequencies could be beneficial.

Results from this project have transitioned into ONR 6.1 research on SR and its implementation in specific devices (fluxgate magnetometer, superconducting quantum interference devices [SQUIDs], and phase-locked-loop arrays) for commercial and Navy applications. SSC San Diego project MA19 is funded at $500K for FY 01. Program officer is Dr. Mike Shlesinger, ONR 331, (703) 696–4220, shlesim@onr.navy.mil.

Applications of Stochastic Nonlinear Dynamics to Communication Arrays

Principal Investigator: Dr. Brian Meadows, (619) 553–2823, bmeadows@spawar.navy.mil

SSC San Diego ILIR project ZU71 was initiated in FY 99 and is continuing in FY 00. This research is an investigation of nonlinear dynamics in coupled-oscillator and phase-locked-loop (PLL) systems that may be incorporated in dynamic nonlinear antennas.

The project leverages recent advances in active antenna design and the theory of non-identical oscillators to generate beam steering and beam forming across an array of nonlinear oscillators. Additionally, compact arrays (antennas with element spacing significantly smaller than a half-wavelength) are possible by *directly* coupling nonlinear elements. Recent results in the design of compact multi-element antenna arrays demonstrate the importance of the mutual coupling effects between elements upon array performance. This research merges nonlinear dynamics and RF microelectronics to create an antenna design that may provide a significant level of directivity in a small volume. By employing non-identical oscillator theory, then "tuning" the *spatial* disorder, the signal-to-noise ratio of an array of PLLs improves as well as the frequency and phase-locking across the array. Beam steering is accomplished simply by adjusting the spatial disorder. Theoretical advances developed under this project include analytical conditions for the beam steering, complete stability analysis for general uniform phase gradients and coupling, and the exact solutions of dynamic beam steering of one- and two-dimensional nonlinear arrays.

Accomplishments under Dr. Meadow's ILIR project have transitioned into the following FY 00 programs:

1. Nonlinear Multi-Element Apertures, 6.2/6.3 research applications to sonobuoy arrays. Project officer is CDR David Falk, NAVAIR PMA-264, (301) 757–5724 falkdc@navair.navy.mil;

2. Nonlinear GPS Technology, (SSC San Diego project MA23), 6.2 research for GPS antennas. Project officer is Dr. William Stachnik, ONR 313, (703) 696–1438, stachnw@onr.navy.mil;

3. Dynamics of Nonlinear Antennas (SSC San Diego project MA24), 6.1 research into nonlinear wide band antennas. Project officer is Dr. Michael F. Shlesinger, ONR 331, (703) 696–4220, shlesim@onr.navy.mil.

High-Isolation Fiber-Optic Add/Drop Multiplexers for Shipboard Networking Applications

Principal Investigator: Richard Orazi, (619) 553–1065, orazi@spawar.navy.mil

SSC San Diego ILIR project ZU59 was completed in FY 99. The effort was directed to studying a novel method for producing add/drop multiplexers for fiber-optic systems operating with multiple, closely spaced wavelengths of signal light. The approach was to create Bragg gratings within fused-fiber biconical tapered couplers. Interference-patterned ultraviolet illumination was used to generate spatial variations of the refractive index to create the Bragg gratings. This project explored the effects of material, fabrication, and device design in controlling the light-coupling phenomena.

Several significant accomplishments were reported from this research. The technology for producing add/drop multiplexers by writing fiber Bragg gratings in the coupling region of fused-fiber couplers was demonstrated. Gratings were written in couplers made from standard photosensitive optical fiber with a drop efficiency of better than 60%. Fused-fiber-coupler fabrication process variables were shown to have a significant effect on the strength of grating formation in the couplers.

Results from this project have transitioned to ONR 6.2 funding under a program to improve wavelength division multiplexers used in undersea surveillance systems. Program officer is Don Davison, ONR 321, (703) 696–3160, davisd@onr.navy.mil. SSC San Diego project number SUBD is managed locally by Ken Rogers, (619) 553–1521, krogers@spawar.navy.mil.

Telesonar Channel Models

Co-Principal Investigators: Paul Baxley, (619) 553–5634, baxley@spawar.navy.mil and Joseph A. Rice, (619) 553–3107, rice@spawar.navy.mil

SSC San Diego Co-Investigators: Dr. Homer Bucker and Vincent McDonald

Academia and Industry Associates: Professors John Proakis and Milica Stojanovic, Northeastern University; Professor Michael Porter, New Jersey Institute of Technology; and Dale Green, Benthos, Inc.

SSC San Diego ILIR project ZU61 was initiated in FY 98 and is continuing in FY 00. This project seeks to understand undersea acoustic communication channels through theoretical and numerical modeling of the propagation physics.

"Telesonar" is undersea acoustic signaling for wireless networks of distributed sensors in shallow and very shallow water. Telesonar technology relies on signal-processing techniques to overcome deleterious aspects of the physical channel and to exploit advantageous channel features. The technology employs various spread-spectrum modulation techniques with signal energy typically in the 8- to 16-kHz acoustic band. In shallow water, a complex multipath structure and the nonhomogeneous, nonstationary nature of the medium and its boundaries impair propagation of acoustic signals. This project is developing a physics-based numerical propagation model that attempts to account for these effects.

Transitions for telesonar channel models include the following items:

1. The Stage-1 model developed under this ILIR project has been used extensively for experiment planning and data analysis associated with the SSC San Diego *Seaweb Science & Technology Capabilities Initiative*, an internally funded umbrella program to advance telesonar C4ISR concepts and to coordinate the various telesonar R&D projects. Sponsorship is under the cognizance of Dr. Eric Hendricks, SSC San Diego D11, (619) 553–3014, ehendric@spawar.navy.mil.

2. The Stage-1 model has also been used extensively for experiment planning and the data analysis associated with the SSC San Diego/ONR 321SS *Telesonar Technology Project* (6.2), which develops signaling techniques, networking philosophies, telesonar testbeds, DSP-based modems, link-layer handshake protocols, adaptive modulation, directional transducers, gateways to manned command centers, submarine installations, transmission-security strategies, and command-center user interfaces. Program officer is Dr. Don Davison, ONR 321SS, (703) 696–3160, davisod@onr.navy.mil.

3. The Stage-1 model has been used extensively for experiment planning and data analysis associated with the SSC San Diego/ONR 321 *Telesonar Surveillance Applications Project* (6.3), advancing communications infrastructure for future naval capabilities in littoral ASW. The Stage-1 model was instrumental in securing funding for this project, which began in FY 00. Program officer is Dr. Don Davison, ONR 321SS, (703) 696–3160, davisod@onr.navy.mil.

4. The Stage-1 model has been used extensively for experiment planning and data analysis associated with the SSC San Diego/ONR 322OM *Telesonar Signaling Measurements Project* (6.2), quantifying the relative performance of telesonar signaling techniques with respect to the probed channel response, observed ocean environment, and model predictions. Program officer is Dr. Tom Curtin, ONR 322OM, (703) 696–4119, curtint@onr.navy.mil.

5. The Stage-1 model has been used extensively for experiment planning and data analysis associated with the SSC San Diego/PD 18E Project X1933 *Telesonar Sublink Task* (6.3), integrating telesonar technology into submarine UQC-2 underwater telephone systems for digital data and digital voice links with other platforms and off-board systems. Program officer is Phil Depauk, SPAWAR PD 18E, (619) 524–7640, depaukp@spawar.navy.mil.

6. Additionally, the Stage-1 model has been used in support of the SSC San Diego/ONR 322BC *Telesonar Network for the Front-Resolving Observational Network with Telemetry (FRONT) Project,* which began in FY 99. FRONT is a major National Oceanographic Partnership Program (NOPP) initiative led by University of Connecticut scientists and involving several academic, government, and industrial partners. SSC San Diego is using telesonar technology for interconnecting remote undersea sensors on the continental shelf and linking this distributed ocean observatory with the terrestrial internet via cell-phone gateway buoys. The model has been used extensively for experiment planning and data analysis for experiments associated with this project. Program officer is James Eckman, ONR 321BC, (703) 696–4119, eckmanj@onr.navy.mil.

7. The Swedish Navy contracted Benthos, Inc., to demonstrate second-generation telesonar modems and third-generation telesonar signaling in the Baltic Sea. SSC San Diego observed these tests

and used the model developed under this ILIR project to perform channel analysis to help interpret performance in the Baltic waters.

Robust Control of Information-Flow for Network-Centric Warfare

Principal Investigator: Dr. Sri Sritharan, (619) 553–1201, srith@spawar.navy.mil

SSC San Diego ILIR project ZU68 was initiated in FY 99 and transitioned to the Defense Advanced Research Projects Agency (DARPA) funding in FY 00. The goal of the research is to mathematically model global information flow dynamics on a large-scale command-control network system and to devise control and game theoretic methods to counter network attacks. The research employs several powerful mathematical approaches (e.g., fluid-flow models based on deterministic and stochastic Navier–Stokes equations) to attack this complex problem. Several publications and presentations have resulted from the first-year efforts.

The FY 00 transition effort, SSC San Diego project CB57, is funded under the DARPA Autonomic Information Assurance program. Program officer is Brian Witten, (703) 696–2323, bwitten@darpa.mil.

PUBLICATIONS AND PRESENTATIONS

REFEREED PAPERS (PUBLISHED OR ACCEPTED)

Bucker, H. and P. Baxley. 1999. "Automated Matched-Field Tracking with Table Lookup," *Journal of the Acoustical Society of America*, vol. 106, no. 6, pp. 3226–3230.

Bulsara, A., M. Locher, W. Ditto, K. Wiesenfeld, P. Hanggi, L. Gammaitoni, J. Neff, and M. Inchiosa. 2000. "Theory of Controlling Stochastic Resonance," *Physical Review E*, to appear.

Chandross, M. and J. C. Hicks. 1999. "Density-Matrix Renormalization-Group Method for Excited States," *Physical Review B*, vol. 59, no. 15, pp. 9699–9702.

Chandross, M. and J. C. Hicks. 1999. "Low-Lying Optically Excited States of Conjugated Polymers with DMRG," *Synthetic Metals*, vol. 102, pp. 928–929.

Finneran, J. J., C. W. Oliver, K. M. Schaefer, and S. H. Ridgway. 2000. "Source Levels and Estimated Yellowfin Tuna (*Thunnus albacares*) Detection Ranges for Dolphin Jaw Pops, Breaches, and Tail Slaps," *Journal of the Acoustical Society of America*, vol. 107, no. 1, pp. 649–656.

Gammaitoni, L., M. Löcher, A. Bulsara, P. Hänggi, J. Neff, K. Wiesenfeld, W. Ditto, and M. E. Inchiosa. 1999. "Controlling Stochastic Resonance," *Physical Review Letters*, vol. 82, pp. 4574ff.

Goodman, I. R. and H. T. Nguyen. 1999. "Probability Updating Using Second-Order Probabilities and Conditional Event Algebra," *Information Sciences*, vol. 121, pp. 295–347.

Lindner, J. F., S. Chandramouli, A. R. Bulsara, M. Löcher, and W. L. Ditto. 1998. "Noise Enhanced Propagation," *Physical Review Letters*, vol. 81, pp. 5048–5051.

Lindner, J. F., B. K. Meadows, T. L. Marsh, W. L. Ditto, and A. R. Bulsara. 1998. "Can a Neuron Distinguish Chaos from Noise?," *International Journal of Bifurcation and Chaos*, vol. 8, no. 4, pp. 767–781.

Löcher, M., D. Cigna, E. R. Hunt, G. A. Johnson, F. Marchesoni, L. Gammaitoni, M. E. Inchiosa, and A. R. Bulsara. 1998. "Stochastic Resonance in Coupled Nonlinear Dynamic Elements," *Chaos*, vol. 8, pp. 604–615.

Lorincz, K., Z. Gingl, L. B. Kiss, and A. R. Bulsara. 1999. "Higher Order Stochastic Resonance in a Level-Crossing Detector," *Physical Letters A*, vol. 254, pp. 154–157.

Mosier–Boss, P. A. and S. H. Lieberman. 1999. "Comparison of Three Methods to Improve Adherence of Thin Gold Films to Glass Substrates and Their Effect on the SERS Response," *Applied Spectroscopy*, vol. 53, pp. 862–873.

Pattison, T. and S. I. Chou. 2000. "Sensitivity Analysis of Dual-Satellite Geolocation," *IEEE Transactions on Aerospace and Electronic Systems*, vol. 36, no. 1, pp. 56–71.

Rice, J. and V. K. McDonald. 1999. "Telesonar Testbed: Advances in Undersea Wireless Communications," *Sea Technology*, vol. 40, no. 2, pp. 17–23.

Ridgway, S. H. 1999. "An Illustration of Norris' Acoustic Window," *Marine Mammal Science*, vol. 15, no. 4, pp. 926–930.

Ridgway, S. H., D. A. Carder, T. Kamolnick, C. E. Schlundt, W. Elsberry, M. Hastings. 1999. Comments on "Broadband Spectra of Seismic Survey Air-Gun Emissions, with Reference to Dolphin Auditory Thresholds," [*J. Acoust. Soc. Am.*, vol. 103, no. 4, pp. 2177–2184 (1998)], *Journal of the Acoustical Society of America*, vol. 105, no. 3, pp. 2047–2048.

Robinson, J. W. C., D. E. Asraf, A. R. Bulsara, and M. E. Inchiosa. 1998. "Information-Theoretic Distance Measures and a Generalization of Stochastic Resonance," *Physical Review Letters*, vol. 81, pp. 2850–2853.

Russell, S. and A. Ramirez. 1999. "In-Situ Boron Incorporation and Activation in Silicon Carbide Using Excimer Laser Recrystallization," *Applied Physics Letters*, vol. 74, no. 22 (May), pp. 3368–3370.

Sritharan, S. S. 2000. "Deterministic and Stochastic Control of Viscous Flow with Linear, Monotone and Hyper Viscosities," *Applied Mathematics and Optimization*, vol. 41, no. 2, pp. 255–308.

Sritharan, S. S. and P. Sundar. 1999. "The Stochastic Magnetohydrodynamic System," *Infinite Dimensional Analysis, Quantum Probability and Related Topics*, vol. 2, no. 2, pp. 241–265.

Stein, D. W. J. "Robust Implementations of an Exponential Mixture Detector with Applications to Radar," *IEEE Transactions on Aerospace and Electronic Systems*, vol. 35, no. 2, pp. 519–532.

Wahlen, B. E. and C. Y. Mai. 2000. "Turbo Coding Applied to Pragmatic Trellis-Coded Modulation," *IEEE Communications Letters*, vol. 4, no. 2, pp. 65–67.

BOOKS/CHAPTERS (PUBLISHED OR ACCEPTED)

Bulsara, A. R. 1998. "Noise-Mediated Cooperative Behavior in Integrated-Fire Models of Neuron Dynamics," *Brain-Like Computing and Intelligent Information Systems* (S. Amari and N. Kasabov, eds.), Springer–Verlag, NY.

Goodman, I. R. and H. T. Nguyen. 2000. "Fuzziness and Randomness," *Statistical Modeling, Analysis & Management of Fuzzy Data* (D. A. Ralescu, C. Bartoluza, M. A. Gil, eds.), Springer–Verlag, New York, NY, chapter 1, to appear.

Inchiosa, M. E. and A. R. Bulsara. 2000. "Noise-Mediated Cooperative Behavior and Signal Detection in dc SQUIDs," *Stochastic and Chaotic Dynamics in the Lakes* (D. S. Broomhead, E. A. Luchinskaya, P. V. E. McClintock, and T. Mullin, eds.), American Institute of Physics, Melville, NY, pp. 583–595.

Mosier–Boss, P. A. and S. H. Lieberman. 1999. "Environmental Applications of Surface Enhanced Raman Spectroscopy (SERS)," *Recent Research Developments in Applied Spectroscopy*, Research Signpost, Kerala, India, vol. 2, pp. 83–98.

Murray, S. A. and B. S. Caldwell. 1998. "Operator Alertness and Human–Machine System Performance during Supervisory Control Tasks," *Automation Technology and Human Performance: Current Research and Trends* (M. Scerbo and M. Mouloua, eds.), Lawrence Erlbaum, Mahwah, NJ, pp. 208–212.

Ridgway, S. H. 1999. "The Cetacean Central Nervous System," *Encyclopedia of Neuroscience*, 2nd edition (G. Adelman and B. Smith, eds.), Springer–Verlag, NY, pp. 352–357.

Ridgway, S. H. and W. W. L. Au. 1999. "Dolphin Hearing and Echolocation: The Bottlenose Dolphin *Tursiops truncatus*," *Encyclopedia of Neuroscience*, 2nd edition (G. Adelman and B. Smith, eds.), Springer–Verlag, NY, pp. 858–862.

Ridgway, S. H. 2000. "The Auditory Central Nervous System of Dolphins," *Hearing in Whales and Dolphins* (W. W. L. Au, A. Popper, and R. Fay, eds.), Springer–Verlag, NY, pp. 363–391.

Sritharan, S. S. and P. Sundar. 2000. "Ergodic Control of Navier-Stokes Equation," *Nonlinear Problems in Aerospace*, (S. Sivasundaram, ed.), Gordon and Breach, to appear.

REFEREED PAPERS (SUBMITTED)

Bamber, D. E., I. R. Goodman, and H. T. Nguyen. "Extension of the Concept of Propositional Deduction from Classical Logic to Probability: Part 1, An Overview of Probability-Selection Approaches," submitted to *Information Sciences*.

Hanson, F. "Coherent Laser Radar Performance in Littoral Environments," submitted to *Optical Engineering*.

Hitney, H. V. "Evaporation Duct Assessment from Meteorological Buoys," submitted to *Radio Science*.

Murray, S. A. "Operator Alertness Fluctuations and Cognitive Function," submitted to IEEE Transactions on *Systems, Man, and Cybernetics*.

Sritharan, S. S. and V. Barbu. "Flow Invariance Preserving Feedback Controllers for the Navier-Stokes Equation," submitted to the *Journal of Mathematical Analysis & Applications*.

Sritharan, S. S. and V. Barbu. "On the Convergence Viscous-Euler Splitting Methods for Controlled and Uncontrolled Navier-Stokes Equation," submitted to *SIAM Journal of Control and Optimization*.

Sritharan, S. S. and J. L. Menaldi. "Impulse Control of Stochastic Navier-Stokes Equation," submitted *to Probability Theory and Related Fields*.

Sritharan, S. S. and J. L. Menaldi. "Stochastic 2-D Navier-Stokes Equation," submitted to *Applied Mathematics & Optimization*.

MONOGRAPH

Sritharan, S. S. *Optimal Control of Turbulence*, under current contract with Gordon and Breach Publishers, (to be submitted).

PROCEEDINGS

Abawi, A. T. 1999. "An Energy-Conserving One-Way Coupled-Mode Propagation Model," *Journal of the Acoustical Society of America*, vol. 105, no. 2 (February), pt. 2, p. 1362.

Baxley, P. A., H. P. Bucker, and J. A. Rice.1999. "First Results from an Acoustic-Communications Transmission Model Using 3D Gaussian Beams and Quadrature Detection," *Journal of the Acoustical Society of America*, vol. 105, no. 2 (February), pt. 2, p. 1364.

Baxley, P. A., H. P. Bucker, J. A. Rice, and M. D. Green. 1999. "Acoustic Communication Channel Modeling for the Baltic," *Proceedings of the IEEE Oceans '99 Conference*, CD-ROM, Poster Session.

Beaven, S. G., L. E. Hoff, and E. M. Winter. 1999. "Comparison of SEM and Linear Unmixing Approaches for Classification of Spectral Data," *Imaging Spectrometry V* (Proceedings of SPIE), vol. 3753, pp. 300–307.

Bogden, P. S., J. A. Rice, et al. 2000. "Front-Resolving Observational Network with Telemetry," *Transactions, American Geophysical Union (AGU), Ocean Sciences.*

Bulsara, A. R. and M. E. Inchiosa. 1999. "Enhanced Magnetic Signal Detection Using Stochastic Resonance in a rf SQUID," *Proceedings of the International Conference on Noise in Physical Systems and 1/f Fluctuations*, in press.

Bulsara, A. R. and M. E. Inchiosa. 2000. "Noise-Mediated Cooperative and Signal Detection in dc SQUIDs," *Stochastic and Chaotic Dynamics in the Lakes*, American Institute of Physics (AIP), Melville, NY, pp. 583–595.

Finneran, J. J., D. A. Carder, S. H. Ridgway, and C. E. Schlundt. 1999. "Technique for the Generation and Frequency Compensation of Bandlimited White Noise and Its Application in Studies of Masked Hearing Thresholds," *Journal of the Acoustical Society of America*, vol. 106, no. 4, pt. 2, p. 2130.

George, M. J. and I. R. Goodman. 1999. "Numerical and Implementational Studies of Conditional and Relational Event Algebra, Illustrating Use and Comparison with Other Approaches to Modeling of Information," *Proceedings of the Second International Conference on Information Fusion (Fusion '99)*, vol. 1, pp.273–280.

Goodman, I. R. 1999. "A Decision-Aid for Nodes in Command and Control Systems, Based on Cognitive Probability Logic," *Proceedings of the 1999 Command and Control Research and Technology Symposium.* vol. 2, pp. 898–941.

Goodman, I. R., R. P. S. Mahler, and H. T. Nguyen. 1999. "What is Conditional Event Algebra and Why Should You Care?" *Proceedings of SPIE Conference on Signal Processing, Sensor Fusion, and Target Recognition VIII*, vol. 3720, pp. 2–13.

Goodman, I. R. and H. T. Nguyen. 1999. "Application of Conditional and Relational Event Algebra to the Defining of Fuzzy Logic Concepts," *Proceedings of SPIE Conference on Signal Processing, Sensor Fusion, and Target Recognition VIII*, vol. 3720, pp. 25–36.

Goodman, I. R. and H. T. Nguyen. 2000. "Computational Aspects of Quantitative Second-Order Probability Logic and Fuzzy If–Then Rules: Part 1, Basic Representations as Integrals," *Proceedings of the Fifth Joint Conference on Information Sciences (JCIS 2000)*, vol. 1, pp. 64–67.

Green, M. D. and J. A. Rice. 1999. "Statistics-Governed Channel Simulator," *Journal of the Acoustical Society of America*, vol. 105, no. 2 (February), pt. 2, p. 1365.

Hanson, F. and E. Schimitschek. 1999. "Relative Ladar Performance in Littoral Environments—The Case for Mid-IR Coherent Laser Radars," *Meeting of the Infrared Information Symposia (IRIS) Specialty Group on Active Systems*, vol. 1, pp. 59–76.

Kramer, G. F. and I. R. Goodman. 1999. "Application of the Possibilistic Approach to Correlation and Tracking," *Proceedings of SPIE Conference on Signal Processing, Sensor Fusion, and Target Recognition VIII*, vol. 3720, pp. 37–46.

Lange, D. 1999. "Hypermedia Potentials for Analysis Support Tools," *Proceedings of Hypertext '99*, Association for Computing Machinery (ACM), pp. 165–166.

Lange, D. 1999. "Integration of Complex Information," *Proceedings of The Technical Cooperation Programme (TTCP) Coordinated Maritime Battlespace Management Symposium*, unclassified paper published on classified CD-ROM (contact author).

McDonald, V. K., J. A. Rice, M. B. Porter, and P. A. Baxley. 1999. "Performance Measurements of a Diverse Collection of Undersea Acoustic Communication Signals," *Proceedings of the IEEE Oceans '99 Conference*, CD-ROM, Session 3F.

Porter, M. B., V. K. McDonald, J. A. Rice, and P. A. Baxley. 2000. "Acoustic Communication Modeling and ModemEx'99 Analysis," *Proceedings of the ONR Conference on Shallow-Water Acoustic Modeling*, Kluwer Academic Press, to appear.

Rice, J. A. 1997. "Acoustic Signal Dispersion and Distortion by Shallow Undersea Transmission Channels," *Proceedings of the NATO SACLANT Undersea Research Centre Conference on High-Frequency Acoustics in Shallow Water*, pp. 435–442.

Ridgway, S. H. 1999. "Hot Topics in Animal Bioacoustics," *Journal of the Acoustical Society of America*, vol. 106, no. 4, p. 2224.

Schlundt, C. E., J. J. Finneran, D. A. Carder, and S. H. Ridgway. 1999. "Masked Hearing Thresholds and Critical Bandwidths for Dolphins and a White Whale at 20 and 30 kHz," *Journal of the Acoustical Society of America*, vol. 106, no. 4, p. 2190.

Sritharan, S. S. and V. Barbu. 2000. "M-Accretive Quantization of the Vorticity Equation," *Proceedings of the First World Conference on Semigroup Theory and Applications*, to appear.

Sritharan, S. S. and J. L. Minaldi. 2000. "Optimal Stopping Time and Impulse Control Problems of Stochastic Navier-Stokes Equation," *Proceedings of the Conference on Stochastic Analysis*, to appear.

Stein, D. W., S. E. Stewart, G. D. Gilbert, and J. S. Schoonmaker. 1999. "Band Selection for Viewing Underwater Objects Using Hyperspectral Sensors," *Airborne and In-Water Underwater Imaging*, Proceedings of SPIE, vol. 3761, pp. 50–61.

PRESENTATIONS TO PROFESSIONAL MEETINGS

Abawi, A. T., W. A. Kuperman, and M. D. Collins. 1999. "The Coupled Mode Parabolic Equation," 137th Meeting of the Acoustical Society of America and 2nd Convention of the European Acoustics Association, February, Berlin, Germany.

Anderson, A. A., E. M. Arias, and R. D. George. 1999. "Surface Properties of Thin-Films and Coatings Prepared from Fluorinated Acrylates," 217th American Chemical Society National Meeting, March, Anaheim, CA.

Baxley, P. A., H. P. Bucker, and J. A. Rice.1999. "First Results from an Acoustic-Communications Transmission Model Using 3D Gaussian Beams and Quadrature Detection," 137th Meeting of the Acoustical Society of America and 2nd Convention of the European Acoustics Association, February, Berlin, Germany.

Baxley, P. A., H. P. Bucker, J. A. Rice, and M. D. Green. 1999. "Acoustic Communication Channel Modeling for the Baltic," IEEE Oceans '99 Conference, 13 to 16 September, Seattle, WA.

Beaven, S. G., L. E. Hoff, and E. M. Winter. 1999. "Comparison of SEM and Linear Unmixing Approaches for Classification of Spectral Data," Imaging Spectrometry V Conference, SPIE International Symposium on Optical Science and Technology, 18 to 23 July, Denver, CO.

Bogden, P. S., J. A. Rice, et al. 2000. "Front-Resolving Observational Network with Telemetry," American Geophysical Union (AGU) Ocean Sciences Meeting, special session on Coastal Ocean Dynamics and Prediction, 24 to 28 January, San Antonio, TX.

Bulsara, A. R. 1999. "Enhanced Magnetic Signal Detection Using Stochastic Resonance in a rf SQUID," invited presentation at the International Conference on Noise in Physical Systems and 1/f Fluctuations, August, Hong Kong.

Bulsara, A. R. 1999. "Enhanced Signal Detection in dc SQUIDs," invited presentation at STOCHAOS: Stochastic and Chaotic Dynamics in the Lakes, August, Ambleside, United Kingdom.

Bulsara, A. R. 1999. "Stochastic Resonance: Noise-Enhanced Signal Detection in Nonlinear Dynamic Devices," invited presentation at the International Meeting on Noise and Nonlinearity in Engineering Applications, Catania, Sicily.

Bucker, H. 1999. "Automatic Matched-Field Tracking with Table Lockup," invited presentation to the Office of Naval Research (ONR) Deployable Sensors Signal Processing Group, 17 November, San Diego, CA.

Finneran, J. J., D. A. Carder, S. H. Ridgway, and C. E. Schlundt. 1999. "Technique for the Generation and Frequency Compensation of Bandlimited White Noise and Its Application in Studies of Masked Hearing Thresholds," 138th Meeting of the Acoustical Society of America, 1 to 5 November, Columbus, OH.

George, M. J. and I. R. Goodman. 1999. "Numerical and Implementational Studies of Conditional and Relational Event Algebra, Illustrating Use and Comparison with Other Approaches to Modeling of Information," Second International Conference on Information Fusion (Fusion '99), 6 to 8 July, Sunnyvale, CA.

George, R. D. 1999. "Bulk and Surface Properties of Low Surface Energy Perfluoroalkyl Polymer Coatings," Paint Research Association's 3rd International Conference on Fluorine in Coatings (Fluorine in Coatings III), January, Grenelefe (Orlando), FL.

Goodman, I. R. 1999. "A Decision-Aid for Nodes in Command and Control Systems, Based on Cognitive Probability Logic," 1999 Command and Control Research and Technology Symposium, 29 June to 1 July, Naval War College, Newport, RI.

Goodman, I. R. 2000. "Extension of the Concept of Propositional Deduction from Classical Logic to Probability: Part 1, An Overview of Probability-Selection Approaches," invited plenary presentation at the Joint Conference on Information Sciences (JCIS 2000), 27 February to 3 March, Atlantic City, NJ.

Goodman, I. R. 2000. "Explorations of New Directions in Tying Together Linguistic/Fuzzy Reasoning and Probablistic Reasoning," presentation to special panel on Fuzzy Logic and Its Applications, Joint Conference on Information Sciences (JCIS 2000), 27 February to 3 March, Atlantic City, NJ.

Goodman, I. R., R. P. S. Mahler, and H. T. Nguyen. 1999. "What is Conditional Event Algebra and Why Should You Care?," invited presentation at the SPIE Conference on Signal Processing, Sensor Fusion, and Target Recognition VIII, part of SPIE 13th Annual International Symposium on Aerosense, 5 to 9 April, Orlando, FL.

Goodman, I. R. and H. T. Nguyen. 1999. "Application of Conditional and Relational Event Algebra to the Defining of Fuzzy Logic Concepts," invited presentation at the SPIE Conference on Signal Processing, Sensor Fusion, and Target Recognition VIII, part of SPIE 13th Annual International Symposium on Aerosense, 5 to 9 April, Orlando, FL.

Goodman, I. R. and H. T. Nguyen. 2000. "Computational Aspects of Quantitative Second-Order Probability Logic and Fuzzy If–Then Rules: Part 1, Basic Representations as Integrals," Fifth Joint Conference on Information Sciences (JCIS 2000), 27 February to 3 March, Atlantic City, NJ.

Green, M. D. and J. A. Rice. 1999. "Statistics-Governed Channel Simulator," 137th Meeting of the Acoustical Society of America and 2nd Convention of the European Acoustics Association, February, Berlin, Germany.

Hanson, F. and E. Schimitschek. 1999. "Relative Ladar Performance in Littoral Environments—The Case for Mid-IR Coherent Laser Radars," Meeting of the Infrared Information Symposia (IRIS) Specialty Group for Active Systems, February, Monterey, CA.

Hitney, H. V. 2000. "Evaporation Duct Assessment from Meteorological Buoys," National Radio Science Meeting, 5 to 8 January, University of Colorado, Boulder, CO.

Kramer, G. F. and I. R. Goodman. 1999. "Application of the Possibilistic Approach to Correlation and Tracking," invited presentation at the SPIE Conference on Signal Processing, Sensor Fusion, and Target Recognition VIII, part of SPIE 13th Annual International Symposium on Aerosense, 5 to 9 April, Orlando, FL.

Lange, D. 1999. "Hypermedia Potentials for Analysis Support Tools," Hypertext '99, Association for Computing Machinery (ACM), 21 to 25 February, Darmstadt, Germany.

Lange, D. 1999. "Integration of Complex Information," The Technical Cooperation Programme (TTCP) Coordinated Maritime Battlespace Management Symposium, 24 to 28 May, SSC San Diego, CA.

McDonald, V. K., J. A. Rice, M. B. Porter, and P. A. Baxley. 1999. "Performance Measurements of a Diverse Collection of Undersea Acoustic Communication Signals," IEEE Oceans '99 Conference, 13 to 16 September, Seattle, WA.

Meadows, B. K. 1999. "Nonlinear Dynamics and Antenna Design," invited seminar at the University of California at Santa Barbara, Electrical and Computer Engineering Department, 19 April, Santa Barbara, CA.

Meadows, B. K. 1999. "Chaos in San Diego: Nonlinear Dynamics Research at SSC San Diego," invited seminar at the Naval Research Laboratory (NRL), 26 May, Washington, DC.

Meadows, B. K. 1999. "Dynamic Nonlinear Antenna Design," opening talk at the Nonlinear Antenna Kick-Off Meeting, 30 to 31 September, SSC San Diego, CA.

Meadows, B. K. 2000. "The Dynamics of Disordered Arrays," invited seminar at the Georgia Institute of Technology, Biomedical Engineering Department, 13 January, Atlanta, GA.

Porter, M. B., V. K. McDonald, J. A. Rice, and P. A. Baxley. 1999. "Acoustic Communication Modeling and ModemEx'99 Analysis," ONR Conference on Shallow-Water Acoustic Modeling, 8 to 10 September, Naval Postgraduate School, Monterey, CA.

Rice, J. A. 1997. "Acoustic Signal Dispersion and Distortion by Shallow Undersea Transmission Channels," NATO SACLANT Undersea Research Centre Conference on High-Frequency Acoustics in Shallow Water, July, Lerici, Italy.

Ridgway, S. H. 1999. "Hot Topics in Animal Bioacoustics," invited presentation at the 138th Meeting of the Acoustical Society of America, 1 to 5 November, Columbus, OH.

Schlundt, C. E., J. J. Finneran, D. A. Carder, and S. H. Ridgway. 1999. "Masked Hearing Thresholds and Critical Bandwidths for Dolphins and a White Whale at 20 and 30 kHz," 138th Meeting of the Acoustical Society of America, 1 to 5 November, Columbus, OH.

Sritharan, S. S. 1998. "Kalman Filters: Past, Present, and Future," 3 November, Mathematics Department, University of California at Riverside, CA.

Sritharan, S. S. 1998. "H-Infinity (Robust) Control of Fluid Dynamics," Applied Mechanics and Engineering Science Colloquium, 21 November, University of California at San Diego, La Jolla, CA.

Sritharan, S. S. 1998. "Control of Fluid Flow with State Constraints," International Conference on Semigroups and Applications, 16 December, Newport Beach, CA.

Sritharan, S. S. 1999. "Quantum Field Theoretic Methods in Turbulence Estimation," Colloqium, 26 January, Mathematics Department, Louisiana State University (LSU), Baton Rouge, LA.

Sritharan, S. S. 1999. "Quantum Field Theoretic Methods in Turbulence Estimation," Colloqium 27 January, Mathematics Department, Wayne State University, Detroit, MI.

Sritharan, S. S. 1999. "Ergodic Control of Turbulence," American Mathematical Society, Special Session on Control of Partial Differential Equations, Sectional Meeting, 10 April, Las Vegas, NV.

Sritharan, S. S. 1999. "Impulse Control of Turbulence," Minisymposium of Advances in Theoretical and Computational Methods in Control of Fluids, SIAM Annual Meeting, 14 May, Atlanta, GA,

Sritharan, S. S. 1999. "Erodicity, Controllability, and Optimal Impulse Control of Turbulence," National Science Foundation (NSF) Flow Control Workshop, 30 May, University of California at San Diego (UCSD), La Jolla, CA.

Sritharan, S. S. 1999. "Some Problems in Deterministic and Stochastic Control of Navier-Stokes Equation," Colloqium, 11 September, Department of Mathematics, University of Iasi, Romania.

Sritharan, S. S. 1999. "Nonlinear Semigroups, M-Accretive Operators and Control of Fluids," Colloqium, 18 October, Department of Mathematics, University of Southern California (USC), Los Angeles, CA.

Sritharan, S. S. 1999. "M-Accretive Operators and Control of Navier-Stokes Equations," National Science Foundation Workshop on Control of Distributed Parameter Systems, 23 October, Texas A&M University, College Station, TX.

Sritharan, S. S. 2000. "Some Control Problems in Deterministic and Stochastic Navier-Stokes Equations," Center for Nonlinear Studies, 4 January, Los Alamos National Laboratory, Los Alamos, NM.

Sritharan, S. S. 2000. "Some Control Problems in Deterministic and Stochastic Navier-Stokes Equations," Center for Nonlinear Dynamic Systems, 24 January, Georgia Institute of Technology, Atlanta, GA.

Sritharan, S. S. and V. Barbu. 1999. "M-Accretive Quantization of the Vorticity Equation," First World Conference on Semigroup Theory and Applications, 14 to 16 December, Los Angeles, CA.

Sritharan, S. S. and J. L. Menaldi. 1997. "Impulse Control of Stochastic Navier-Stokes Equation," SIAM Annual Meeting, July, Orlando, FL.

Sritharan, S. S. and J. L. Minaldi. 2000. "Optimal Stopping Time and Impulse Control Problems of Stochastic Navier-Stokes Equation," Conference on Stochastic Analysis, January, University of Trento, Italy.

Stein, D. W., S. E. Stewart, G. D. Gilbert, and J. S. Schoonmaker. 1999. "Band Selection for Viewing Underwater Objects Using Hyperspectral Sensors," Airborne and In-Water Underwater Imaging Conference, SPIE International Symposium on Optical Science and Technology, 18 to 23 July, Denver, CO.

Wahlen, B. E. 1998. "Navy Applications of Turbo Codes to Bandwidth Efficient Modulation Techniques," invited presentation at the Turbo Codes Workshop, jointly sponsored by the Office of Naval Research and the Naval Research Laboratory, 3 December, Washington, DC.

HONORS AND AWARDS

HONORS AND AWARDS

Paul Baxley continues as President of the San Diego Chapter of the Acoustical Society of America (ASA). He is Chairman of the ASA Public Relations Committee, a Member of the ASA External Affairs Committee, and Co-Chair of the ASA Home Page Committee. He is also a member of the ASA Underwater Acoustics Technical Committee and is a member of the Institute of Electrical and Electronic Engineers (IEEE) Marine Technology Society.

Douglass Evans received a Navy Exemplary Achievement Award in June 1998 for superlative performance and contributions to the Navy and SSC San Diego.

Dr. I. R. Goodman was selected as an ongoing associate editor of *Information Sciences*. Also, Professor J. Tyzkiewicz, visiting Professor at the University of New South Wales, Sydney, Australia, met with Dr. Goodman on 21 April 1999 at special request to discuss Dr. Goodman's work in conditional event algebra.

Dr. Frank E. Hanson is a program committee member for the Military Sensing Symposia Specialty Group on Active Electro-Optic (E-O) Systems.

Dr. Wayne C. McGinnis received an SSC San Diego Distinguished Publication Award for Technical Report 1741, "High-Tc Superconducting Thick-Film Spiral Magnet: Development and Characterization of a Single Spiral Module," coauthored with Dr. Thomas E. Jones.

Dr. Brian Meadows is currently providing scientific and technical support to the Assistant Secretary of the Navy for Research, Development, and Acquisition (ASN RDA). He is also the technical team leader of the Global Positioning System (GPS) and Navigation Warfare (NAVWAR) modernization review and reports directly to the ASN RDA. Dr. Meadows was also nominated to serve on a Central Intelligence Agency (CIA) panel to study future threats to national security; members of the panel include a former President, a former director of the CIA, and a MacArthur grant winner. Additionally, Dr. Meadows coordinated the "Nonlinear Antenna Kick-Off Meeting" at SSC San Diego from 30 to 31 September 1999. Over 30 participants representing ONR, NAVAIR, NAWC China Lake, SSC San Diego, UC Santa Barbara, Georgia Tech, and Information Systems Laboratory attended.

Steven A. Murray received an SSC San Diego Distinguished Award for "Underwater Telerobotics and Virtual Reality: A New Technology Partnership," a conference proceedings article he coauthored with Douglas W. Murphy.

Joseph Rice received the Navy Meritorious Civilian Service Award in 1998 for contributions that have been of high value to the Navy. This is the third highest Navy award. Mr. Rice is also a member of IEEE and ASA and has served as a lecturer for the Physics Department at the Naval Postgraduate School.

Dr. Sam H. Ridgway and **Dr. James J. Finneran** were appointed to the Animal Bioacoustics Technical Committee of the Acoustical Society of America (ASA). Dr. Ridgway was invited to represent the Animal Bioacoustics Technical Committee and present "Hot Topics in Animal Bioacoustics" at the 138th Meeting of ASA. Dr. Ridgway was also invited to be guest editor of *Marine Mammal Science* for "Recollections of Kenneth S. Norris." (Dr. Norris was the nation's leading marine mammalogist and professor at the University of California at Santa Cruz.)

Dr. Sri S. Sritharan served as organizer and Chair of a four-part mini-symposium on "Advances in Optimal Control of Fluid Dynamics," during the July 1999 Society of Industrial and Applied Mathematics (SIAM) Annual Meeting in Atlanta, GA.

Dr. Stephen E. Stewart chaired the "Modeling and Analysis" session of the Airborne and In-Water Underwater Imaging Conference, which was part of the Society of Photo-Optical Instrumentation Engineers' (SPIE's) 1999 International Symposium on Optical Science and Technology.

Dr. Po-Yun Tang served on the Composite Committee of the Material Division of the American Society of Mechanical Engineering (ASME).

Dr. Bruce E. Wahlen has been invited to serve as a consultant to the Naval Air Warfare Center Aircraft Division and to Rockwell Collins, Inc., during fiscal year 2000 for their combined effort on Bandwidth Efficient Advanced Modulation (BEAM) Technology for UHF SATCOM.

PATENT ACTIVITY

INDEPENDENT RESEARCH
Patents Issued

Jerome F. DeJaco
Willard F. Rask

<div align="right">

**"Impulsive Snap-through
Acoustic Projector (ISnAP)"**

</div>

An impulsive snap-through acoustic pulse generator may be used to generate an acoustic
pulse in an aqueous environment without gas bubbles. The impulsive snap-through acoustic
pulse generator includes a support structure having an open end, a resilient shell mounted to
the support structure to define a chamber, and a gas vent in fluid communication with the
chamber through which a gas passes for changing the pressure in the chamber so that the
resilient shell transitions from a first stable state to a second stable state, thereby generating
an acoustic pulse.

Patent 5,894,451 Navy case 77,245 (Serial 08/955,339) filed 21 October 1997; issued 13 April 1999.

Steven D. Russell
Shannon Kasa
Howard W. Walker

<div align="right">

**"Chemical Sensor Using
Ring-Oscillator Thermometry"**

</div>

This invention describes a novel structure using ring-oscillator thermometry for use as a
chemical or biological sensor. Combustible gas sensors based on thermal sensors have been
demonstrated in the prior art. These sensors, called pellistors, depend on a rise in temperature
at a catalytic surface due to catalytic oxidation of the combustible gas. The pellistor measures
this rise in temperature with a thermistor. The novel gas sensor incorporates a catalytic plati-
num layer deposited on top of a ring oscillator. Combustible gases will be catalytically oxi-
dized at the platinum surface. The heat released by the reaction will cause local heating of the
ring oscillator and thus, affect its frequency.

Patent 5,895,629 Navy case 76,462 (Serial 08/977,720) filed 25 November 1997; issued 20 April
1999.

David W. J. Stein

<div align="right">

"Coherent Hidden-Markov Detector"

</div>

This method for processing coherent radar-return data detects targets in nonstationary radar
clutter. Advantages and new features of this method over Doppler processing include mod-
eling the clutter using Markov models and applying a phase-coherent detection statistic based
on a likelihood ratio that allows for the clutter level to fluctuate over the duration of the time
series being analyzed.

Patent 5,900,835 Navy case 78,933 (Serial 09/112,906) filed 9 July 1998; issued 4 May 1999.

Stanislaw J. Szpak
Pamela A. Boss
**"Electrochemical Cell Having a
Beryllium Compound Coated Electrode"**

This invention describes a procedure to modify metal-hydride electrodes so as to increase hydrogen storage capabilities as well as increase the cycling lifetime of the electrode. Such an invention improves the performance of fuel cells and/or rechargeable metal-hydride batteries.

Patent 5,928,483 Navy case 76,707 (Serial 08/969,175) filed 12 November 1997; issued 27 July 1999.

Stephen M. Hart
"Optoelectronically Controlled Waveguide"

An optoelectronically controlled waveguide (OCW) is composed of a metallic waveguide, a finline, and a PVFET. (A PVFET is a field-effect transistor with a gate controlled by a photovoltaic cell.) The finline is inserted into the waveguide making electrical contact, and the PVFET is affixed to the finline in a shunt configuration. The resulting device is capable of attenuating the energy propagating in the waveguide to any desired degree. In this fashion, the OCW can function as an attenuator or a switch.

Patent 5,969,581 Navy case 76,916 (Serial 09/093,849) filed 28 May 1998; issued 19 Oct 1999.

Adi R. Bulsara
Mario E. Inchiosa
Luca Gammaitoni
Frank E. Gordon
**"Stochastic Resonance Detector
for Weak Signals"**

This device exploits the dynamical symmetry-breaking property of a weak dc signal in an *a priori* symmetric nonlinear dynamic device, to detect and quantify the dc signal. Simultaneously, the technique offers a novel way to circumvent detector low-frequency noise constraints by shifting the detection to a more acceptable part of the frequency spectrum.

Patent 6,008,642 Navy case 78,154 (Serial 08/917,655) filed 25 August 1997; issued 6 July 1999.

Michael J. Winton
Stephen D. Russell
**"Method of Making Improved
Electrical Contact to Porous Silicon"**

This is an improved method of making electrical contact to porous silicon and porous silicon device structures by controlling the global or large-scale surface morphology. The inventive process uses the supply of holes, ions of other charged species to control the etching dynamics of the porous silicon formation. The intensity of the light emitted by porous silicon layers and devices can therefore be increased by the improved electrical interconnection between the mechanically, chemically, and thermally fragile porous silicon and the device electrodes.

Patent 6,017,811 Navy case 77,603 (Serial 08/944,746) filed 6 October 1997; issued 25 January 2000.

Terence R. Albert
Adi R. Bulsara
Gabor Schmera
Mario Inchiosa

"Noise-Assisted Signal Processor
with Nonlinearly Coupled Arrays
of Nonlinear Dynamic Elements"

A signal processor uses a globally nonlinearly coupled array of nonlinear dynamic elements. In one embodiment of the invention, these elements take the form of bistable overdamped oscillators. The processor exploits the phenomenon of stochastic resonance to amplify a weak periodic signal embedded in noise. A detailed numerical analysis of the full dynamics of the bistable element represented by the reference oscillator has shown that the signal-to-noise ratio (SNR) of the entire processor system reaches a maximum at a critical noise variance value.

By using a number of overdamped oscillators working together, an enhancement of SNR can be achieved over that attained with the use of a single oscillator.

Patent 6,020,782 Navy case 78,545 (Serial 08/893,907) filed 11 July 1997; issued 1 February 2000.

David W. J. Stein

"Method for Detecting Weak Signals
in a Non-Gaussian and Non-Stationary
Background"

This method detects weak signals in a non-Gaussian and non-stationary background by using a hidden Markov parameter estimator. A detection output signal is generated if any of the normalized values of the detection statistics exceeds a threshold.

Patent 6,038,526 Navy case 79,280 (Serial 09/111,369) filed 24 June 1998; issued 14 March 2000.

INDEPENDENT RESEARCH
Claims Allowed; Notice of Allowance

Willard M. Cronyn

"Compact, Phasable, Multioctave,
Planar, High-Efficiency Spiral-Mode
Antenna"

The antenna consists of eight planar windings, each one of which is an exponential spiral. The windings are connected in groups of three to a balanced transmission line, with a "floating" winding between each of the two groups. For the purpose of phasing elements together for directional-beam control, the particular grouping of windings can be changed. A sinuous variation is imposed on the spiral windings to increase the path length for each winding rotation so that the circumference through which the phase increases by 360 degrees is correspondingly decreased. This element integrates a planar structure, wideband compact design, and phasability into a single physical structure.

Navy case 76,188 (Serial 09/107,901) filed 18 June 1998; Notice of Allowance 2 August 1999.

Allen Shum   **"Asynchronous Transfer Mode Cell Loss Estimation Algorithms"**

A software program for estimating traffic loss of an asynchronous transfer mode (ATM) statistical multiplexer comprises a communication channel having traffic sources and a buffer. Traffic is generated by the traffic sources and removed by the communication channel. When total traffic exceeds the capacity of the communication channel, excess traffic is stored in the buffer. When the buffer is full, excess traffic is lost. Estimating the amount of traffic that will be lost by an ATM statistical multiplexer, therefore, has application in the design of ATM networks.

Navy case 77,443 (Serial 08/707,284) filed 3 September 1996; Notice of Allowance 12 May 1998.

Monti E. Aklufi   **"Thin-Film Improvement Method and Apparatus"**
Stephen D. Russell

This invention provides a novel apparatus and an improved method by using a contoured laser beam to improve the electrical, optical, and material properties of thin films.

Navy case 77,921 (Serial 08/934,037) filed 19 September 1997; Notice of Allowance 15 October 1999.

Gregory A. Theriault   **"A Translation System for Directing an Optical Signal to Predetermined Coordinates"**
Leonard J. Martini
Leon V. Smith

A translation system for directing an optical signal through predetermined coordinates of a window mounted in a soil penetration probe includes a tube having a sidewall and an aperture through said sidewall; an optically transparent window mounted in said aperture; an optical system for emitting an optical signal through said aperture; and a translation mechanism mounted within said tube. The translation mechanism may be selectively operated to translate independently and simultaneously the optical system along two orthogonal vectors so that the optical signal scans across the window. Scanning the optical signal extends the useful life of the window before its transmissibility becomes too impaired by damage caused from the optical signal.

Navy case 78,881 (Serial 09/015,431) filed 29 January 1998; Notice of Allowance 22 November 1999.

David W. J. Stein   **"Hidden-Markov Amplitude Detector"**

This invention provides a means of detecting incoherent signals in non-Gaussian noise.

Navy case 79,280 (Serial 09/111,369) filed 24 June 1999; Notice of Allowance 2 September 1999.

INDEPENDENT RESEARCH
Patent Applications Filed

Stanislaw J. Szpak
Pamela A. Boss

"Electrode and Method for Preparation of Electrode for Electrochemical Compression of Deuterium into a Metal Lattice"

This invention provides an electrode and method for preparing the electrode that may be employed to electrochemically compress deuterium into a metal lattice of the electrode. An electrochemical cell is constructed that includes an electrolyte solution comprising a metallic salt and a supporting electrolyte. The metallic salt, when in a reduced state, absorbs deuterium. Both the electrolytic solution and supporting electrolyte are dissolved in heavy water. An anode and cathode are immersed and stable within the electrolytic solution. The anode is stable when polarized. A voltage is applied across the anode and cathode while a constant potential is maintained at the cathode. The constant potential is measured with respect to a reference electrode immersed within the electrolytic solution so that deposition of metallic ions occurs in the presence of evolving deuterium during electrolysis of the electrolytic solution. By this method, the cathode is transformed into the electrode.

Navy case 73,311 (Serial 07/632,896) filed 24 December 1990; pending.

Stephen M. Hart

"Optoelectronically Controlled Frequency-Selective Surface"

A photovoltaic field-effect transistor (PVFET) is used to control the impedance, scattering frequency, and scattering cross-section of the scattering elements on a frequency-selective surface. The PVFETs are implanted in the arms of either wire or slot scatterers to make their scattering properties adjustable. The resulting optoelectronically controlled frequency-selective surface (OCFSS) becomes a programmable electromagnetic shield or pattern control device.

Navy case 76,915 (Serial 09/253,504) filed 19 February 1999; pending.

Richard Scheps

"Underwater Imaging Technique for the Detection of Shallow Submerged Objects"

This high-resolution underwater imaging and ranging device scans an area underwater with a pulsed laser and records the reflected signal from the illuminated area with a gated photomultiplier.

Navy case 77,222 (Serial 08/908,778) filed 7 August 1997; pending.

Parviz Soltan
John A. Trias
Weldon J. Dahlke
Robert V. Belfatto
Frank Sanzone
Christopher J. Poulos
Neil P. Acantilado

"Computer-Controlled
Three-Dimensional
Volumetric Display"

A three-dimensional display system comprises a display volume selectively partitioned into distinct display regions: a display surface for scattering light beams from the display volume; at least two optical scanners for modulating the light beams and for directing the light beams to the display surface within each distinct display region, respectively; and a display controller. The display controller comprises a world-coordinate interface for inputting world coordinates, a data processor for transforming the world coordinates into view coordinates and device coordinates, and an optical-scanner controller for sensing and controlling the motion of the display surface and for outputting the device coordinates to the optical scanners to generate a three-dimensional image within the display volume.

Navy case 78,445 (Serial 08/926,854) filed 10 September 1997; pending.

Stephen D. Russell
Randy L. Shimabukuro
Yu Wang

"Transmissive Surface-
Plasmon Light Valve

The invention provides a light valve or optical modulating device that exploits color-selective absorption at a metal-dielectric interface by surface plasmons. The invention includes an electrode layer formed of an optically transparent substrate. A layer of electro-optic material is formed on the electrode. The electro-optic material has an index of refraction that may be modulated by an electrical bias. A second electrode is formed over the electro-optic material. Changes in a voltage bias across the electrodes modulate the index of refraction of the electro-optic material so that it selectively absorbs light (at different wavelengths) that passes through the light valve, depending on the index of refraction. The electrodes are made of a transparent or semitransparent material, such as indium tin oxide. Multiple light valves may be arranged in an array to form a flat-screen video display.

The novelty of the invention is that it provides a new mode of operation in that it is a transmissive device, rather than a reflective device.

Navy case 78,518 (Serial 09/172,581) filed 14 October 1998; pending.

Carol A. Becker   **"Light-Activated Polymeric Actuators"**

Visible light causes a pH charge *in situ* to the polymer backbone. The pH charge expands and contracts the polymeric actuator in a timeframe suitable for robotics. A mechanism is provided for reversible dissipation of any heat produced by the light.

Navy case 78,990 (Serial 09/137,008) filed 20 August 1998; pending.

Frank E. Hanson
Peter M. Poirier

<div align="right">

**"Technique for Operating High-
Energy Q-switched 0.9-μm
Neodymium Lasers"**

</div>

This invention describes a wavelength discriminating filter and procedure to efficiently operate a Q-switched neodymium laser on the 4F3/2 to 4I9/2 transition near 0.9 μm by suppressing the higher gain emissions near 1 μm. The invention applies in general to all neodymium-based lasers operating at 0.9 μm and, in particular, to neodymium-doped yttrium aluminum garnet (Nd:YAG) operating at 0.0946 μm.

Navy case 79,523 (Serial 09/252,610) filed 4 February 1999; pending.

INDEPENDENT RESEARCH
Invention Disclosures Authorized

Pamela A. Boss
Stephen H. Lieberman

<div align="right">

**"The Use of Microelectrode Arrays for
the Detection of Volatile Organic
Contaminants in the Air"**

</div>

The invention is used to detect organic contaminants in the gas phase. The invention comprises a working electrode separated from an auxiliary electrode by an insulator. The electrodes are coated with self-assembled monolayers, and a voltage bias is applied across the electrodes while the resulting current is measured. The electrode materials and monolayers are selected so that when a gaseous analyte of interest contacts the electodes, the current changes by a detectable amount. Multiple microelectrodes may be configured into arrays whereby each microelectrode is responsive to a particular analyte. In this way, many different gaseous contaminants may be detected with a single instrument. The microelectrodes may be fabricated onto chips using photo-lithographic techniques.

An important novelty of the invention is that it provides an instrument capable of monitoring contaminants over time and provdes the real-time detection of drugs and explosives. The use of the self-assembled monolayers as a coating to enhance the response of the electrodes is novel.

Navy case 78,928; authorized for preparation of patent application 9 Februrary 1999.

Richard Scheps

<div align="right">

"Compact Solid-State Dye Laser"

</div>

This invention describes a compact solid-state dye laser that is diode-pumpable. The laser in its preferred embodiment consists of a monolithic state of materials including a solid-state 1-μ–emitting laser gain element, a passive Q-switch, a second-harmonic doubling crystal, and the solid-state dye gain element.

Navy case 79,094; authorized for preparation of patent application 6 December 1999.

Pamela A. Boss
Stephen H. Lieberman

**"Spectroelectrochemical Device
to Detect Airborne Contaminants"**

The invention is a gas sensor that combines the sensitivity of electrochemistry with the specificity of spectroscopy for detecting organic contaminants in the gas phase. The sensing unit consists of a micro-electrode assembly comprising an inner working disk electrode and an outer auxiliary ring electrode. The inner working disk electrode is coated with a thiol coating. The micro-electrode portion of the sensor is used to continuously monitor the environment. When current flow between the two electrodes of the sensor occurs, a spectrum of the working electrode can be obtained to identify the electro-active species. The invention can operate in either a flowing stream or a quiescent environment. It can also be used to monitor for dangerous volatile organics, explosives, or drugs. The invention may also be used to perform surface-enhanced Raman spectroscopy (SERS).

An important novelty of the invention is that it incorporates micro-electrodes and SERS, which combine to have the capability of detecting organic contaminants in the ppm level. The micro electrodes can be arranged in arrays and require reduced capacitive charging currents. Micro-electrodes exhibit reduced signal-to-noise characteristics over standard-sized electrodes and can be configured into a variety of shapes.

Navy case 79,709; authorized for preparation of patent application 15 December 1999.

INDEPENDENT RESEARCH
Invention Disclosures Submitted

Stephen D. Russell
Philip R. Kesten

"Interactive Display Device"

This invention is a monolithically integrated display and sensor array that provides for interactive real-time changes to the display image.

Navy case 78,287; disclosure submitted 24 October 1996.

Stephen D. Russell
Randy L. Shimabukuro
Yu Wang

"Microdynamic Optical Device"

This invention describes a light valve, display, optical modulating device or optical filter that uses a microdynamic construction to exploit the color-selective absorption at a metal-dielectric interface by surface plasmons. This invention has applications for displays in command and control, for multispectral imaging in surveillance and reconnaissance, and for filtering in optical communications and scientific instrumentation.

Navy case 78,968; disclosure submitted 19 November 1997.

Ayax D. Ramirez
Stephen D. Russell
Randy L. Shimabukuro
"Resonance-Tunable Optical Filter"

This invention exploits color-sensitive absorption at a metal dielectric interface by surface plasmons. The invention provides a resonance-tunable optical filter that includes a dielectric and a metal layer through which electromagnetic radiation may be transmitted or reflected. A beam-steering apparatus is used to change the incident angle of the electromagnetic radiation whose optical properties are modified by choice of incident angle. The incident medium and exit medium are optically transmissive.

Unlike the prior art, the invention device does not require spacers, alignment layers, and seals previously used to make liquid crystal filled surface-plasmon devices.

Navy case 79,095; disclosure submitted 26 February 1998.

Stephen D. Russell
Randy L. Shimabukuro
Yu Wang
"Solid-State Light Valve
and Tunable Filter"

This invention describes an all solid-state light valve, optical modulating device or optical filter that uses color-selective absorption at a metal-dielectric interface by surface plasmons. The invention has applications for displays in command and control, for multispectral imaging in surveillance and reconnaissance, and for filtering in optical communications and scientific instrumentation.

Navy case 79,542; disclosure submitted 3 November 1997.

Stephen D. Russell
"Spatially Conformable Tunable Filter"

The invention provides a flexible or pliable optical modulating device, light-valve or optical filter. It uses a sheet of polymer-dispersed liquid crystal (PDLC) material and specifically selected thin-metal electrodes on either side of the PDLC to form a capacitor structure. When a voltage is applied to the capacitor, the refractive index of the liquid crystal changes since it is an electro-optic material. The optical properties of one of the thin-metal electrodes are selected in combination with the PDLC to have a surface-plasmon resonance that is either narrow band or broadband depending on the application. The surface plasmon is then used to selectively absorb incident light at the metal-PDLC interface, while the remaining light gets reflected (or transmitted). By varying the applied voltage, and its corresponding change in PDLC refractive index, we can modulate the light valve or tune the filter.

The improvement over the prior art is that this can be configured conformably over a surface to improve the acceptance angle for the filter and to simplify the fabrication of the device as compared to conventional liquid crystals.

Navy case 79,545; disclosure submitted 1 June 1998.

David F. Schwartz
J. William Helton
Jeffery C. Allen

"Predictor for Optimal Broadband Matching"

A predictor for optimal broadband matching of the present invention comprises a computer program that inputs samples of load reflectance normalized to characteristic line impedance, the frequencies associated with the normalized reflectance samples, and a parameter specifying the number of frequency increments for calculation. The program calculates and outputs the highest power gain obtainable by any matching circuit and two associated system parameters: the power mismatch and the voltage standing-wave ratio.

Navy case 79,796; disclosure submitted 1 December 1998.

James D. Warner
Thomas A. Knoebel
James R. Deuth

"Small-Boat Captive System"

The small-boat capture device consists of two major components. The first component is a spring loop attached to the trailer and intersects the bow of the boat as it comes aboard the trailer. For the 10,000-lb small boat used in the initial application, a closing speed of 4.5 kn and a 1.5-inch-diameter nylon line provided the correct spring constant to provide a 2.5-g decelerate. The second component is a stainless-steel latching mechanism mounted to the bow of the small boat. The latch catches the line as it slides down the bow.

Navy case 79,950; disclosure submitted 22 January 1999.

Pamela A. Boss
Roger D. Boss
Stephen H. Lieberman

**"Method of Preparing Durable
Gold or Silver Film Substrates
for Surface-Enhanced Raman
Spectroscopy (SERS)"**

This invention describes a process to prepare durable gold or silver films on substrates containing metal-oxide bonds for use in SERS. Steps in the process are (1) roughen the surface of the substrate, (2) react the roughened surface with a silanization agent such as (3-mercaptopropy) trimethoxy silane, (3) vacuum-deposit silver or gold onto the silanized surface, and (4) react with thiol coating. Depending upon the thiol coating used, these substrates can be used to detect VOCs, metal ions, and anions. Substrates prepared in this manner exhibit excellent adherence between the substrate surface and the metal film. The films can be immersed in water over extended periods of time. The silver or gold metal film can be used as the sensing layer of an optical waveguide device.

The substrates can be used by either the Navy or Marine Corps for environmental monitoring. The chemical modification of these substrates enables them to be used to detect and identify explosives, nerve agents, drugs, etc.

Navy case 79,987; disclosure submitted 8 October 1998.

Richard Scheps

"Efficient Laser for High-Frequency Modulation"

A dye laser pumped by a laser diode allows highly efficient modulation into the 100-Ghz range for high bandwidth communications.

Navy case 80,110; disclosure submitted 11 February 1999.

Pamela A. Boss
Stephen H. Lieberman
Leonard J. Martini
Leon Smith

"Fiber-Optic Sensor for Surface-Enhanced Raman Spectroscopy (SERS) to Detect Subsurface Contaminants"

The present invention comprises a fiber-optic probe fitted into a cone penetrometer module that draws a liquid sample from subsurface soil. The fiber-optic probe illuminates the sample and collects a Raman emission spectrum from the sample. The sample may then be purged from the module to allow another sample to be taken at a different soil depth.

Navy case 80,175; disclosure submitted 3 November 1999.

Steven J. Cowen

"Method for Incorporating Total Internal Reflection into a Flexible Lithographic Mask"

The novelty of the invention resides in the incorporation of critically angled surfaces to reflect unwanted optical energy out of the pattern mask. In the prior art, pattern masks that perform the frequency up-shifting function used energy-absorbing occluding layers to block unwanted light. However, such occluding layers had a tendency to accumulate heat energy that could damage the masks, and required low optical intensities to prevent mask damage. The invention allows the use of more intense optical irradiation of the pattern mask, thereby resulting in faster processing time.

Navy case 80,180; disclosure submitted 15 October 1999.

Stanislaw Szpak
Pamela A. Boss

"Power Conversion Unit"

This invention describes a power-conversion unit consisting of a working electrode and counter electrode. Palladium and deuterium are co-deposited on the working electrode. During co-deposition, nuclear events of unknown origin occur resulting in enormous heat release. This heat can be used to provide power for a number of applications.

Navy case 80,181; disclosure submitted 17 September 1998.

Pamela A. Boss
Stephen H. Lieberman

**"Hand-Held, Fiber-Optic Sensor
for Either Normal Raman (NR)
Spectroscopy of Surface-Enhanced
Raman Spectroscopy (SERS)"**

The invention is a hand-held, fiber-optic sensor used to detect and identify VOCs, inorganic anions, metal ions, etc., by either normal Raman spectroscopy or SERS. The sensor head consists of an optical window and a fiber-optic bundle. For SERS, the window is coated with a thin silver or gold film that is optically transparent. The metal film is then reacted with a thiol to form a self-assembled monolayer (SAM). The chemical nature of the coating determines its selectivity.

SSC San Diego case 384; disclosure submitted 6 December 1999.

Pamela A. Boss
Stephen H. Lieberman
Greg Theriault
Leonard J. Martini
Leon Smith

**"Thermo-Electrically Cooled
Sensor for Normal Raman (TE-NR)
Spectoscopy or Surface-Enhanced
Raman Spectroscopy (TE-SERS) to
Detect Subsurface Contaminants"**

The invention incorporates either a TE-NR or a TE-SERS sensor module inside a sampling, cone penetrometer probe. The inside of the probe is subdivided into three chambers—a lower sample chamber, a middle chamber housing either the TE-NR or TE-SERS sensor module, and an upper chamber housing the fiber optics. A water sample is taken into the lower chamber. It is then sparged with an inert gas to displace VOCs. VOC vapors are transported through a hydrophobic membrane and are concentrated onto a TE-cooled SERS substrate. The VOCs are identified and quantitated by either their Raman or SERS emissions.

SSC San Diego case 385; disclosure submitted 6 December 1999.

James Alsup

"Improved Comb-Spectrum Sensor"

A triplet-pair waveform for an active sonar is generated by an algorithm that provides good range resolution, high Doppler sensitivity, moderate bandwidth, and good power efficiency.

SSC San Diego case 386; disclosure submitted 14 December 1999.

Pamela A. Boss
Stephen H. Lieberman

**"Device to Detect Anionic Nutrients
by Surface-Enhanced Raman
Spectroscopy (SERS)"**

This invention is a sensor that uses cationic-coated SERS substrates to detect anionic nutrients *in-situ* and in real time. For the Navy, information on nutrient dynamics is used to understand chemical reactions that impact marine environmental quality and to predict the distribution, growth, and community structure of biota in the coastal ocean.

SSC San Diego case 389; disclosure submitted 19 January 2000.

Douglass C. Evans
Joseph D. Aboumrad
Earl E. Floren

**"Blazed-Grating Optical Fiber
Polarizing Coupler"**

This invention develops a technique to selectively remove one polarization state of light propagating in a single-mode optical fiber more than the other polarization state over a large range of wavelengths. The light-carrying fiber is induced to radiate an accurately controllable percentage of its light by the introduction of a blazed Bragg grating into its core region for a few millimeters of length. The blaze, or tilt, of the periodic perturbation is selected to maximize polarization discrimination. The scattered light is incident on the outer surface of an identical fiber that is located in close proximity and in parallel to the first fiber. The identical grating in the second fiber scatters light radiated from the first fiber into its guided direction of propagation with maximum polarization discrimination.

SSC San Diego case 398; disclosure submitted 12 April 2000.

INDEPENDENT EXPLORATORY DEVELOPMENT
Patents Issued

Neil P. Acantilado

**"Computer Program for a Three-
Dimensional Volumetric Display"**

This method for transforming world coordinates into device coordinates comprises the following steps: inputting a set of world coordinates to be displayed; scaling the world coordinates into view coordinates bounded by a display volume; finding a control memory location of a light-beam deflector corresponding to a Y-axis position for each of the view coordinates; calculating X-axis and Z-axis device coordinates from the view coordinates for deflecting a light beam to a selected point within the display volume, corresponding to each of the view coordinates; and loading the device coordinates into the control memory locations corresponding to the Y-axis position for each of the view coordinates, to cause the light beam to be deflected to each selected point.

Patent 5,945,966 Navy case 77,782 (Serial 08/726,305) filed 2 October 1996; issued 31 August 1999.

Pamela A. Boss
Roger D. Boss

"Thin-Layer Spectroelectro-Chemical Cell"

This invention describes the design of a low-volume, thin-layer cell constructed of chemically resistant materials capable of performing spectroelectrochemistry. Such a cell can be used as a flow-through cell to continuously monitor manufacturing processes.

Patent 6,015,479 Navy case 77,803 (Serial 08/900,983) filed 25 July 1997; issued 18 January 2000.

PROJECT TABLES

SSC San Diego FY 99 ILIR Database

SSC SD Proj. #	DTIC DN No.	Project Title	Principal Investigator	SSC SD Code	Phone (619)55	ONR SE#	DoD MA1	DoD MA2	JMA	DoD CT	FY 98 $(K)	FY 99 $K	Planned FY 00 $(K)	Keywords	Most Strongly Supported ONR/NRL Thrust	Next Most Strongly Supported ONR/NRL Thrust
ZU54	307777	3-D Propagation in Shallow Water Overlaying an Elastic Bottom	Dr. A. T. Abawi	D857	33101	14	ASW	OSV	2	19	80	63	0	propagation; parabolic equation model; coupled mode	311-03	NRL710-04
ZU78	308521	Detection of Ionic Nutrients in Aqueous Environments Using Surface-Enhanced Raman Spectroscopy (SERS)	Dr. P. A. Boss	D363	31603	13	MWT		8	12	0	79.8	100	sensors; Surface-Enhanced Raman Spectroscopy (SERS)	342-04	361-08
ZU69	308519	Public-Key Cryptosystems Based on Groups on Elliptic Curves	Dr. V. P. Broman	D712	31641	15	CCC		4	7	0	92.4	0	cryptosystems; public key; elliptic curve; discrete logarithm; cryptanalysis	NRL550-03	NRL570-02
ZU55	307778	Environmentally Adaptive Autonomous Matched-Field Tracking	Dr. H. P. Bucker	D857	33093	14	OSV	ASW	3	19	68	58.8	0	underwater sound; signal processing	320-11	320-12
ZU79	308522	Frequency Mixing in Nonlinear Dynamic Devices	Dr. A. R. Bulsara	D364	31595	14	CCC		4	6	0	110	0	heterodyne signal; nonlinear device; target frequency	331-04	331-03
ZU72	308510	Geolocation Error Modeling and Reduction	Dr. S. I. Chou	D73A	32541	14	INT	ELW	4	19	0	63	0	time difference of arrival; time of arrival; constant pulse repetition interval	NRL570-01	320-08
ZU73	308513	In-Fiber Polarizers Using Blazed Fiber Gratings	D. Evans	D746	31978	11	CCC		3	6	0	55	0	fiber optics; gratings	313-06	NRL680-01
ZU57	307780	Anti-Ice Coatings: New Low Surface Free Energy Coatings for Easy Ice Release	Dr. R. D. George	D361	32776	13	MOB		8	17	90	29.4	0	polymers; coatings; ice-release; environmental; anti-ice	NRL600-01	361-07
ZU58	307781	Deduction in Data Fusion Based upon Algebraic Representation of Probabilistic Models	Dr. I. R. Goodman	D44215	34014	14	CCC		4	6	185	96.6	110	data fusion; expectation of random sets; generalized estimation; relational event algebras	311-02	NRL700-01
ZU80	308516	Coherent Mid-IR Optical Parametric Oscillator	Dr. F. E. Hanson	D853	32094	11	AAW		3	19	0	92.4	100	lasers; nonlinear optics; laser radar	313-06	331-03

NOTES: SE = Subelement (codes); MA = Mission Area; JMA = Joint Mission Area (codes); CT = Critical Technology (codes)
See Glossary for numbered codes, thrusts, and other abbreviations.

155

SSC SD Proj. #	DTIC DN No.	Project Title	Principal Investigator	SSC SD Code	Phone (619)55	ONR SE#	DoD MA1	DoD MA2	JMA	DoD CT	FY 98 $(K)	FY 99 $K	Planned FY 00 $(K)	Keywords	Most Strongly Supported ONR/NRL Thrust	Next Most Strongly Supported ONR/NRL Thrust
ZU53	306770	Exact Diagonalization of Large Sparse Matrices	Dr. C. Hicks	D3604	31593	11	MWT	CCC	4	6	40	29.4	0	high-performance computing; large matrix diagonalization	NRL550-01	NRL600-04
ZU74	308509	Evaporation Duct Assessment from Meteorological Buoys	H. V. Hitney	D858	31428	21	OSV		3	19	0	91.2	0	radar; evaporation ducting; propagation	320-02	NRL100-01
ZU75	308527	Floating Antenna Propagation	B. R. Hunt	D7303	35345	21	ELW	INT	4	10	0	98.4	0	RF propagation; floating antennas	313-04	313-11
ZU84	308530	Speech Enhancement	R. R. Johnson	D44213	33653	15	CCC		4	6	0	117	0	speech enhancement; noise reduction	342-05	342-08
ZU35	305529	Parallel Sparse Factorizations through Recursive Bordered Block Diagonalization	Dr. A. K. Kevorkian	D712	32058	14	MWT		3	22	84	29.4	0	least squares; sparse matrices; indefinite systems; linear and nonlinear programming	NRL550-01	NRL710-01
ZU48	306760	Propwash/Wake Resuspension in San Diego Bay (The Grand Plan III)	D. M. Ladd	D363	31617	23	FSO	MWT	8	12	80	80.6	0	critical shear stress; resuspension	361-08	342-04
ZU66	308507	Integration of Complex Information	D. Lange	D4223	36534	15	CCC		3	6	0	53.8	50	hypermedia; knowledge base; plan	311-02	342-05
ZU70	308511	Wireless Network Resource Allocation with QoS Guarantees	S. K. Lapic	D822	33073	21	CCC		3	6	0	92.4	105	communications; wireless networks	313-02	313-07
ZU81	309260	Electronic Properties of Cubic Boron Nitride	Dr. W. C. McGinnis	D364	35610	21	MWT		3	9	0	46.2	80	semiconductors; electronics	312-02	312-04
ZU71	308514	Applications of Stochastic Nonlinear Dynamics to Communication Arrays	Dr. B. K. Meadows	D364	32823	14	CCC		3	6	0	90	150	command and communications; nonlinear dynamics; stochastic	313-02	313-07
ZU67	308520	Innovative Methods for Alertness Management	S. A. Murray	D374	36350	15	CCC		4	15	0	91.3	70	alertness; human factors; human computer interaction; psychophysiology	342-05	342-06
ZU82	308524	Laser Optical Parametric Oscillator for mid-IR	J. F. Myers	D743	32599	11	CCC		3	6	0	84	50	laser; optical parametric oscillator (OPO)	NRL680-01	331-03

NOTES: SE = Subelement (codes); MA = Mission Area; JMA = Joint Mission Area (codes); CT = Critical Technology (codes)
See Glossary for numbered codes, thrusts, and other abbreviations.

156

SSC San Diego FY 99 ILIR Database (contd)

SSC SD Proj. #	DTIC DN No.	Project Title	Principal Investigator	SSC SD Code	Phone (619)55	ONR SE#	DoD MA1	DoD MA2	JMA	DoD CT	FY 98 $(K)	FY 99 $K	Planned FY 00 $(K)	Keywords	Most Strongly Supported ONR/NRL Thrust	Next Most Strongly Supported ONR/NRL Thrust
ZU59	307782	High-Isolation Fiber-Optic Add/Drop Multiplexers for Shipboard Networking Applications	R. J. Orazi	D825	31065	11	CCC		4	6	90	79	0	wavelength division multiplexing; Bragg gratings; fused-fiber couplers	331-03	NRL680-01
ZU61	307784	Telesonar Transmission Channel Models	J. A. Rice	D857	33107	11	CCC		4	19	105	96.6	135	underwater acoustic propagation; trans-mission channels; propagation models; telesonar; sound scattering	320-11	311-01
ZU83	308518	Sensitivity of Marine Mammals to Low-Frequency Acoustic Pressure and Particle Motion	Dr. S. H. Ridgway	D3503	31374	31	ASW	MIW	3	19	0	50.4	60	marine mammals; acoustics; particle motion	342-07	361-08
ZU68	309262	Robust Control of Information-Flow for Network-Centric Warfare	Dr. S. Sritharan	D73H	31201	15	CCC		4	6	0	105	0	C^4I, network-centric warfare; optimal control; information	NRL570-02	311-06
ZU76	308523	Advanced Hyperspectral Data Processing	Dr. S. E. Stewart	D743	32546	14	MWT		3	19	0	75.6	140	hyperspectral data; data processing; stochastic; linear unmixing; detection	311-03	NRL570-07
ZU77	308532	Super Composite Slotted Cylinder Projector	Dr. P. Y. Tang	D746	31938	11	ASW		3	19	0	84	90	laminated composite materials; actuator; active materials; wall-driven projector; slotted cylinder projector	320-11	320-14
ZU63	307786	Development and Analysis of Turbo Codes for Navy Applications	Dr. B. E. Wahlen	D841	35622	21	CCC		4	6	0	109.2	0	forward error correction; turbo codes; trellis-coded modulation	313-02	313-07

NOTES: SE = Subelement (codes); MA = Mission Area; JMA = Joint Mission Area (codes); CT = Critical Technology (codes)
See Glossary for numbered codes, thrusts, and other abbreviations.

157

SSC San Diego FY 00 ILIR Database

SSC SD Proj. #	DTIC DN No.	Project Title	Principal Investigator	SSC SD Code	Phone (619)55	ONR SE#	DoD MA1	DoD MA2	JMA	DoD CT	FY 98 $(K)	FY 99 $(K)	Actual FY 00 $(K)*	Keywords	Most Strongly Supported ONR/NRL Thrust	Next Most Strongly Supported ONR/NRL Thrust
ZU93	309352	Sonar Waveform Design	J. Alsup	D711	32498	14	OSV	ASW	2	19	0	0	89	acoustic detection and detectors; undersea and anti-submarine warfare	320-11	320-14
ZU61	307784	Telesonar Transmission Channel Models	P. A. Baxley	D857	35634	11	CCC	ASW	4	19	105	96.6	119	underwater acoustic propagation; transmission channels; propagation models; telesonar; sound scattering	320-11	311-01
ZU78	308521	Detection of Ionic Nutrients in Aqueous Environments Using Surface-Enhanced Raman Spectroscopy (SERS)	Dr. P. A. Boss	D363	31603	13	MWT	MWT	8	12	0	79.8	89	sensors; Surface-Enhanced Raman Spectroscopy (SERS)	342-04	361-08
ZU94	309353	Automatic Matched-Field Tracking	Dr. H. P. Bucker	D857	33093	14	OSV	ASW	3	19	0	0	71	acoustics; acoustic detection and detectors	320-11	320-12
ZU97	309356	Fiber-Optic Gyroscope Dead-Band Analysis	J. J. Del Colliano	D314	31516	21	CCC	MOB	1	6	0	0	80	navigation and guidance	313-09	NRL680-01
ZU85	309343	Change Blindness: Understanding Our Visual Representation of Objects and Scenes	J. C. DiVita	D44209	36461	15	CCC		4	6	0	0	45	change blindness, scene perception, visual memory, object perception	342-05	342-06
ZU86	309344	Distributed Quality Collaboration	J. J. Drummond	D4123	34131	15	CCC		4	6	0	0	27	computer systems; command and control; situation awareness	311-02	333-01
ZU98	309357	Antijam Techniques for GPS Using Nonlinear Processing	Dr. H. L. Dyckman	D313	33829	14	CCC	MOB	1	6	0	0	89	GPS; antijam; nonlinear	313-09	331-02
ZU58	307781	Deduction in Data Fusion Based on Algebraic Representation of Probabilistic Models	Dr. I. R. Goodman	D44215	34014	14	CCC		4	6	185	96.6	98	data fusion; expectation of random sets; generalized estimation; relational event algebras	311-02	NRL700-01
ZU90	309348	Development of Improvements to the UHF Advanced Digital Waveform	S. J. Graser	D844	39691	14	CCC		4	6	0	0	98	radio communications	313-02	313-07

NOTES: SE = Subelement (codes); MA = Mission Area (codes); JMA = Joint Mission Area (codes); CT = Critical Technology (codes)
See Glossary for numbered codes, thrusts, and other abbreviations.
* FY 00 funding includes a $300K carryover from FY 99.

SSC San Diego FY 00 ILIR Database (contd)

SSC SD Proj. #	DTIC DN No.	Project Title	Principal Investigator	SSC SD Code	Phone (619)55	ONR SE#	DoD MA1	DoD MA2	JMA	DoD CT	FY 98 $(K)	FY 99 $(K)	Actual FY 00 $(K)*	Keywords	Most Strongly Supported ONR/NRL Thrust	Next Most Strongly Supported ONR/NRL Thrust
ZU87	309345	Adaptive Intelligent Agents in Informative Environments	B. J. Hafner	D4123	35538	15	CCC		5	6	0	0	54	computer systems; command and control	311-04	311-02
ZU80	308516	Coherent Mid-IR Optical Parametric Oscillator	Dr. F. E. Hanson	D853	32094	11	AAW		3	19	0	92.4	89	lasers; nonlinear optics; laser radar	313-06	331-03
ZU66	308507	Integration of Complex Information	D. Lange	D4223	36534	15	CCC		3	6	0	53.8	45	hypermedia; knowledge base; plan	311-02	342-05
ZU70	308511	Wireless Network Resource Allocation with QoS Guarantees	Dr. S. K. Lapic	D822	33073	21	CCC		3	6	0	92.4	94	communications; wireless networks	313-02	313-07
ZU88	309346	Reasoning with Uncertainty about Complex Information and Events	Dr. R. W. Larsen	D441	34142	14	CCC		5	6	0	0	28	multi-process algebra data; conditional event algebra and probability logic; maximum entropy	311-02	342-05
ZU89	309347	Software Agents for Dissemination of Sensor Information and Tasking	J. R. McDonnell	D745	35762	15	CCC		5	6	0	0	72	miscellaneous detection and detectors	311-02	311-04
ZU81	309260	Electronic Properties of Cubic Boron Nitride	Dr. W. C. McGinnis	D364	35610	21	MWT		3	9	0	46.2	72	semiconductors; electronics	312-02	312-04
ZU71	308514	Applications of Stochastic Nonlinear Dynamics to Communication Arrays	Dr. B. K. Meadows	D364	32823	14	CCC		3	6	0	90	134	command and communications; nonlinear dynamics; stochastic	313-02	331-07
ZU67	308520	Innovative Methods for Alertness Management	S. A. Murray	D374	36350	15	CCC		4	15	0	91.3	62.5	alertness; human factors; human computer interaction; psychophysiology	342-05	342-06
ZU82	308524	Laser Optical Parametric Oscillator for mid-IR	J. F. Myers	D743	32599	11	CCC		3	6	0	84	45	laser; optical parametric oscillator (OPO)	NRL680-01	331-03

NOTES: SE = Subelement (codes); MA = Mission Area; JMA = Joint Mission Area (codes); CT = Critical Technology (codes)
See Glossary for numbered codes, thrusts, and other abbreviations.
* FY 00 funding includes a $300K carryover from FY 99.

159

SSC San Diego FY 00 ILIR Database (contd)

SSC SD Proj. #	DTIC DN No.	Project Title	Principal Investigator	SSC SD Code	Phone (619)55	ONR SE#	DoD MA1	DoD MA2	JMA	DoD CT	FY 98 $(K)	FY 99 $(K)	Actual FY 00 $(K)*	Keywords	Most Strongly Supported ONR/NRL Thrust	Next Most Strongly Supported ONR/NRL Thrust
ZU91	309350	High-Linearity Broadband Fiber-Optic Link Using Electroabsorption Modulators with a Novel Dual-Wavelength Second-Harmonic Cancellation Scheme	R. Nguyen	D859	35435	11	CCC		3	6	0	0	98	fiber optics; photonic link, electro-absorption (EA) modulator	313-02	312-01
ZU83	308518	Sensitivity of Marine Mammals to Low-Frequency Acoustic Pressure and Particle Motion	Dr. S. H. Ridgway	D3503	31374	31	ASW	MIW	3	19	0	50.4	54	marine mammals; acoustics; particle motion	342-07	361-08
ZU99	300314	Knowledge Mining for Command and Control Systems	Dr. S. H. Rubin	D73H	33554	15	CCC		4	6	0	0	295	knowledge mining; mining tools	360-02	342-08
ZU95	309354	Liquid Elastic Flextensional Broad-Band Acoustic Projector	Dr. L. S. Sheiba	D364	32046	11	ASW		3	19	0	0	85	flextensional acoustic projector	320-11	320-14
ZU76	308523	Advanced Hyperspectral Data Processing	Dr. S. Stewart	D743	32546	14	MWT		3	19	0	75.6	125	hyperspectral data; data processing; stochastic; linear unmixing; detection	311-03	NRL570-07
ZU77	308532	Super-Composite Slotted Cylinder Projector	Dr. P. Y. Tang	D746	31938	11	ASW		3	19	0	84	80	laminated composite materials; actuator; active materials; wall-driven projector; slotted cylinder projector	320-11	320-14
ZU96	309355	Enhanced Coordinate Registration for ROTHR	Dr. W. C. Torrez	D7212	32020	14	MWT	AAW	3	19	0	0	55.5	active and passive radar detection	313-08	NRL700-04
ZU92	309351	Robust Waveform Design for Tactical Communication Channels	Dr. J. R. Zeidler	D8505	31581	14	CCC		4	6	0	0	385	radio communications	313-02	313-07

NOTES: SE = Subelement (codes); MA = Mission Area; JMA = Joint Mission Area (codes); CT = Critical Technology (codes)
See Glossary for numbered codes, thrusts, and other abbreviations.

* FY 00 funding includes a $300K carryover from FY 99.

GLOSSARY

GLOSSARY

AC	Alternating Current
ACM	Association for Computing Machinery
A/D	Add/Drop
ADCP	Acoustic Doppler Current Profiler
ADNS	Automated Digital Network System
AGU	American Geophysical Union
AIP	American Institute of Physics
AMS	American Mathematical Society
ASA	Acoustical Society of America
ASCEE	American Society for Engineering Education
ASN(RDA)	Assistant Secretary of the Navy for Research, Development, and Acquisition
ASW	Antisubmarine Warfare
ATM	Asynchronous Transfer Mode
bbd	Bordered Block Diagonal
b-e	Bending-Extension
BEAM	Bandwidth.Efficient Advanced Modulation
BER	Bit Error Rate
BRF	Birefringent Filter
C^2	Command and Control
C^4ISR	Command, Control, Communications, Computers, Intelligence, Surveillance, and Reconnaissance
CBMS	Conference Board of the Mathematical Sciences
c-BN	Cubic phase of Boron Nitride
CEP	Circular Error Probable
CFAR	Constant False Alarm Rate
CIA	Central Intelligence Agency
CIC	Combat Information Center
COMM	Communications
COTS	Commercial-off-the-Shelf
CPM	Continuous-Phase Modulation
Cr	Chromium
CTD	Conductivity, Temperature, and Depth
CW	Continuous Wave
CY	Cysteamine (hydrochloride)
CYE	L-cysteine ethyl ester (hydrochloride)

DARPA	Defense Advanced Research Projects Agency
DEA	Diethylamino-ethanethiol (hydrochloride)
DIA	Defense Intelligence Agency
DISA	Defense Information Systems Agency
DMA	Dimethylamino-ethanethiol (hydrochloride)
DMRG	Density Matrix Renormalization Group
DRT	Diagnostic Rhyme Test
DSP	Digital Signal Processor
EA	Electro-Absorption
EC	Elliptic Curve
ECC	Elliptic Curve Cryptosystem
EEG	Electroencephalogram
EO	Electro-Optic
FFT	Fast Fourier Transform
FIFO	First-In/First-Out
FRONT	Front-Resolving Observational Network with Telemetry
FWN	Flat White Noise
GaN	Gallium Nitride
GEV	Generalized Eigenvector
GPS	Global Positioning Satellite
	Global Positioning System
HPCMP	High Performance Computing Modernization Program
HWY	Highway
ICA	Independent Components Analysis
ID	Identification
IEEE	Institute of Electrical and Electronic Engineers
ILIR	In-house Laboratory Independent Research
ILS	Intercavity Laser Sensor
IP	Internet Protocol
IR	Infrared
IRIS	Infrared Information Symposia
IRS-CPM	Interleaved Reed–Solomon-encoded Continuous Phase Modulation
ISM	Industrial, Scientific, and Medical
ISnAP	Impulsive Snap-through Acoustic Projector
ISNS	Integrated Shipboard Network Systems
ISR	Intelligence, Surveillance, and Reconnaissance

JCIS	Joint Conference on Information Sciences
JIEO	Joint Interoperability and Engineering Organization
KTA	Potassium tri-arsenate
LFM	Linear Frequency Modulated
LOD	Limit of Detection
LOP	Lines of Position
LOS	Line of Sight
LUM	Linear Unmixing
MAI	Multiple-Access Interference
MCTMS	3-mercaptopropyl trimethoxysilane
MFP	Matched-Field Processing
MFT	Matched-Field Tracking
MMP	Mercapto-methylpyrimidine (hydrochloride)
MNF	Maximum Noise Fraction
Mo	Molybdenum
MSK	Minimum Shift Keying
NAVWAR	Navigation Warfare
NCSC	Naval Coastal Systems Center
NCW	Network-Centric Warfare
Nd:YAG	Neodium: Yttrium Aluminum Garnet
NMCI	Navy/Marine Corps Intranet
NOPP	National Oceanographic Partnership Program
NR	Normal Raman
NRL	Naval Research Laboratory
NSF	National Science Foundation
OCFSS	Optoelectronically Controlled Frequency-Selective Surface
OCW	Optoelectronically Controlled Waveguide
ONR	Office of Naval Research

ONR/NRL Thrusts	ONR/NRL Code and Description
NRL 100-01	NRL Code 1001, Environmental Effects
NRL 100-02	NRL Code 1001, Spacecraft Technology
NRL 550-01	NRL Code 5500, Computational Methods
NRL 550-02	NRL Code 5500, Decision Aids
NRL 550-03	NRL Code 5500, Security
NRL 570-01	NRL Code 5700, Autonomous Real-Time Targeting
NRL 570-02	NRL Code 5700, Network-Centric EW
NRL 570-03	NRL Code 5700, Offboard/Expendables
NRL 570-04	NRL Code 5700, Onboard Jammers
NRL 570-05	NRL Code 5700, Radar Arrays
NRL 570-06	NRL Code 5700, Simulation/Visualization/Planning
NRL 570-07	NRL Code 5700, Threat Detection/Classification/ID
NRL 600-01	NRL Code 6000, Functional Materials
NRL 600-02	NRL Code 6000, Prediction/Simulation
NRL 600-03	NRL Code 6000, Survivability/Lethality
NRL 600-04	NRL Code 6000, Synthesis, Processes, Characterization
NRL 680-01	NRL Code 6800, Electro-Optics
NRL 680-02	NRL Code 6800, Nanoelectronics
NRL 680-03	NRL Code 6800, Plasma Science and Technology
NRL 680-04	NRL Code 6800, Solid-State Electronics
NRL 680-05	NRL Code 6800, Vacuum Electronics
NRL 700-01	NRL Code 7000, Data Assimilation and Information
NRL 700-02	NRL Code 7000, Environmental Processes
NRL 700-03	NRL Code 7000, Model Development
NRL 700-04	NRL Code 7000, Sensors and Data
NRL 700-05	NRL Code 7000, Validation Studies
NRL 710-01	NRL Code 7100, Environmental Adaptive Sonar
NRL 710-02	NRL Code 7100, Mine Countermeasures
NRL 710-03	NRL Code 7100, Shallow Water Active ASW
NRL 710-04	NRL Code 7100, Shallow Water Signal Processing
NRL 710-05	NRL Code 7100, Warfare Effectiveness
ONR 00B-01	ONR 00B1, Naval Science Assistance Program
ONR 01A-01	ONR 01A, ILIR
ONR 311-01	ONR 311, Common Operational/Tactical Picture
ONR 311-02	ONR 311, Decision Support and Collaboration for Optimal Mission Planning and Execution
ONR 311-03	ONR 311, Image Processing, Analysis, and Exploitation for Target Recognition
ONR 311-04	ONR 311, Intelligent Software and Robotic Systems
ONR 311-05	ONR 311, Modeling and Simulation for Design, Engineering, and Acquisition

ONR 311-06	ONR 311, Networked Combat System and Operations
ONR 312-01	ONR 312, EO/IR Electronics
ONR 312-02	ONR 312, High-Power Solid-State Macro Electronics
ONR 312-03	ONR 312, Nanoelectronics
ONR 312-04	ONR 312, RF Solid-State Electronics
ONR 312-05	ONR 312, Vacuum Electronics
ONR 313-01	ONR 313, Advanced Multi-Function RF System
ONR 313-02	ONR 313, Dynamic Wireless Networks
ONR 313-03	ONR 313, Electronic Combat Mission Support
ONR 313-04	ONR 313, Electronic Combat Self-Protection
ONR 313-05	ONR 313, Electronic Combat Threat Warning
ONR 313-06	ONR 313, EO/IR Sensors for Surface/Aerospace Surveillance
ONR 313-07	ONR 313, Maritime/Military Radio
ONR 313-08	ONR 313, Multi-Sensor Fusion for Surface/Aerospace Surveillance
ONR 313-09	ONR 313, Navigation
ONR 313-10	ONR 313, RF Sensors for Surface/Aerospace Surveillance
ONR 313-11	ONR 313, Submarine Communications
ONR 320-01	ONR 32 BSE, Data Assimilation and Information Exploitation
ONR 320-02	ONR 32 BSE, Environmental Processes
ONR 320-03	ONR 32 BSE, Model Development
ONR 320-04	ONR 32 BSE, Sensors & Data
ONR 320-05	ONR 32 BSE, Validation Studies
ONR 320-06	ONR 32 ISR/Spa, Remote/Space Sensing Processes
ONR 320-07	ONR 32 ISR/Spa, Space/Airborne Sensor Development
ONR 320-08	ONR 32 ISR/Spa, Space/Airborne Sensor Exploitation and Demonstration
ONR 320-09	ONR 32 USW/ASW, Battlegroup ASW Defense
ONR 320-10	ONR 32 USW/ASW, Cooperative ASW
ONR 320-11	ONR 32 USW/ASW, Wide-Area ASW Surveillance
ONR 320-12	ONR 32 USW/MIW, Advanced Force Operations
ONR 320-13	ONR 32 USW/MIW, Mine Sweeping/Jamming
ONR 320-14	ONR 32 USW/MIW, Mine/Obstacle Neutralization
ONR 320-15	ONR 32 USW/MIW, Mining
ONR 320-16	ONR 32 USW/MIW, Organic Minehunting
ONR 331-01	ONR 331, Logistics
ONR 331-02	ONR 331, Navigation and Timekeeping
ONR 331-03	ONR 331, Photonics and Electronics
ONR 331-04	ONR 331, Sensing, Diagnostics, and Detectors
ONR 332-01	ONR 332, Maintenance Reduction Technology
ONR 332-02	ONR 332, Naval Materials
ONR 333-01	ONR 333, Dependable, Real-Time, High-Assurance Information System
ONR 333-02	ONR 333, Energy Conversion
ONR 333-03	ONR 333, Hydromechanics

ONR 333-04	ONR 333, Undersea Weaponry
ONR 334-01	ONR 334, Advanced Electrical Power Systems
ONR 334-02	ONR 334, Automation to Reduce Manning
ONR 334-03	ONR 334, Hull Life Assurance
ONR 334-04	ONR 334, Reduced Signatures
ONR 341-01	ONR 341, Chemical-Biological Defense
ONR 341-02	ONR 341, Combat Casualty Care
ONR 341-03	ONR 341, Infectious Disease
ONR 341-04	ONR 341, Military Operational Medicine
ONR 342-01	ONR 342, BioRobotics
ONR 342-02	ONR 342, Biosensors, Biomaterials, and Biotechnology
ONR 342-03	ONR 342, Condition-Based Maintenance
ONR 342-04	ONR 342, Environmental Quality and Environmental Health
ONR 342-05	ONR 342, Human Factors
ONR 342-06	ONR 342, Manpower and Personnel
ONR 342-07	ONR 342, Marine Mammals
ONR 342-08	ONR 342, Pattern Recognition
ONR 342-09	ONR 342, SC-21 Manning Affordability
ONR 342-10	ONR 342, Training
ONR 351-01	ONR 351, Air Superiority
ONR 351-02	ONR 351, Air Vehicle
ONR 351-03	ONR 351, Integrated Avionics, Displays, and Advanced Cockpit
ONR 351-04	ONR 351, Naval Fire Support
ONR 351-05	ONR 351, Precision Strike
ONR 351-06	ONR 351, Propulsion and Power
ONR-351-07	ONR 351, Ship-Based Defense
ONR 351-08	ONR 351, Strategic Systems Sustainment
ONR 351-09	ONR 351, Survivability and Signature Control
ONR 351-10	ONR 351, Uninhabited Combat Air Vehicle
ONR 352-01	ONR 352, Cruise/Theater Air Missile Defense
ONR 352-02	ONR 352, Expeditionary Operations
ONR 352-03	ONR 352, Extending the Littoral Battlespace
ONR 360-01	ONR 36, Commercial Research and Development
ONR 360-02	ONR 36, Data Mining
ONR 361-01	ONR 361, Advanced Composites for Naval Sea Structures (MANTECH NTO)
ONR 361-02	ONR 361, Advanced Forming Techniques for Metallic Engine Components (MANTECH NTO)
ONR 361-03	ONR 361, Advanced Metallic Processing for Ship Structures (MANTECH NTO)
ONR 361-04	ONR 361, Advanced, Affordable Energetics (MANTECH NTO)
ONR 361-05	ONR 361, Affordable Electro-Optic Components

ONR 361-06	ONR 361, Affordable Radar Components
ONR-361-07	ONR 361, Composites Processing for Advanced Aircraft (MANTECH NTO)
ONR 361-08	ONR 361, Environmental Compliance for Navy Shipyards and Depots (MANTECH NTO)
ONR 361-09	ONR 361, Improved Joining Technology for Naval Sea Structures (MANTECH NTO)
ONR 361-10	ONR 361, Low-Cost Manufacturing Processes for Next-Generation Marine Amphibious Assault (MANTECH NTO)
ONR 361-11	ONR 361, MANTECH Non-NTO
ONE 361-12	ONR 361, Non-Invasive Testing and Inspection Methods for Improved Sustainment (MANTECH NTO)
ONR 362-01	ONR 362, Acquisition Center of Excellence
ONR 362-02	ONR 362, Affordability Programs
ONR 362-03	ONR 362, Dual-Use Program
ONR 362-04	ONR 362, SLICE Program
ONR 362-05	ONR 362, Technology Transfer Program/IR&D
ONR 363-01	ONR 363, Historically Black Colleges and Universities/Minority Institutions
ONR 364-01	ONR 364, SBIR/STTR Program
ONR SE	Office of Naval Research Subelement
OPO	Optical Parametric Oscillator
PADL	Posterior-Averaged Deduction Level
PC	Personal Computer
	Principal Component
PDLC	Polymer-Dispersed Liquid Crystal
PKI	Public-Key Infrastructure
PLL	Phase Locked Loop
ppb	Parts Per Billion
PPLN	Periodically Poled $LiNbO_3$
ppm	Parts Per Million
PSD	Power Spectral Densities
p/v	Particle Velocity
PVFET	Photovoltaic Field-Effect Transistor
PZT	Piezoelectric Translator
QD	Quadrature-Detector
QoS	Quality of Service
RF	Radio Frequency
RS	Reed–Solomon

RV	Research Vessel
RX	Reed–Xioali (algorithm)
SAE	Society of Automotive Engineers
SAM	Self-Assembled Monolayer
SBIR	Small Business Innovation Research
SDSU	San Diego State University
SEM	Stochastic Expectation Maximization
SERS	Surface-Enhanced Raman Spectroscopy
SGS	Silver Gallium Sulfide
SIAM	Society of Industrial and Applied Mathematics
SiC	Silicon Carbide
SIO	Scripps Institution of Oceanography
SMP	Stochastic Mixture Processing
SNR	Signal-to-Noise Ratio
SOPL	Second-Order Probability Logic
SPIE	Society of Photo-Optical Instrumentation Engineers (also known as The International Society for Optical Engineering)
SQUIDs	Superconducting Quantum Interference Devices
SR	Stochastic Resonance
ST	Schmitt Trigger
SwellEX-96	Shallow-Water Environmental Cell Experiment, 1996
TCM	Trellis-Coded Modulation
TC TCM	Turbo-Coded TCM
TDOA	Time Difference of Arrival
TE-NR	Thermo-Electrically Cooled Sensor for Normal Raman
TE-SERS	Thermo-Electrically Cooled Sensor for Surface-Enhanced Raman Spectroscopy
Ti	Titanium
TOA	Time of Arrival
TTCP	The Technical Cooperation Programme
UCSD	University of California at San Diego
UV	Ultraviolet
VCO	Voltage-Controlled Oscillator
WDM	Wavelength Division Multiplexers
WFQ	Weighted Fair Queuing

REPORT DOCUMENTATION PAGE		Form Approved OMB No. 0704-01-0188

The public reporting burden for this collection of information is estimated to average 1 hour per response, including the time for reviewing instructions, searching existing data sources, gathering and maintaining the data needed, and completing and reviewing the collection of information. Send comments regarding this burden estimate or any other aspect of this collection of information, including suggestions for reducing the burden to Department of Defense, Washington Headquarters Services Directorate for Information Operations and Reports (0704-0188), 1215 Jefferson Davis Highway, Suite 1204, Arlington VA 22202-4302. Respondents should be aware that notwithstanding any other provision of law, no person shall be subject to any penalty for failing to comply with a collection of information if it does not display a currently valid OMB control number.
PLEASE DO NOT RETURN YOUR FORM TO THE ABOVE ADDRESS.

1. REPORT DATE (DD-MM-YYYY) May 2000	2. REPORT TYPE Final	3. DATES COVERED (From - To) October 1998 through September 1999

4. TITLE AND SUBTITLE ILIR '99: SSC SAN DIEGO IN-HOUSE LABORATORY INDEPENDENT RESEARCH 1999 ANNUAL REPORT	5a. CONTRACT NUMBER
	5b. GRANT NUMBER
	5c. PROGRAM ELEMENT NUMBER
6. AUTHORS	5d. PROJECT NUMBER 0601152N
	5e. TASK NUMBER
	5f. WORK UNIT NUMBER

7. PERFORMING ORGANIZATION NAME(S) AND ADDRESS(ES) SSC San Diego San Diego, CA 92152–5001	8. PERFORMING ORGANIZATION REPORT NUMBER TD 3095
9. SPONSORING/MONITORING AGENCY NAME(S) AND ADDRESS(ES) Office of Naval Research 800 North Quincy Street Arlington, VA 22217–5000	10. SPONSOR/MONITOR'S ACRONYM(S)
	11. SPONSOR/MONITOR'S REPORT NUMBER(S)

12. DISTRIBUTION/AVAILABILITY STATEMENT
Approved for public release; distribution is unlimited.

13. SUPPLEMENTARY NOTES

14. ABSTRACT
The work detailed in this report was carried out in FY 99 as part of the Office of Naval Research In-house Laboratory Independent Research (ILIR) program, which supports basic scientific research in several areas of interest to the Navy, including command and control; communications; intelligence, surveillance, and reconnaissance; and other research areas such as navigation. This document describes the accomplishments and funding of 29 ILIR projects during the period 1 October through 30 September 1999.

15. SUBJECT TERMS
In-house Laboratory Independent Research (ILIR)
command and control; communications; intelligence, surveillance, and reconnaissance
navigation; other research

16. SECURITY CLASSIFICATION OF:			17. LIMITATION OF ABSTRACT	18. NUMBER OF PAGES	19a. NAME OF RESPONSIBLE PERSON Flesner, Larry
a. REPORT	b. ABSTRACT	c. THIS PAGE			19B. TELEPHONE NUMBER (Include area code) (619) 553–1044
U	U	U	U	182	

Standard Form 298 (Rev. 8/98)
Prescribed by ANSI Std. Z39.18

AUTHOR INDEX

Code	Contributor	Page	Code	Contributor	Page
D857	Abawi, Ahmad T.	57	D363	Ladd, Daniel M.	93
D857	Baxley, Paul A.	33	D4223	Lange, Doug	22
D363	Boss, Pamela A.	85	D822	Lapic, Stephan K.	42
D712	Broman, Vincent P.	38	D364	McGinnis, Wayne C.	103
D857	Bucker, Homer P.	60	D364	Meadows, Brian K.	46
D364	Bulsara, Adi R.	88	D374	Murray, Steven A.	12
D73A	Chou, S. I.	63	D743	Myers, Joseph F.	101
D746	Evans, Douglass C.	67	D825	Orazi, Richard J.	50
D361	George, Robert D.	90	D857	Rice, Joseph A.	33
D44215	Goodman, I. R.	16	D3503	Ridgway, Samuel H.	104
D853	Hanson, Frank E.	97	D73H	Sritharan, Sri	9
D3604	Hicks, Charles	99	D743	Stewart, Stephen E.	75
D858	Hitney, Herbert V.	70	D746	Tang, Po–Yun	79
D7303	Hunt, Barry R.	72	D841	Wahlen, Bruce E.	53
D44213	Johnson, Ralph R.	25			
D712	Kevorkian, Aram K.	73			

INTERNAL DISTRIBUTION

pdf file available for download from
http://www.spawar.navy.mil/sti/publications/pubs/td/3095/td3095.pdf

173

EXTERNAL DISTRIBUTION

pdf file available for download from
http://www.spawar.navy.mil/sti/publications/pubs/td/3095/td3095.pdf